



**GEOLOGICAL SURVEY OF CANADA**

**OPEN FILE 2635**

This document was produced  
by scanning the original publication.

Ce document a été produit par  
numérisation de la publication originale.

---

**Geomagnetic induced currents:  
assessment of geomagnetic hazard**

---

**R.L. Coles, D.H. Boteler**

**1993**



Energy, Mines and  
Resources Canada

Énergie, Mines et  
Ressources Canada

**Canada**

## ABSTRACT

The object of this study was to determine the occurrence of geomagnetic conditions which may lead to problems on power systems. Maximum rate of change of the magnetic field in each hour has been chosen as the most suitable indicator of geomagnetic hazard conditions. The occurrence frequency of different geomagnetic hazard levels has been analyzed using data from Canadian geomagnetic observatories for the years 1977 to 1989. A general characteristic is that the frequency of occurrence of different hazard levels falls off exponentially with increasing hazard size. The actual occurrence values at particular locations change with time and with position. Hazard events have an essentially random distribution in time, but analysis of sufficient data shows there are underlying changes in the occurrence frequency related to the phase of the solar cycle and to season. Hazard occurrences are also clustered at particular times of day: 16:00 to 01:00 and 03:00 to 11:00 defined in the "local" time of the location. The results show that the hazard occurrence increases sharply as one approaches the auroral zone and then decreases as one goes further north. By using the invariant geomagnetic coordinate system these results can be used to determine the hazard occurrence for a power system anywhere in Canada.

## PRÉAMBULE

La présente étude avait pour objet l'examen de la manifestation des conditions géomagnétiques susceptibles d'entraîner des problèmes sur les réseaux électriques. Comme indicateur le plus approprié pour caractériser les conditions de risque géomagnétique, on a choisi le taux de variation maximal du champ magnétique pendant des périodes d'une heure. La fréquence d'apparition de différents niveaux du risque géomagnétique a été analysée à l'appui des données provenant de station d'observation des phénomènes géomagnétiques au Canada au cours des années 1977 à 1989. Une caractéristique générale que l'on peut dégager est la suivante: la fréquence d'apparition des différents niveaux de risque chute de façon exponentielle avec la taille du risque. Les valeurs effectives liées aux manifestations en des endroits particuliers changent avec le temps, mais l'analyse d'une quantité suffisante de données montre qu'il y a des variations sous-jacentes dans le fréquence des manifestations, qui sont en relation avec la phase du cycle solaire et la saison. Par ailleurs, les manifestations semblent être concentrées à certaines heures particulières de la journée: de 16 h à h et de 3 h à 11 h, définies en heure «locale» de l'endroit. Les résultats montrent que la manifestation du risque géomagnétique s'accroît de façon abrupte à mesure que l'on se rapproche de la one de l'aurore polaire, et puis décroît lorsqu'on se déplace encore plus vers le nord. Grâce à l'utilisation du système invariant de coordonnées géomagnétiques, ces résultats peuvent servir à déterminer l'apparition du risque pour un réseau électrique, n'importe où au Canada.

## ACKNOWLEDGEMENTS

This work was undertaken as a jointly-funded project between CEA and the Geological Survey of Canada. In particular, we wish to acknowledge the able assistance of Mr. K. Rose and Mr. G. Jansen van Beek in the collection, preparation, and analysis of the data.

We thank Mr L. R. Newitt for his careful and constructive review of a draft of the report.

We appreciate the comments and advice given by the project monitors, Dr Léonard Bolduc and Mr Kevin Thompson.

## SUMMARY

Geomagnetic disturbances can have serious effects on power systems. These effects arise because of geomagnetically induced currents flowing through grounded power transmission systems and causing transformer saturation with its associated problems of harmonic generation and increased reactive power demand. The purpose of this study was to determine the occurrence of those geomagnetic conditions that might cause power system problems.

The rate of change of the magnetic field,  $dB/dt$ , was chosen as the most appropriate indicator of the magnetic fluctuations likely to produce significant geomagnetically induced currents. Magnetic field data from 11 observatories across Canada for the years 1977 to 1989 was analyzed to determine rates of occurrence for different levels of  $dB/dt$ . In addition, comparison was made between the occurrence of  $dB/dt$  values and the occurrence of different levels of  $K_p$ , the global index traditionally used to measure geomagnetic activity.

Large disturbances were found to be distributed nearly randomly in time. With the 13-year data set used for the  $dB/dt$  analysis there were no clear variations in occurrence of large  $dB/dt$  values with season or with the solar cycle. However, in the study of 55 years of  $K_p$  data, seasonal and solar cycle trends are apparent. This indicates that the seasonal and solar cycle variations represent only a modulation of the otherwise irregular occurrence pattern of large disturbances.

It was found that the mean occurrence of  $dB/dt$  values decreases exponentially with increasing size of  $dB/dt$ . The results show that the occurrence of larger  $dB/dt$  values increases as one goes north to the auroral zone and then decreases as one goes further north. The occurrence of high  $dB/dt$  values also varies with the time of day (local time) as the rotation of the Earth carries the observing position past the disturbance centres around the auroral zone. Maps are produced showing the probability of occurrence of large  $dB/dt$  values across Canada.

## RÉSUMÉ

Les perturbations géomagnétiques peuvent avoir de graves effets sur les réseaux électriques. Ces effets ont pour origine des courants, induits par les phénomènes géomagnétiques, qui circulent dans les réseaux de transport d'énergie mis à terre et qui provoquent la saturation des transformateurs, donnant ainsi lieu à des problèmes associés comme la génération d'harmoniques et l'accroissement de la demande de puissance réactive. Cette étude avait pour objet l'examen de l'apparition des conditions géomagnétiques particulières qui peuvent entraîner des problèmes sur les réseaux de transport d'énergie.

Le taux de variation du champ magnétique,  $dB/dt$  a été choisi comme l'indicateur le plus approprié pour caractériser les fluctuations magnétiques censées produire d'importants courants induits par géomagnétisme. Les données sur le champ magnétique, couvrant les années 1977 à 1989, et provenant de 11 stations d'observation réparties à travers le Canada, ont été analysées en vue de déterminer le taux de manifestation de différents niveaux de  $dB/dt$ . En outre, on a effectué une comparaison entre les valeurs de  $dB/dt$  obtenues lors des manifestations géomagnétiques et les différents niveaux de  $K_p$ , un indice global utilisé traditionnellement pour mesurer l'activité géomagnétique.

On a constaté que les fortes perturbations étaient réparties quasiment au hasard dans le temps. Malgré un étalement sur 13 ans, l'ensemble de données utilisé pour l'analyse de  $dB/dt$  n'a pas fait ressortir des variations bien définies de l'apparition de grandes valeurs de  $dB/dt$  liées à la saison ou au cycle solaire. En revanche, dans l'étude des données relatives au  $K_p$ , couvrant une période de 55 ans, des tendances saisonnières et liées au cycle solaire apparaissent bel et bien. Ceci indique que la variation saisonnière et celle liée au cycle solaire ne représentent qu'une modulation du schème, apparemment irrégulier, d'apparition de fortes perturbations.

On a constaté que la moyenne d'apparition des valeurs de  $dB/dt$ . Les résultats montrent que l'apparition de valeurs plus grandes de  $dB/dt$  augmente lorsqu'on va en direction du nord, vers la zone de l'aurore polaire, et puis décroît lorsqu'on va encore plus au nord. L'apparition de valeurs élevées de  $dB/dt$  varié également avec l'heure de la journée (en heure locale), à mesure que la rotation de la terre emporte la position d'observation au-delà des centres de perturbation, autour de la zone d'aurore polaire. On a par ailleurs produit des cartes illustrant la probabilité d'apparition de valeurs importantes de  $dB/dt$  partout à travers le Canada.

## CONTENTS

<u>Section</u>		<u>Page</u>
1	INTRODUCTION	1
	1.1 Outline of Report	1
	1.2 Geomagnetic Effects on Electric Power Systems	1
	1.3 The Production of GIC	2
	1.4 Evaluating Problem Disturbances	2
	1.5 Previous Work	3
2	DATA COLLECTION AND ANALYSIS	7
	2.1 Canadian Magnetic Observatory Network	7
	2.2 Coordinate Systems	9
	2.3 Data Analysis	11
3	RESULTS OF RATE-OF-CHANGE ANALYSIS	17
	3.1 Introduction	17
	3.2 Variation of Occurrence with Solar Cycle	17
	3.3 Variation of Occurrence with Season	26
	3.4 Variation of Occurrence with Latitude	26
	3.5 Variation of Occurrence with Local Time	31
4	COMPARISONS OF $dB/dt$ WITH GLOBAL INDICES	33
	4.1 The Magnetic Indices $K_p$ , $a_p$ , and $A_p$	33
	4.2 Comparisons between the $a_p$ Index and Rate-of-Change	33
5	DISCUSSION AND CONCLUSIONS	39
	5.1 Introduction	39
	5.2 Temporal Variations	39
	5.3 Spatial Variations	40
	5.4 Geomagnetic Hazard	42
	5.5 Recommendations for Future Work	45
6	REFERENCES	47
	APPENDIX	49
	A. Latitudinal and Seasonal Variations	49
	B. Variation of Occurrence with Local Time	63
	C. Relations between $dB/dt$ and $a_p$ ( $K_p$ )	69



## LIST OF ILLUSTRATIONS

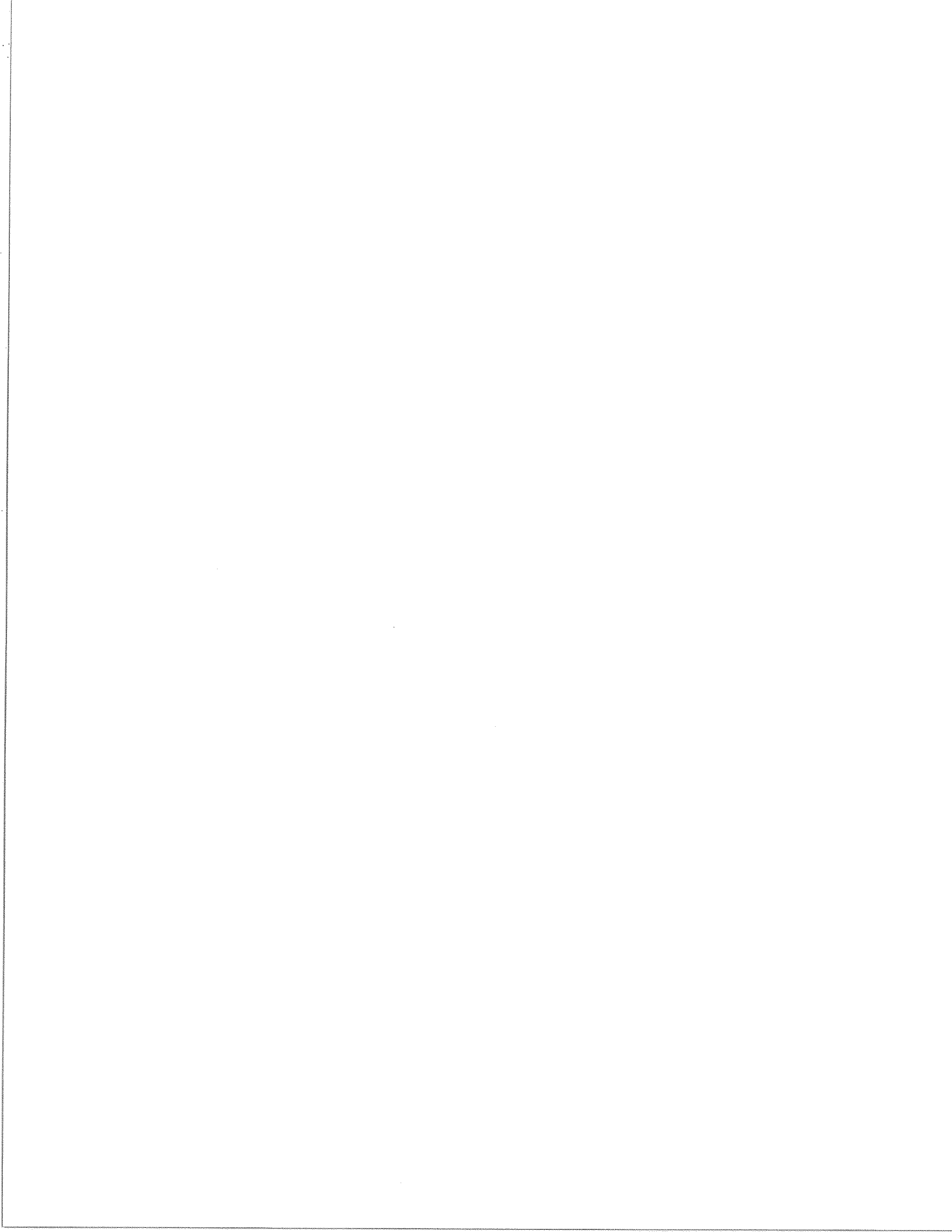
<u>Figure</u>	<u>Page</u>
1	5
<p>Comparison between the unsigned maximum rate-of-change of the magnetic field at Ottawa and the unsigned maximum GIC at Wawa, during intervals of 2 minutes, for March 13, 1989. Both data sets were based on 10-second sampling rates.</p>	
2	5
<p>Correlogram plot of peak GIC versus peak rate-of-change of magnetic field during 2-minute intervals, based on 10-second data. (Note that 50 nT/(10sec) equals 300 nT/min.)</p>	
3	8
<p>The Canadian Magnetic Observatory Network.</p>	
4	10
<p>The relationship between the Geographic Coordinate System and the Invariant Geomagnetic Coordinate System, for the northern regions. Dashed lines indicate the invariant geomagnetic latitudes.</p>	
5	13
<p>Histogram of the events occurring during one year (1989) at Ottawa observatory, within intervals 0-59, 60-119, 120-179, 180-239, 240-299, and 300 and over, nT/min, for each magnetic field component X, Y, and Z. The number of events with rate-of-change in the first interval exceeds 520,000 for all components.</p>	
6	14
<p>Histogram of the events occurring during one year (1989) at Meanook observatory, within intervals 0-59, 60-119, 120-179, 180-239, 240-299, and 300 and over, nT/min, for each magnetic field component X, Y, and Z. The number of events with rate-of-change in the first interval exceeds 520,000 for all components. The number of events in the second interval exceeds 1200 for all components.</p>	
7	19
<p>The number of hours per year (left scale) and percentage probability (right scale) during which at least one event in any magnetic field component equalled or exceeded 180 nT/min, for each observatory.</p>	
8	25
<p>The monthly sunspot numbers and coronal activity index values for the years 1977 to 1989.</p>	
9	27
<p>The average number of hours (left scale) and percentage probability (right scale) during which at least one event in any component equalled or exceeded 300 nT/min, as a function of month. Only those observatories for which the numbers are appreciable are shown.</p>	



10	The average numbers of hours per season for which at least one event in any component equalled or exceeded 180 (solid discs), 300 (squares), 420 (triangles), 540 (diamonds) nT/min. Note the logarithmic horizontal scale. On the vertical scale, the observatories are sequenced according to invariant geomagnetic latitude.	30
11	The average numbers of events equalling or exceeding 300 nT/min, for each hour in local time, for the X magnetic field component, for observatories OTT, MEA, FCC, and BLC as examples.	32
12	Histogram of the distribution of $A_p$ values, in terms of number per year.	34
13	Average occurrence per year (left scale) and percentage probability per year (right scale) for 3-hour intervals with $K_p=7$ , $K_p=8$ , and $K_p=9$ , in terms of number of years after the minimum in the solar sunspot cycle.	35
14	Average occurrence per month (left scale) and percentage probability per month (right scale) for 3-hour intervals with $K_p=7$ , $K_p=8$ , and $K_p=9$ , according to month of the year.	35
15	Examples of correlogram of the maximum dB/dt in a three-hour interval versus the $a_p$ value for that interval. The equivalent $K_p$ values are noted on the top axis.	37
16	Plots of the slopes of the regression lines derived from the set of correlograms, as shown in Figure 14, for southern observatories, according to local time.	38
17	Map of average geomagnetic hazard, expressed as the percentage probability of occurrence of an hour during which dB/dt will equal or exceed 300 nT/min.	43
18	Map of geomagnetic hazard for more active years, expressed as percentage probability of occurrence of an hour during which dB/dt will equal or exceed 300 nT/min.	44

## LIST OF TABLES

<u>Table</u>		<u>Page</u>
1	Probabilities of Occurrence of Hours with Events Equalling or Exceeding 300 nT/min Expressed as Percentages	18
2	Occurrences of large dB/dt during K9 storms	41



# 1. INTRODUCTION

## 1.1 OUTLINE OF REPORT

Section 1 provides the setting for the study described in this report, and discusses some previous work. Section 2 describes the magnetic field measurements that were used for the study and the processing of the data. Section 3 presents the results on the occurrence of different dB/dt values. Section 4 compares dB/dt occurrences with ap values and occurrence patterns of ap. Section 5 provides a general discussion and conclusions. Some results for individual observatories and additional data compilations are presented in a series of appendices.

This initial study presents a summary of the statistical results, looked at from a broad perspective. More detailed analyses may be pursued in the future.

## 1.2 GEOMAGNETIC EFFECTS ON ELECTRIC POWER SYSTEMS

Variations of the geomagnetic field induce electric fields in the Earth that drive electric currents into grounded power system networks. These geomagnetically induced currents (GIC) flowing through power system transformers produce half-cycle saturation of the transformers, leading to distorted waveforms with a high harmonic content. These high harmonic levels, plus increased reactive power demand on the transformers, can lead to a variety of problems with system operation (see (1) for a review of these effects).

Equipment to prevent GIC problems is expensive; therefore the response to GIC problems has concentrated on developing operating strategies for geomagnetically disturbed conditions. However, changing a system operation to a "safe posture" imposes its own costs that can be exacerbated by repeated false alarms. A first step in planning a cost effective response to GIC is to determine how often the problematic geomagnetic conditions can be expected. This is the subject of this report.

### 1.3 THE PRODUCTION OF GIC

The processes leading to power system problems start on the Sun. Eruptions from the surface of the Sun eject clouds of high energy plasma out into space. These plasma clouds travel out from the Sun and, if directed this way, arrive at the Earth several days later. The Earth's magnetic field creates a region of space, the magnetosphere, shielded from the direct penetration of the solar plasma, thus preventing the solar particles from reaching the Earth's surface. However, the plasma cloud compresses the magnetosphere and, depending on the conditions, can generate large electric fields along the boundaries of the magnetosphere. These electric fields drive currents in the magnetosphere that flow down magnetic field lines to the ionosphere, 100 km above the surface of the Earth. It is the magnetic fields of these ionospheric currents that are the predominant cause of the magnetic fluctuations seen at the Earth's surface as geomagnetic disturbances.

The changing geomagnetic field induces a varying electric field in the conducting Earth. The size of electric field produced depends principally on the magnitude and frequency of the magnetic field variations. It also depends on the conductivity of the Earth and how this conductivity varies with depth and geographic location. Also important are horizontal variations in the magnitude of fluctuations of the magnetic field as these affect not only the size of GIC but also their distribution across the power system.

### 1.4 EVALUATING PROBLEM DISTURBANCES

The ultimate aim of this work is to evaluate the occurrence of those geomagnetic events that cause power system problems. Focussing on specific conditions requires information on the threshold levels at which power systems start experiencing problems - information that is not yet available and is likely to vary considerably between power systems. This study therefore evaluates the occurrence of a range of conditions. The next question is: What is an appropriate measure of the geomagnetic conditions that affect power systems? An obvious parameter is the size of geomagnetic variations and this (measured as the range of variation in a 1-hour or 3-hour interval) is the indicator that has traditionally been used. However,

as explained above, the production of electric fields and GIC depends on the frequency of the magnetic field variations; therefore, the rate of change of the magnetic field over a much smaller time interval may be a better indicator of the critical geomagnetic conditions.

Data is available from 13 geomagnetic observatories across Canada. From 1977 data is available in digital form and has been processed to determine the maximum rate of change of the magnetic field in each hour. The occurrences of different values have been determined and the basic results are presented in a series of appendices. However, to make the results more useful and more understandable, considerable work has been done to determine the underlying "structure" of the data and to explain the causes of these features.

It will be shown that the rate of occurrence of a geomagnetic disturbance depends on the magnitude of the disturbance, the solar cycle, and the season. Also, the disturbance observed at a particular site depends on its location relative to the disturbance current systems. This shows up as a strong dependence on latitude. There is also a dependence on the "longitudinal" position of the site relative to the current systems, but as the current systems are fixed with respect to the magnetosphere, a site rotating with the Earth observes this as a variation of occurrence with time of day.

Comparison is also made between Canadian data and the "ap" index of global magnetic activity (the linear equivalent of Kp). This provides a test of the effectiveness of ap (and Kp) as an indicator of a disturbance in different parts of Canada. Also the 55-year ap data set provides a better indication of the variation in the occurrence frequency of different levels of activity with the solar cycle and with season, and also places the Canadian data in the proper historical context.

## 1.5 PREVIOUS WORK

Several studies (2,3,4) have considered some aspects of the variations in magnetic activity with latitude, season, local time, and solar cycle. These studies were concerned primarily with shorter periods of data than used in this study, but their results suggested some

directions to be pursued in this study.

Some previous work relating GICs and rates-of-change of geomagnetic variations has been carried out through collaboration with staff of Ontario Hydro (5,6). In Figure 6 of (5), reproduced here as Figure 1, a graphical comparison was presented between the unsigned maximum GIC and the unsigned maximum rate-of-change of geomagnetic field occurring during two-minute intervals for March 13 1989. Both data sets in that case were based on 10-second sampling rates. A clear qualitative correlation between occurrences of high GIC and high dB/dt was seen.

An alternative form of presentation, the correlogram or scatter plot, was used in (5) in figure 11 of that report. A similar presentation, but solely for the March 13 1989 storm, is shown here in Figure 2. These results are specific to a particular Ontario Hydro site and the Ottawa observatory, but similar comparisons could be developed between other sites and a relevant observatory.

Figure 2 indicates that for an intense storm such as that of March 13 1989, the occurrence, for example, of a rate-of-change of magnetic field of 3 nT/sec (180 nT/min) may correspond to GICs up to about 35 A at Wawa, but no higher, as indicated by the dashed threshold line shown in the figure.

Of course, the net GICs recorded at a station depend on the geology of the region, specifically the electrical conductivity of the Earth in the region, and also on the precise configuration of the distribution grid and of the transformers and neutral connections at the site. In an interconnected system, the net GIC flowing through the neutral connection may be only a part of the total GIC flowing through the transmission line system.

With a more complete understanding of the linkages between the geomagnetic field variations, the Earth's conductivity, and the power systems, the statistical summaries of geomagnetic hazards presented in this report may be used to establish measures of risk to segments of power grids in various parts of the country.

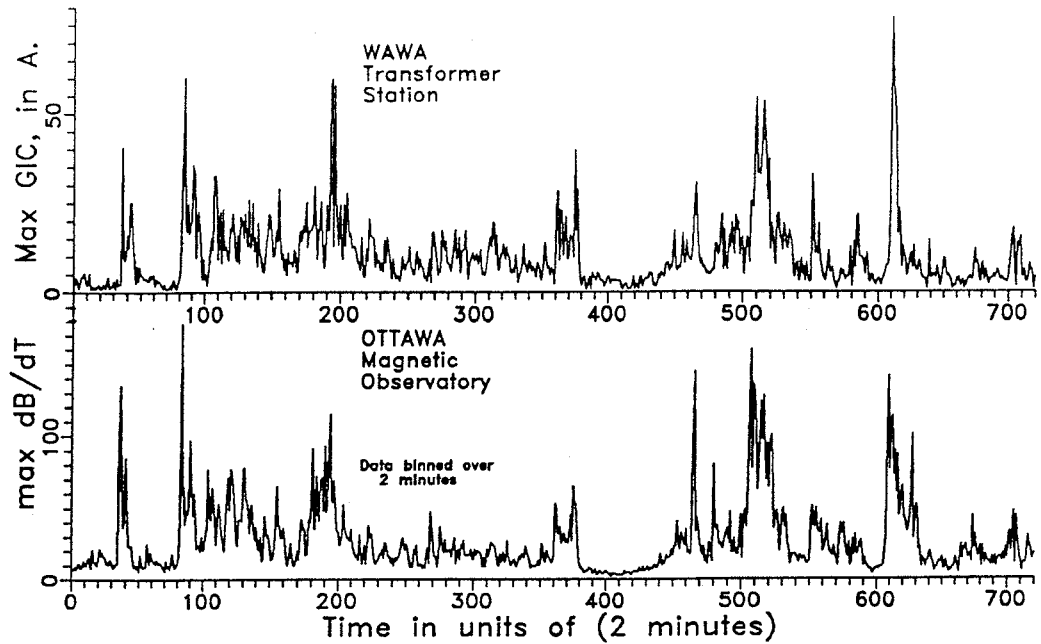


Figure 1 Comparison between the unsigned maximum rate-of-change of the magnetic field at Ottawa and the unsigned maximum GIC at Wawa, during intervals of 2 minutes, for March 13, 1989. Both data sets were based on 10-second sampling rates.

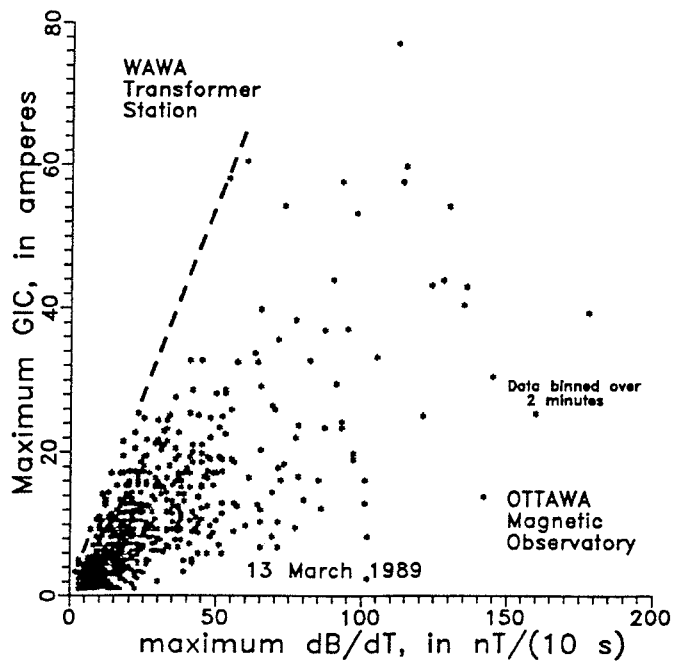
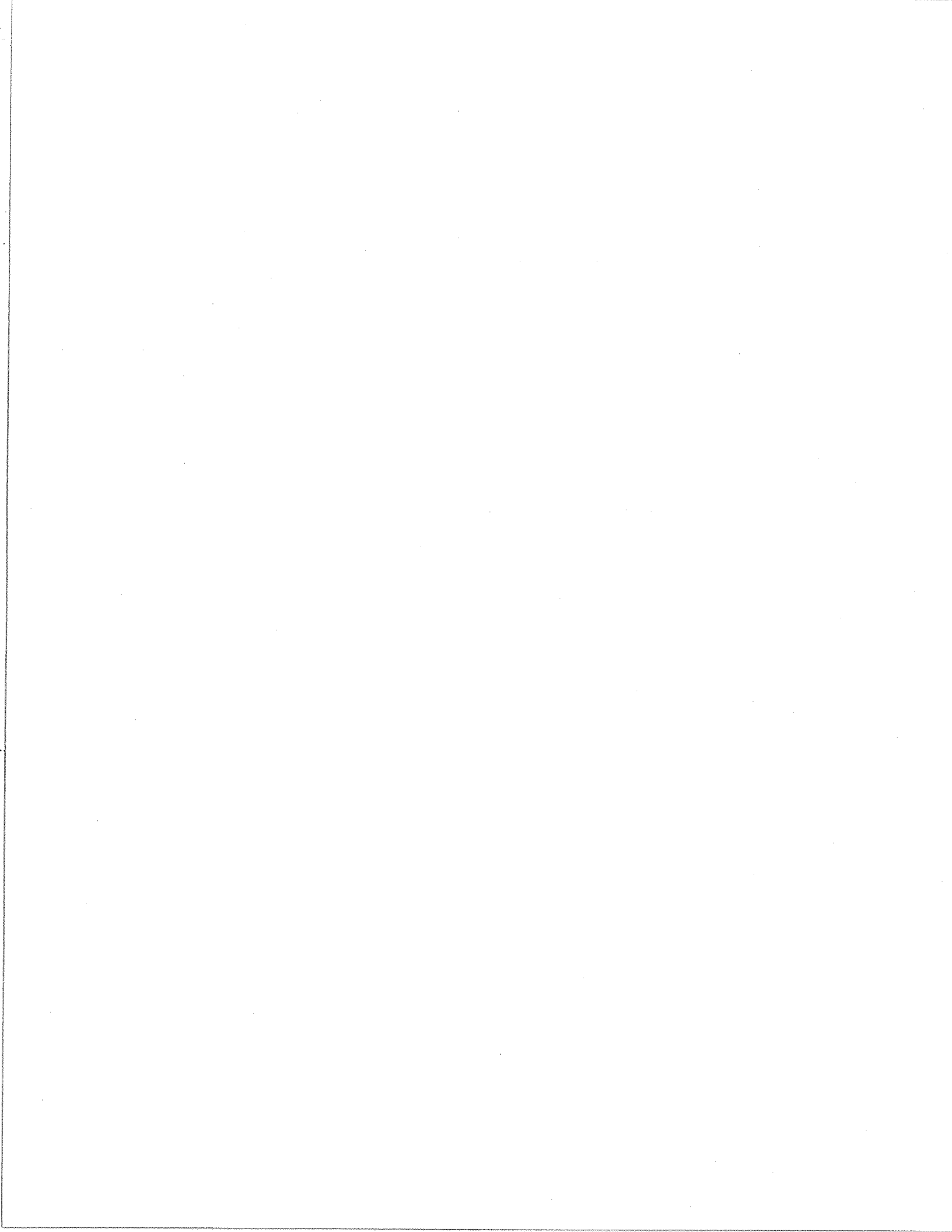


Figure 2 Correlogram plot of peak GIC versus peak rate-of-change of magnetic field during 2-minute intervals, based on 10-second data. (Note that 50 nT/(10sec) equals 300 nT/min.)





## 2 DATA COLLECTION AND ANALYSIS

### 2.1 CANADIAN MAGNETIC OBSERVATORY NETWORK

The Canadian magnetic observatory network (7) consists of 13 digital observatories (Figure 3), providing coverage of the three major magnetic regions in Canada, namely the subauroral, auroral, and polar cap regions (8). In this study, only 11 of the observatories were used, those at Mould Bay and Alert being too far north to contribute pertinent information.

At each observatory, a triaxial fluxgate magnetometer measures the component values of the vector geomagnetic field, in the northward (X), eastward (Y), and downward (Z) directions; in addition, a proton precession magnetometer measures the scalar total intensity of the field (F). Once per minute, digitally filtered values of the X, Y, and Z components, along with one F value for the minute, are recorded.

During the years (1977 - 1989) for which data were studied in this contract, one major instrumentation change was made at all observatories. During the early years, all observatories used the AMOS I instrumentation (9). During 1981, instrumentation at all the observatories was changed to the AMOS III (10). For the purposes of this study, the only consideration is that the one-minute fluxgate values from the AMOS I system were "spot-values", not filtered as in AMOS III. However, such a change is unlikely to affect significantly the conclusions that we draw.

The data from the Canadian magnetic observatories form a major data set of international significance for many facets of scientific research and commercial endeavour. The data undergo stringent quality control procedures before they are archived and made available for final distribution. The data are deposited annually in the World Data Centre A, in Boulder, Colorado, USA. They are archived on optical disc WORM platters in the Geophysics Division, Geological Survey of Canada, in Ottawa.

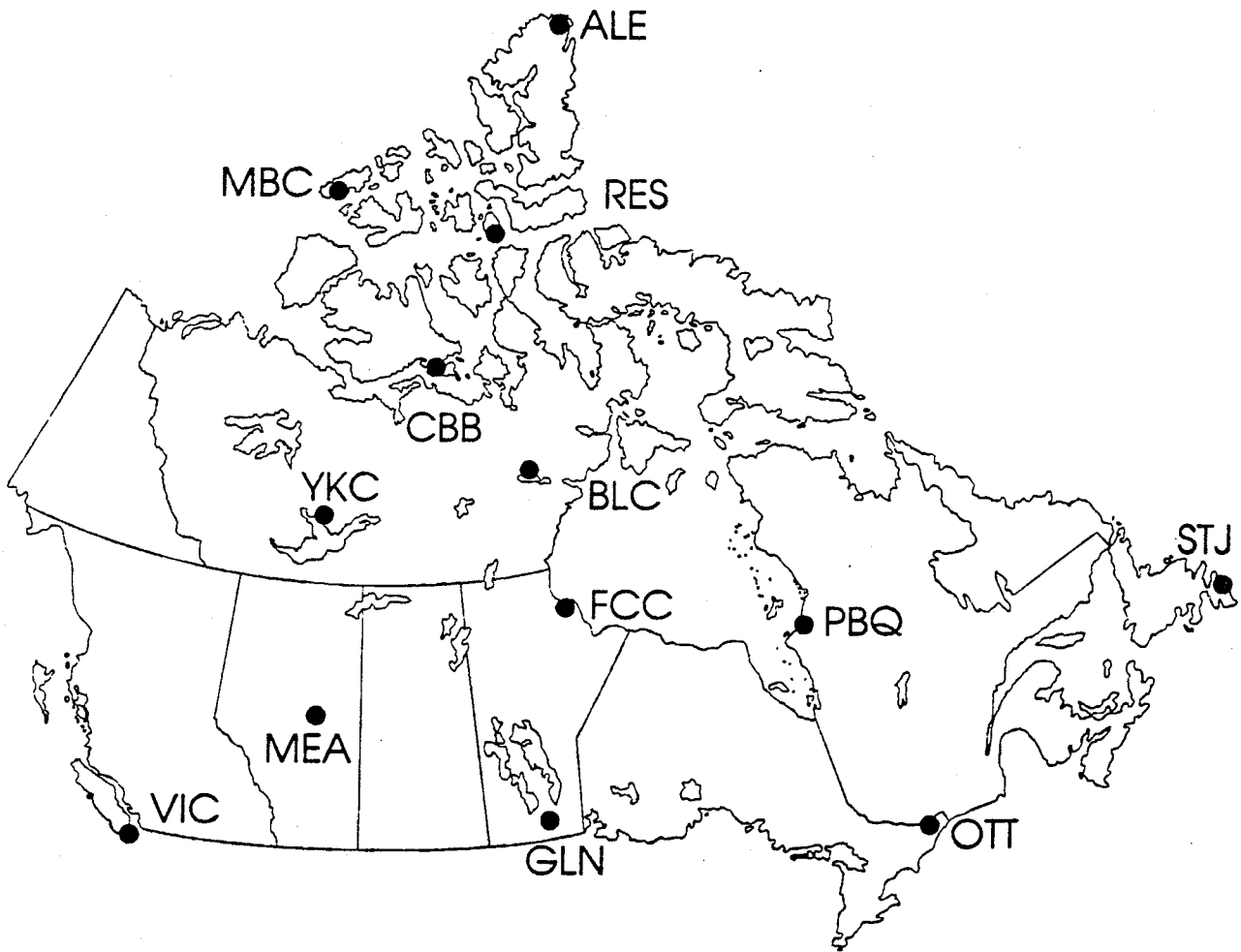


Figure 3 The Canadian Magnetic Observatory Network.

- ALE Alert
- MBC Mould Bay
- RES Resolute
- CBB Cambridge Bay
- BLC Baker Lake
- YKC Yellowknife
- FCC Churchill
- PBQ Poste-de-la-Baleine
- MEA Meanook
- GLN Glenlea
- OTT Ottawa
- STJ St John's
- VIC Victoria

## 2.2 COORDINATE SYSTEMS

The magnetic field fluctuations that occur during a geomagnetic disturbance vary considerably from place to place, especially near the auroral regions such as exist in Canada. The rapid magnetic field fluctuations of concern in studies of GIC are not due to changes of the "internal" magnetic field originating from within the Earth but are due to "external" effects in the magnetosphere and ionosphere. However, the "internal" magnetic field of the Earth exerts a controlling influence on the movements of charged particles arriving from the sun in the solar wind. These moving charged particles constitute electric currents and therefore cause additional fluctuating magnetic fields that may result in GIC. The geographic coordinate system is not the optimum coordinate system, or reference frame, in which to study these phenomena and their effects. A coordinate system that has been found to be appropriate for studies of these phenomena was introduced by McIlwain (11) and practically expounded by Evans et al. (12). It is known as the Invariant Geomagnetic Coordinates System. (The term "invariant" is concerned with the behaviour of the particles, not the coordinate system.)

The relation between the geographic and invariant geomagnetic coordinate systems for the north polar region is shown in Figure 4. In this Figure, the locations of the Canadian magnetic observatories are also shown. Relative to the Invariant Geomagnetic Coordinate System, we can consider an invariant geomagnetic latitude. In some of the presentations in Section 3 and the Appendix of this report, the observatories will be ordered in terms of their invariant geomagnetic latitudes, since this permits a more sensible description of the results, consistent with a global perspective.

As a result of numerous studies over the years, it has been found convenient to divide the Earth into several regions which each experience different types of magnetic disturbance (13). Considered on a global basis, the magnetic variations, or fluctuations, exhibit a dominant zonal character, when viewed in a coordinate system such as the Invariant Geomagnetic Coordinate System. In addition to this dominantly latitudinal characteristic, there is often a strong dependence on longitude, or local time (i.e. time relative to the Sun)

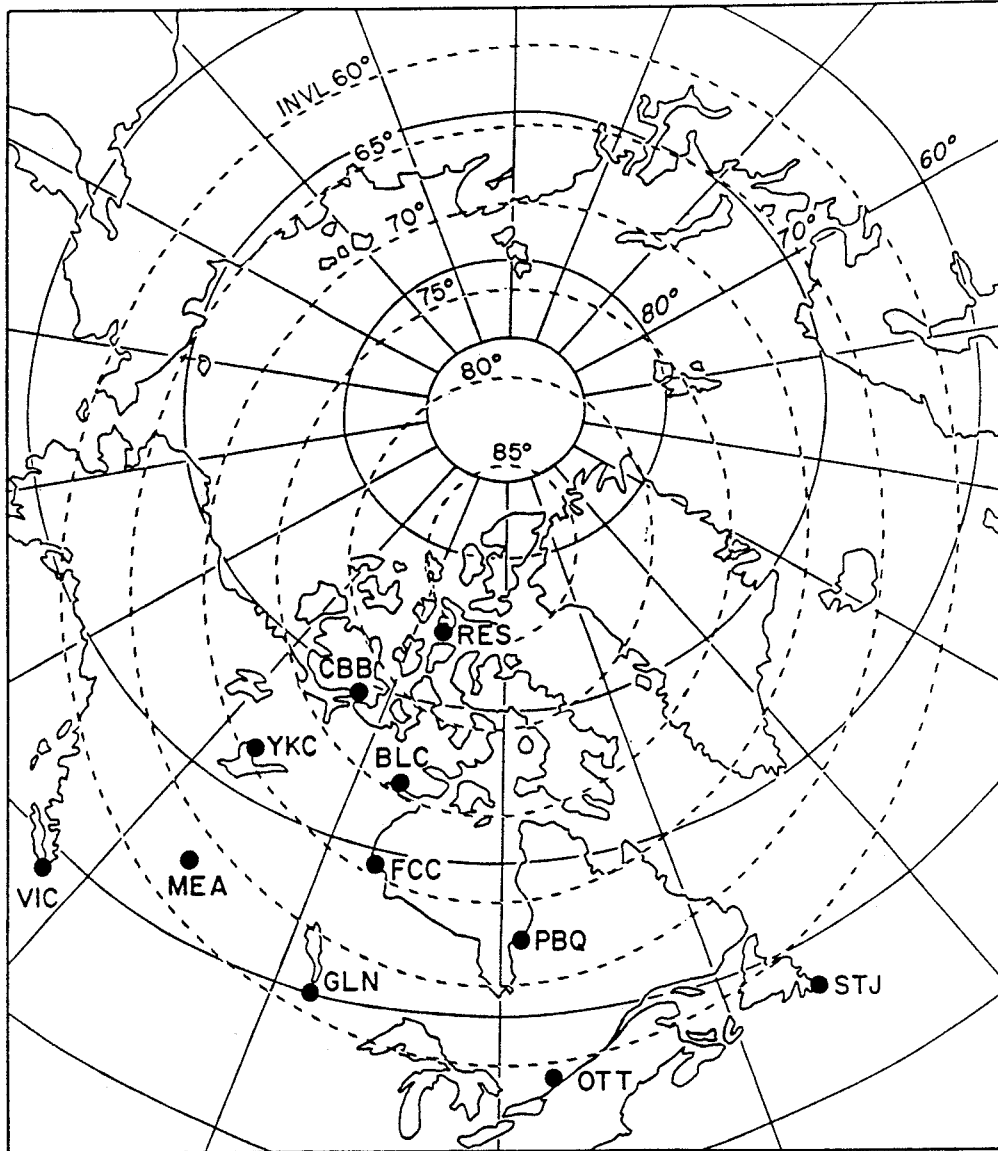


Figure 4 The relationship between the Geographic Coordinate System and the Invariant Geomagnetic Coordinate System, for the northern regions. Dashed lines indicate the invariant geomagnetic latitudes.

since the phenomena that occur in the magnetosphere and the ionosphere, and that cause the magnetic field fluctuations, are strongly influenced by the relative orientations of the Sun, Earth and the Earth's magnetic field.

It is through this dominant latitudinal (zonal) characteristic that we are able to generalize from the results that we obtain in this study of data from individual observatories to conclusions concerning the whole of the Canadian region. Each observatory can be considered as representative of one zone in a set of concentric zones about the pole of the invariant coordinate system.

### 2.3 DATA ANALYSIS

For this study, data for the years 1977 to 1989 were taken from the WORM archive of Canadian observatory network data held in Ottawa. Data prior to 1977 were not consistently available for several of the observatories, and the data for 1990 and 1991 were still undergoing final quality checks and had not been placed in the archive. The period 1977 to 1989 covers slightly more than one solar cycle.

As noted in Section 1, estimates of the rate-of-change of the geomagnetic field provide useful proxy indicators for the occurrence of significant fluctuations in the electric field. Earlier work (such as indicated in (5)) suggests that significant events tend to occur when high rates-of-change of the geomagnetic field last for a minute or more. Thus, it is appropriate to use the large Canadian observatory data-set to determine average rates-of-change for each minute. Shorter events are filtered out in the process.

In terms of the computing process, one simply computes first differences between one-minute values, while testing for the occurrence of data gaps. The resulting values, known variously in this report as "first differences", "dB/dt", and "rate-of-change", represent the average rate-of-change of the geomagnetic field from one minute to the next. The units of these values are nanotesla/minute, or nT/min.

In the archive, data are organized by year. Each optical disc (capacity 400 MB on each of two sides) normally contains data from the network for four years.

In the analysis, first differences were calculated for each component. The values of the first differences (or rates-of-change) were sorted into histogram bins. Prior work (5) and preliminary investigation at the start of this study indicated that it would be useful to select "bin thresholds" of 60, 120, 180, 240, 300, 360, 420, 540, and 600 nt/min. These allow ready comparison with other studies that may use different data sets (again such as in (2) where some data was sampled at 10 second intervals), since they are readily convertible to nT/sec, as 1, 2, 3 nT/sec and so on.

In the first step, computer files were generated that contained for each hour, the histogram data for each component, the maximum rate-of-change ("max dB/dt") in that hour for each component, and the hourly range for each component. Each histogram bin contained the number of occurrences of dB/dt with values falling within that bin's limits.

Examples of histograms showing the distributions of values of rates-of-change are shown in Figures 5 and 6, for Ottawa, a southern observatory, and Meanook, just south of the auroral region. These figures show that the three components, X, Y, Z, have comparable occurrence rates at most stations. Previous work has shown that GIC have similar relationships with the rates-of-change of either X, Y, or Z. As a result, in this study we have selected the largest of  $dX/dt$ ,  $dY/dt$  and  $dZ/dt$  during the specified interval and have labelled it, dB/dt.

It is of limited value to know that there were, say, 5 rate-of-change values within certain threshold limits during a single hour, particularly if they all occurred during, say, a 10 minute period. In the context of this contract study, it is more useful and manageable, from a practical viewpoint, to know that at least one rate-of-change value within the threshold limits has occurred within an hour. A series of files was therefore developed that established histograms of the maximum rates-of-change occurring during every hour. From

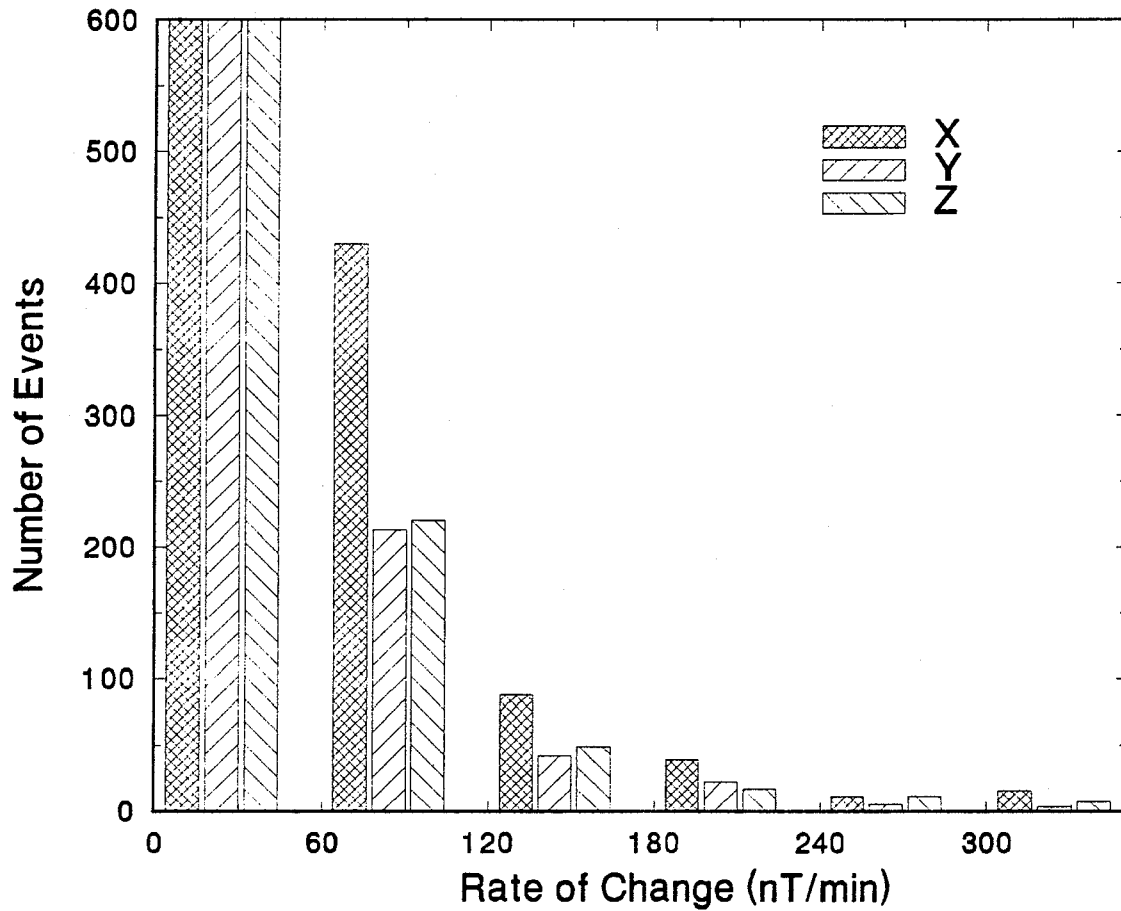


Figure 5 Histogram of the events occurring during one year (1989) at Ottawa observatory, within intervals 0-59, 60-119, 120-179, 180-239, 240-299, and 300 and over, nT/min, for each magnetic field component X, Y, and Z. The number of events with rate-of-change in the first interval exceeds 520,000 for all components.



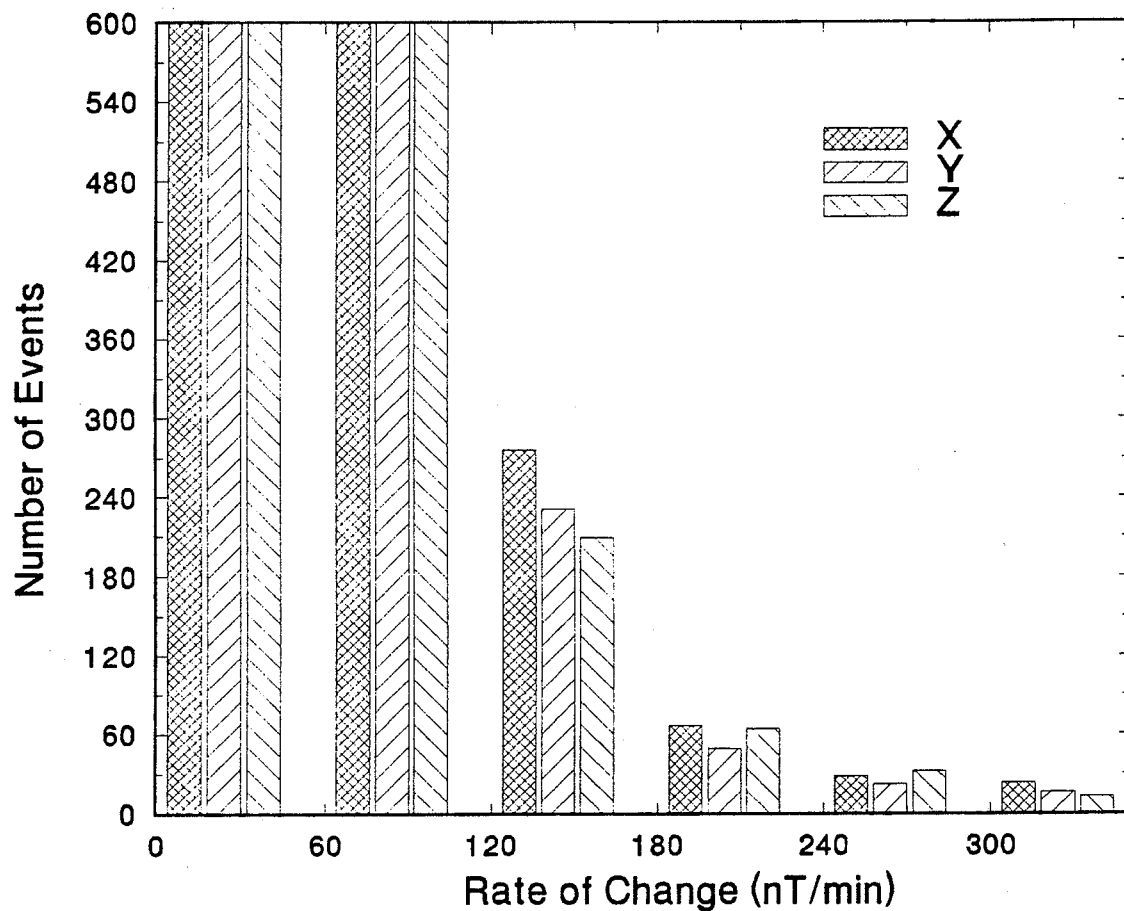
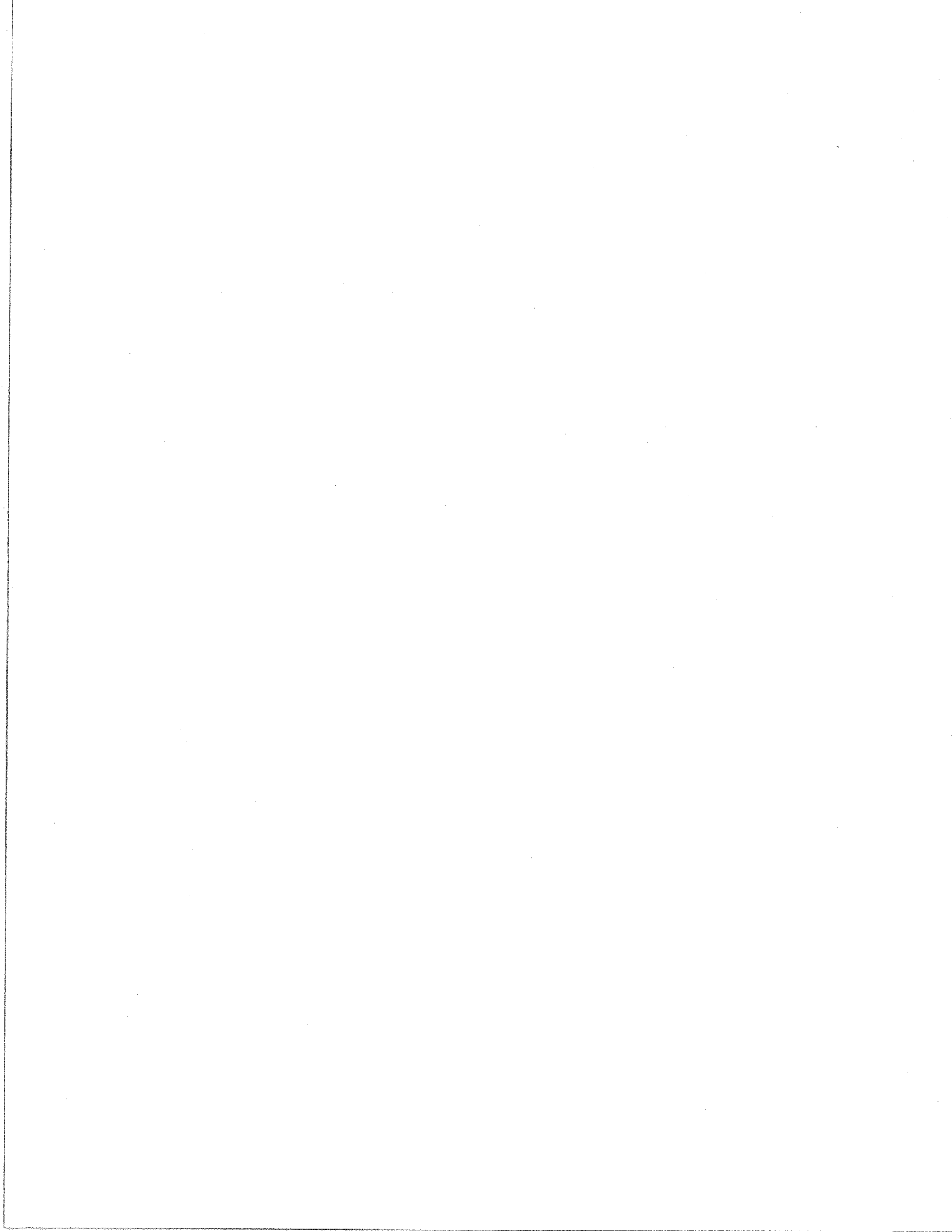


Figure 6 Histogram of the events occurring during one year (1989) at Meanook observatory, within intervals 0-59, 60-119, 120-179, 180-239, 240-299, and 300 and over, nT/min, for each magnetic field component X, Y, and Z. The number of events with rate-of-change in the first interval exceeds 520,000 for all components. The number of events in the second interval exceeds 1200 for all components.

these it was also possible to determine the frequency of occurrence of hours during which defined thresholds were exceeded.

The histogram data were organized in units of hours, months, seasons, and years. This permitted analyses according to time of day, time of year, season, and the solar cycle. The seasons are defined as Equinox (March, April, September, October), Winter (November, December, January, February), and Summer (May, June, July, August).



## 3 RESULTS OF RATE-OF-CHANGE ANALYSIS

### 3.1 INTRODUCTION

In order to summarize a large amount of data in a reasonable number of graphs and figures, decisions were taken concerning threshold levels to be used. For some of the plots, a threshold of 180 nT/min was used to include many lower level events that nonetheless might present problems in some areas. In some other plots, higher thresholds were used, such as 300 nT/min, 420 nT/min and 540 nT/min. Exceedences of these latter two thresholds are very rare, but correspond to some serious problems on power grids.

The 180 nT/min threshold corresponds approximately to levels of activity in the K6 region, using the more familiar K index, for a southern Canada Location. The 300 nT/min threshold falls approximately in the K7 region, and has been used to separate, or highlight, the events most likely to cause serious GIC problems. Further discussion of the relationships between dB/dt and the traditional indices is presented in Section 4 below. The Kp and Ap indices have limitations to their applicability in this context.

In many plots, the values displayed are the number of hours experiencing events within specified limits. In some cases, it is appropriate to express the data also as probabilities of occurrence.

### 3.2 VARIATION OF OCCURRENCE WITH SOLAR CYCLE

Figures 7 (a-k) show, for each observatory, the number of occurrences of dB/dt events equal to or exceeding 180 nT/min for each year, along with the equivalent probabilities. Figure 8 shows the monthly Sunspot Numbers and the Index of Coronal Activity for the same years. Two points emerge from these graphs.

One is the clear variation in the occurrences of dB/dt over the solar cycle, with generally more occurrences near the beginning of the cycle (1977, 1978), a dip near the peak of sunspot activity (1980), and a second broader peak (1982-1986) during the waning phase of the sunspot cycle, but closer to the peak of the coronal activity index. As the latest cycle begins (1988,1989), the occurrences of large dB/dt increase in number again (1988,1989).

The second point is the wide variation in occurrence frequency with latitude. This is developed further in section 3.4.

Table 1 shows the probabilities of occurrence of events equalling or exceeding 300 nT/min, for each observatory for each year, with the probabilities expressed as percentages of the total number of hours in a year.

TABLE 1  
PROBABILITIES OF OCCURRENCE OF HOURS WITH EVENTS  
EQUALLING OR EXCEEDING 300 NT/MIN EXPRESSED AS PERCENTAGES

Obs	77	78	79	80	81	82	83	84	85	86	87	88	89	MEAN
RES	.01	.00	.01	.00	.00	.01	.01	.00	.00	.01	.00	.00	.01	.004
CBB	.04	.03	.00	.01	.01	.02	.06	.08	.11	.05	.05	.02	.00	.038
BLC	.31	.22	.00	.03	.05	.17	.14	.18	.19	.10	.02	.06	.03	.118
YKC	.38	.45	.09	.03	.11	.19	.30	.32	.21	.15	.06	.11	.13	.195
FCC	.35	.34	.22	.01	.16	.21	.31	.30	.29	.16	.06	.17	.18	.212
PBQ	.50	.47	.25	.17	.21	.46	.54	.26	.25	.24	.08	.22	.27	.297
MEA	.19	.38	.11	.05	.14	.27	.14	.06	.06	.06	.01	.16	.24	.143
GLN	.06	.23	.06	.00	.00	.16	.07	.00	.01	.03	.01	.09	.21	.071
OTT	.02	.05	.00	.00	.00	.11	.00	.01	.00	.02	.00	.00	.08	.024
STJ	.01	.01	.00	.00	.00	.02	.00	.00	.00	.01	.00	.00	.02	.006
VIC	.00	.00	.00	.00	.01	.02	.01	.00	.00	.00	.00	.00	.03	.006

Table 1 shows similar variations to those found in Figures 7(a-k). The remaining presentations in section 3 use the 300 nT/min threshold, emphasizing the larger dB/dt occurrences.

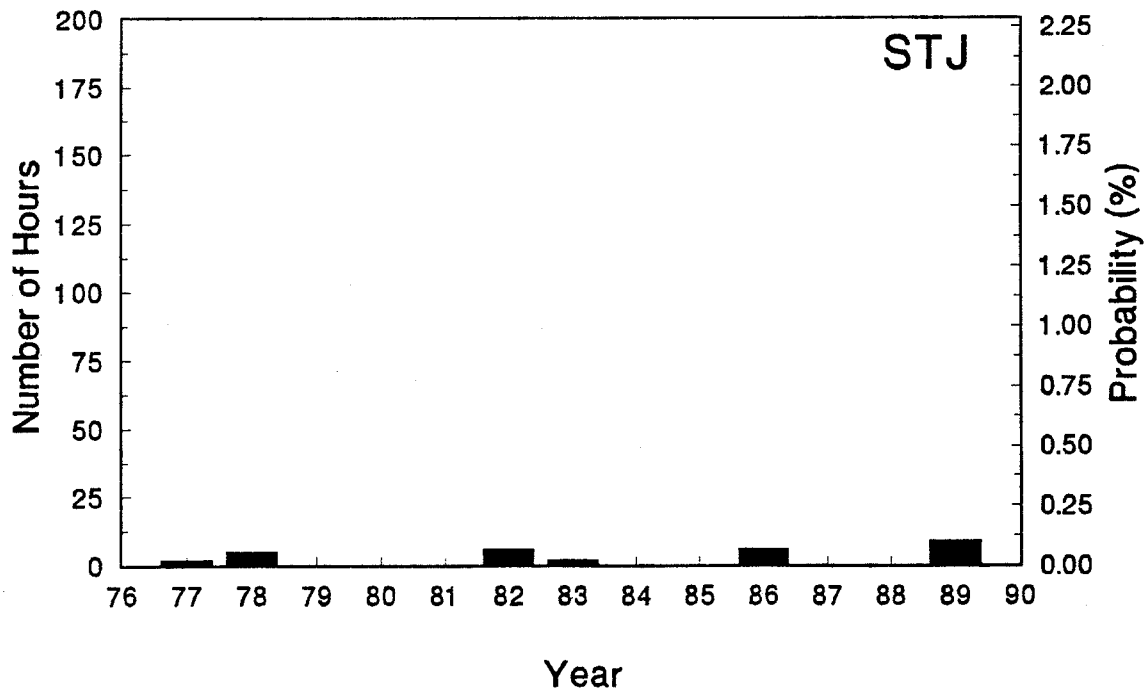
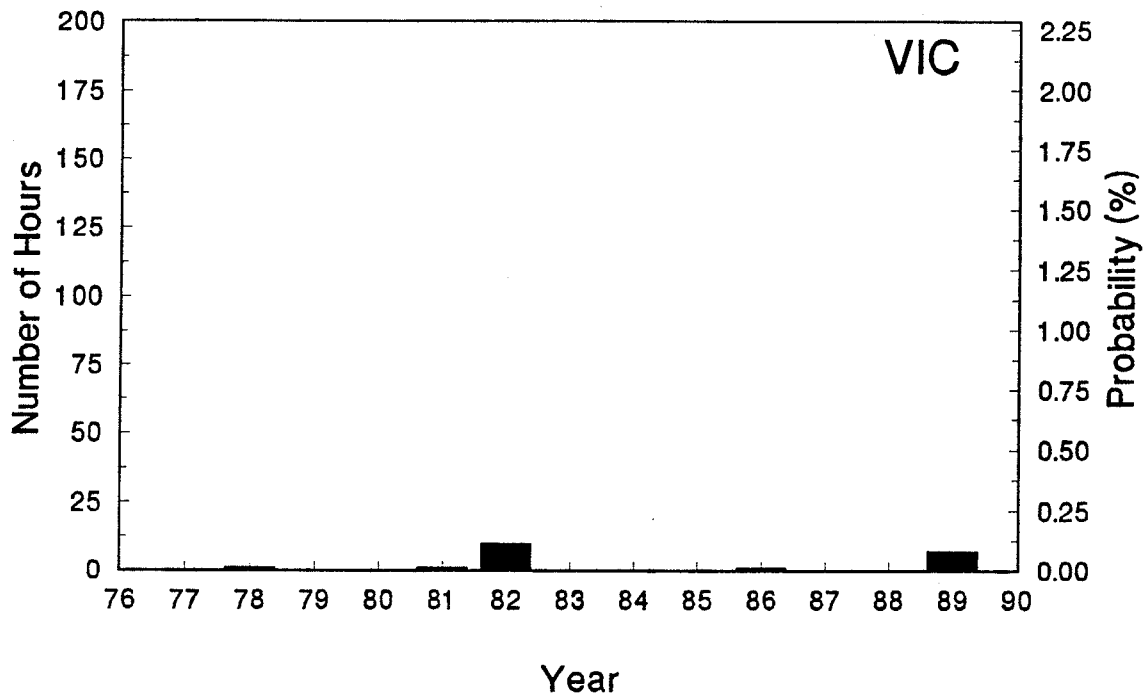


Figure 7a,b The number of hours per year (left scale) and percentage probability (right scale) during which at least one event in any magnetic field component equalled or exceeded 180 nT/min, for each observatory.

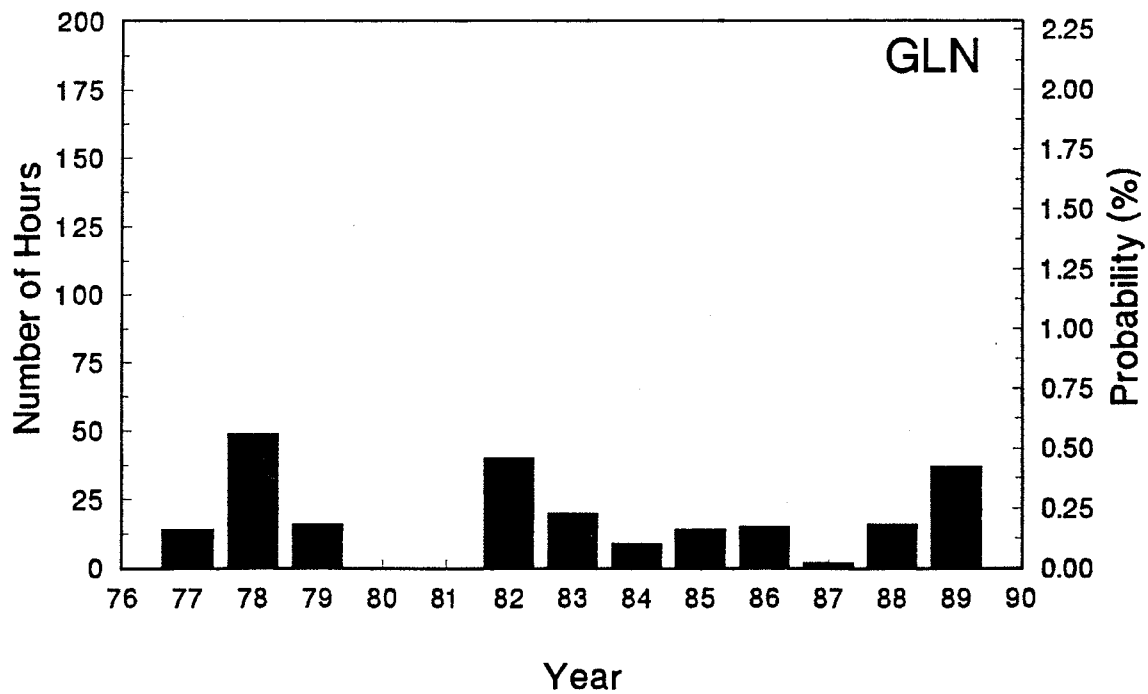
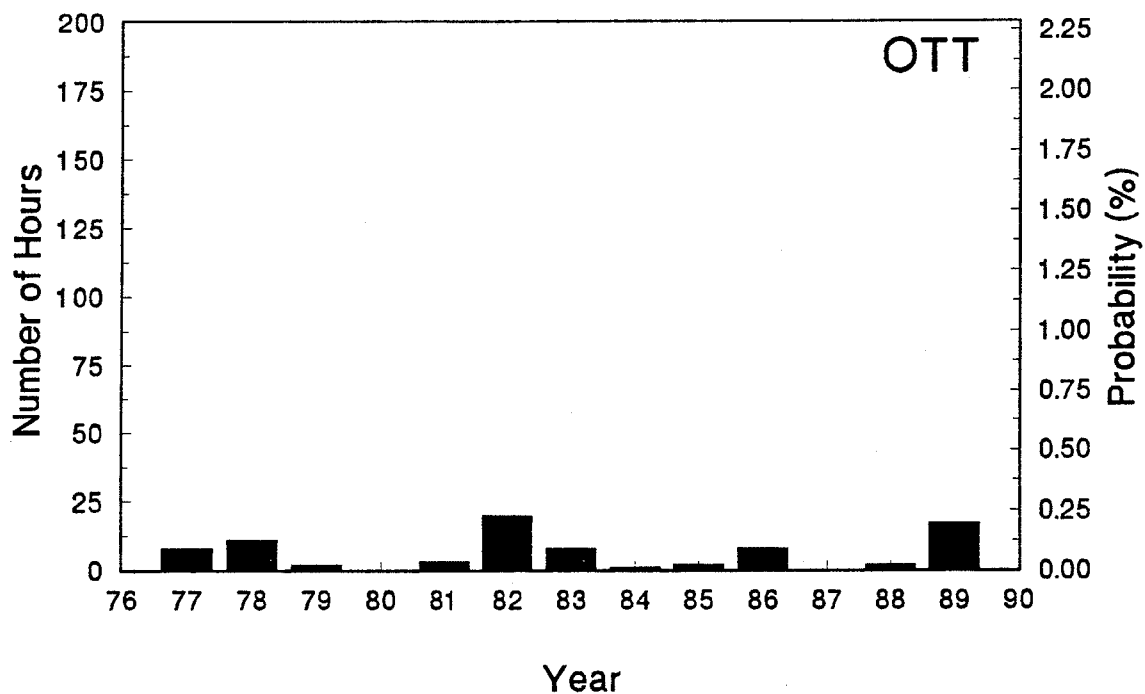


Figure 7c,d The number of hours per year (left scale) and percentage probability (right scale) during which at least one event in any magnetic field component equalled or exceeded 180 nT/min, for each observatory.

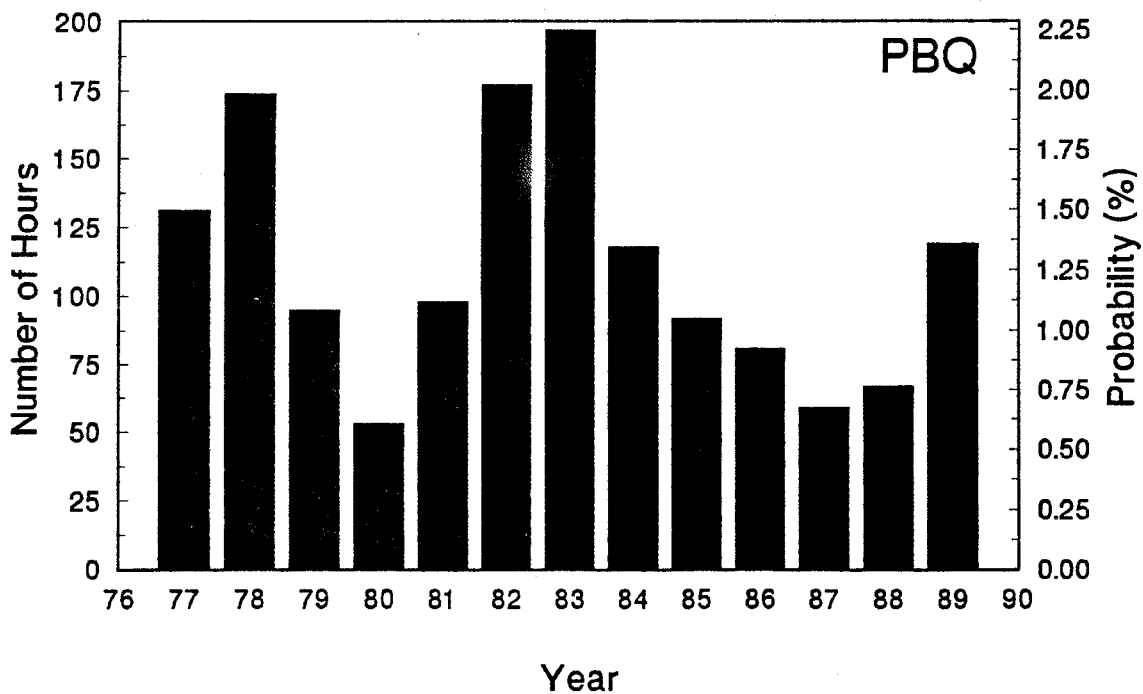
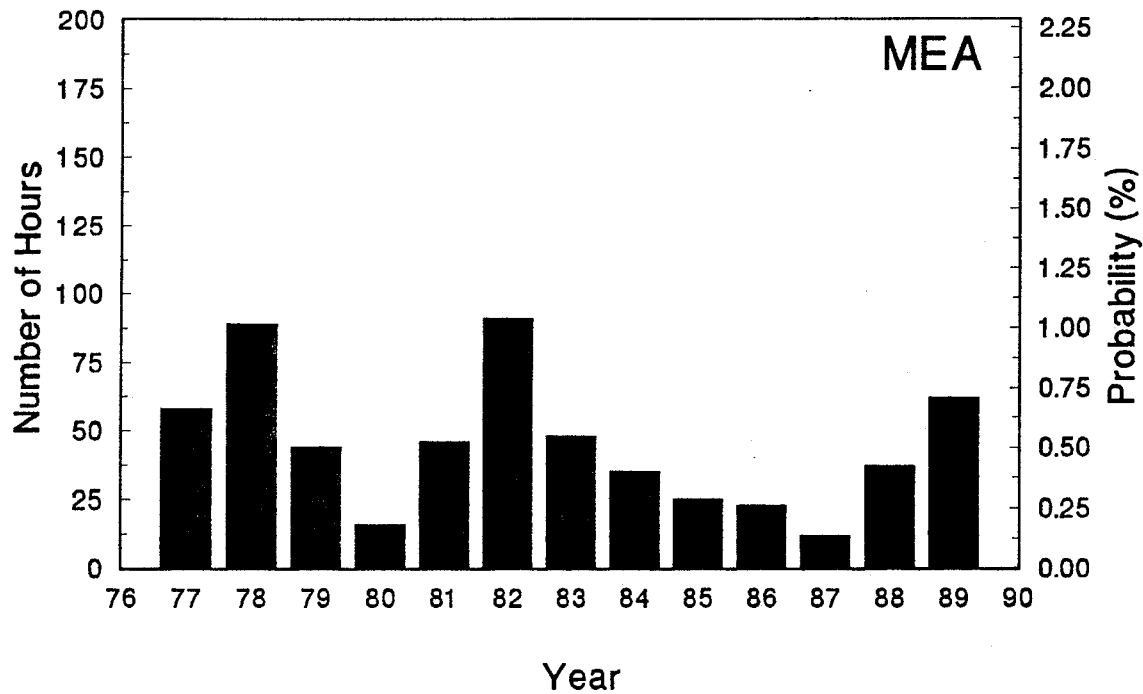


Figure 7e,f The number of hours per year (left scale) and percentage probability (right scale) during which at least one event in any magnetic field component equalled or exceeded 180 nT/min, for each observatory.



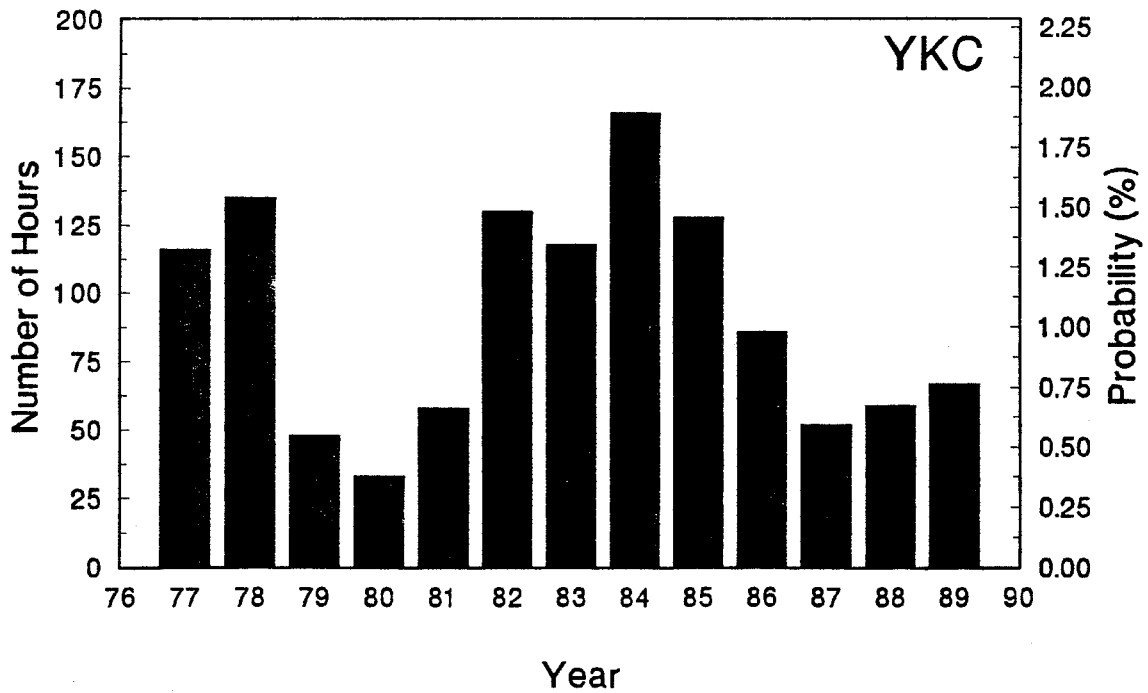
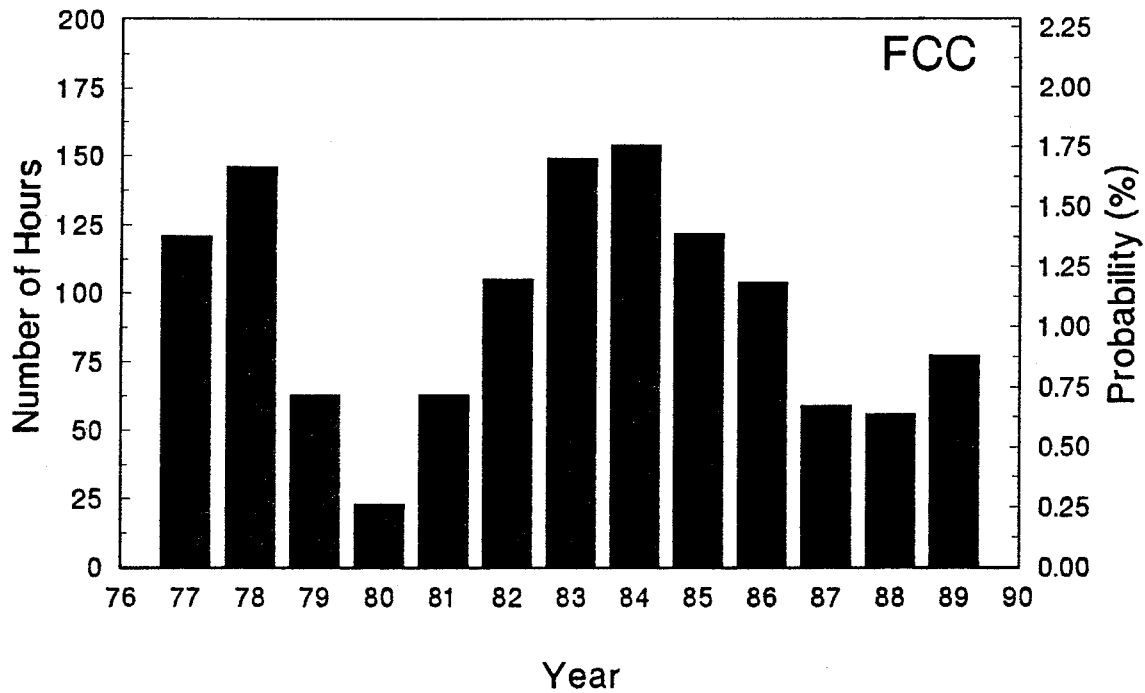


Figure 7g,h The number of hours per year (left scale) and percentage probability (right scale) during which at least one event in any magnetic field component equalled or exceeded 180 nT/min, for each observatory.

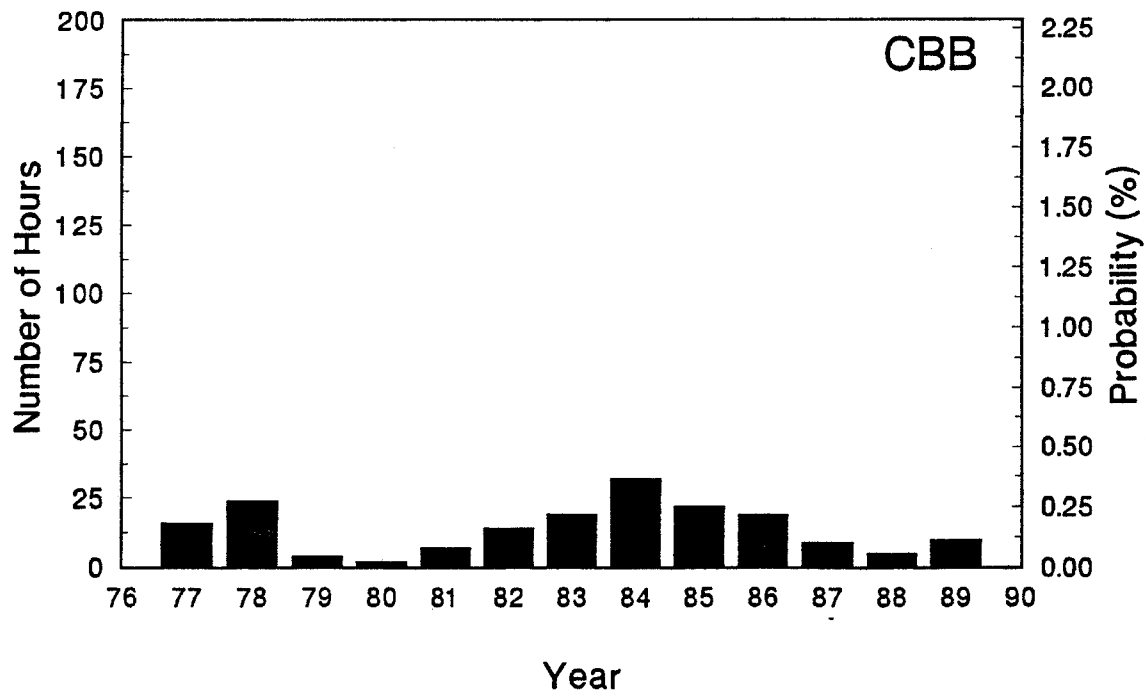
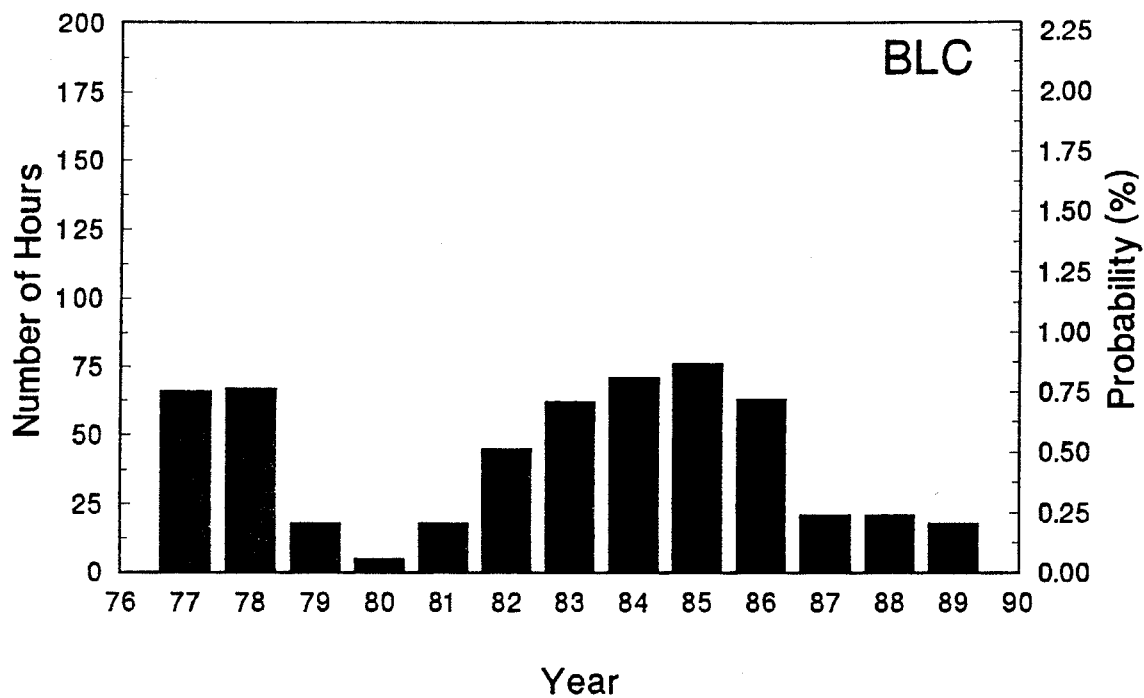


Figure 7i,j The number of hours per year (left scale) and percentage probability (right scale) during which at least one event in any magnetic field component equalled or exceeded 180 nT/min, for each observatory.

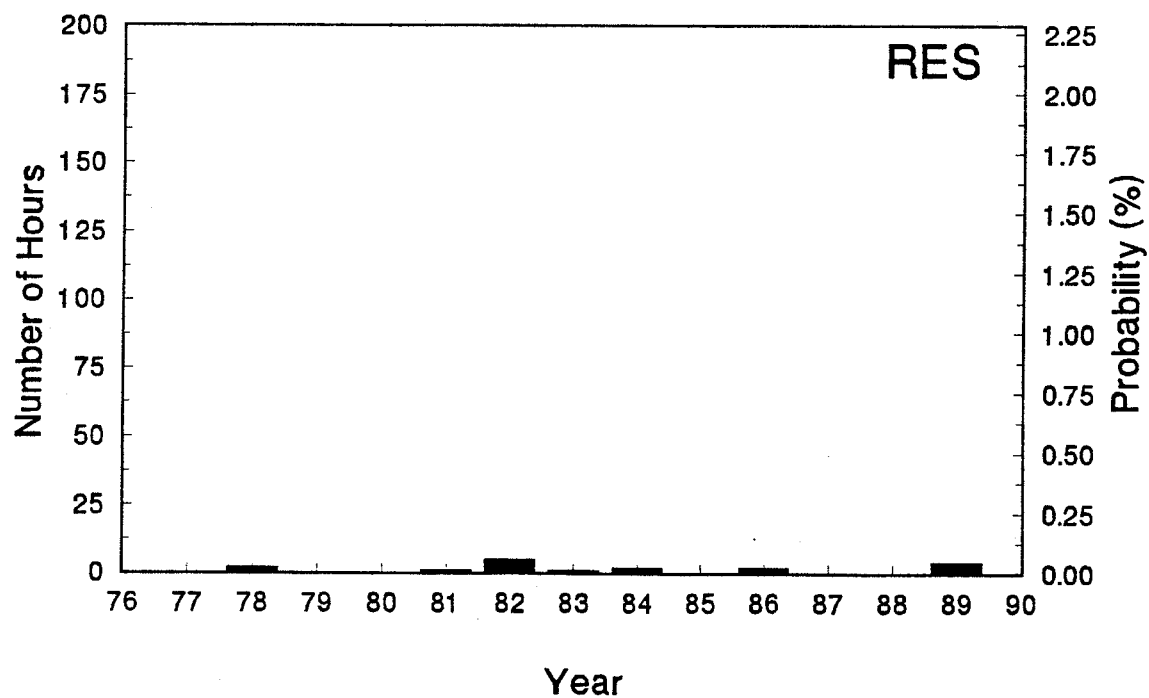


Figure 7k The number of hours per year (left scale) and percentage probability (right scale) during which at least one event in any magnetic field component equalled or exceeded 180 nT/min, for each observatory.

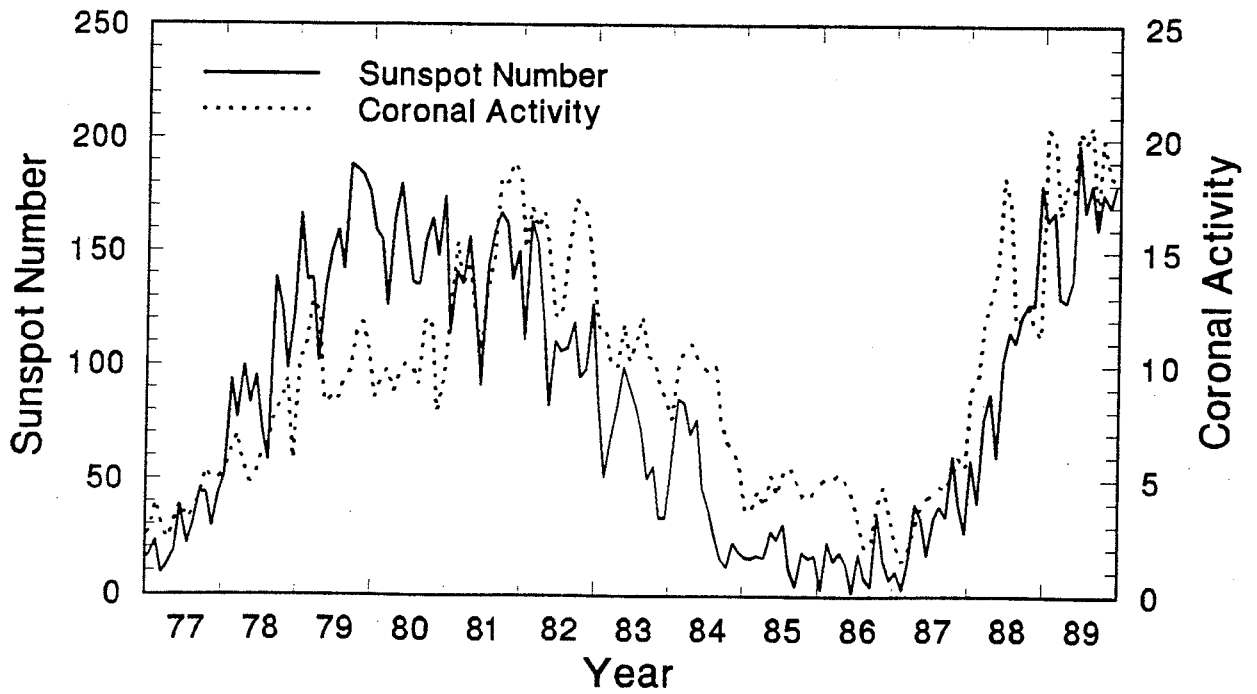


Figure 8 The monthly sunspot numbers and coronal activity index values for the years 1977 to 1989.

### 3.3 VARIATION OF OCCURRENCE WITH SEASON

To examine the typical variation of occurrence throughout the year the number of hours with  $dB/dt > 300$  nT/min each month was determined and the averages calculated for each month over all the years 1977 to 1989. The results, given for some observatories in Figure 9 (a-f), show the same differences in occurrence between observatories as appeared in the previous figures, but also show considerable variability in occurrence from month to month. In this variability, the only consistent feature across all observatories is a low level of occurrence in June. Ottawa shows a peak occurrence in the equinoctial months of March and September, but there is no clear equinoctial peak at the other observatories. To further examine whether there is a seasonal dependence in the occurrence patterns the following results regarding the latitudinal dependence of occurrence are presented separately for equinox, winter, and summer. Equinox includes March, April, September, October. Winter includes November, December, January, February. Summer includes May, June, July, August.

### 3.4 VARIATION OF OCCURRENCE WITH LATITUDE

Figure 10 shows the variation in average occurrence versus latitude, for the three four-month seasons, Equinox, Winter, and Summer. Four different thresholds are shown in the figure. Data for all thirteen years have been combined to form the averages. Graphs for individual years were originally produced; these often showed quite marked differences from season to season. These year-graphs are often highly biased by one or a few major storms. They are included in the Appendix. The averages shown in Figure 10 show no significant differences from season to season. In this figure, the observatories have been ordered according to their invariant geomagnetic latitudes, as discussed in Section 2.1. (Note that FCC and YKC have essentially the same invariant latitude.)

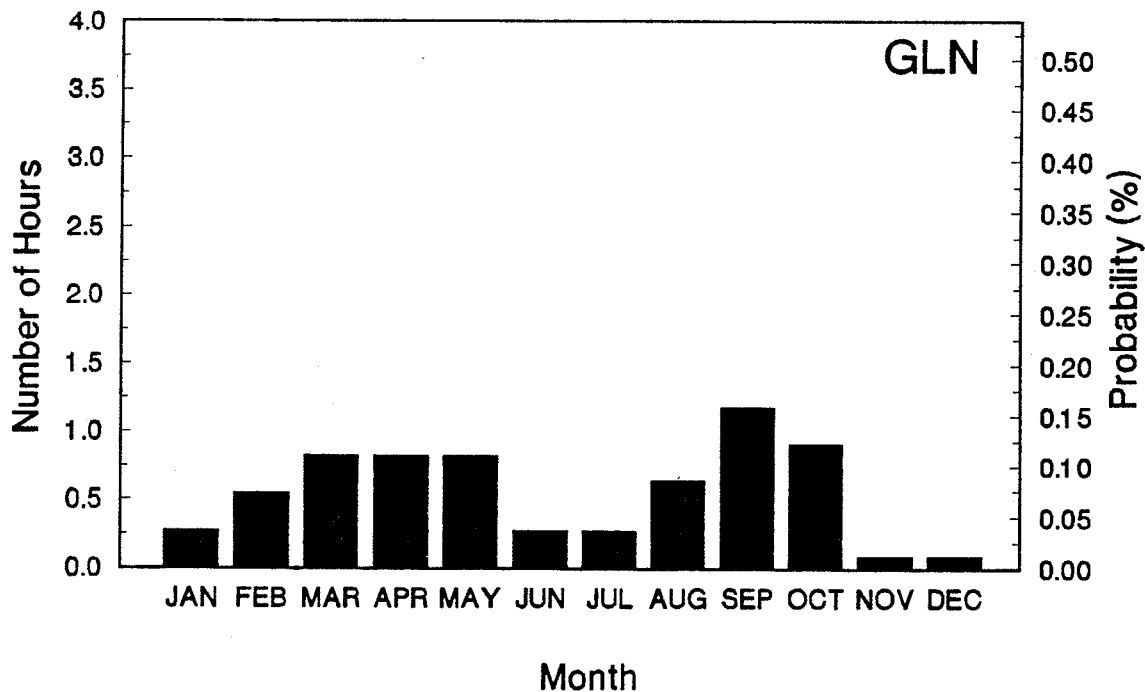
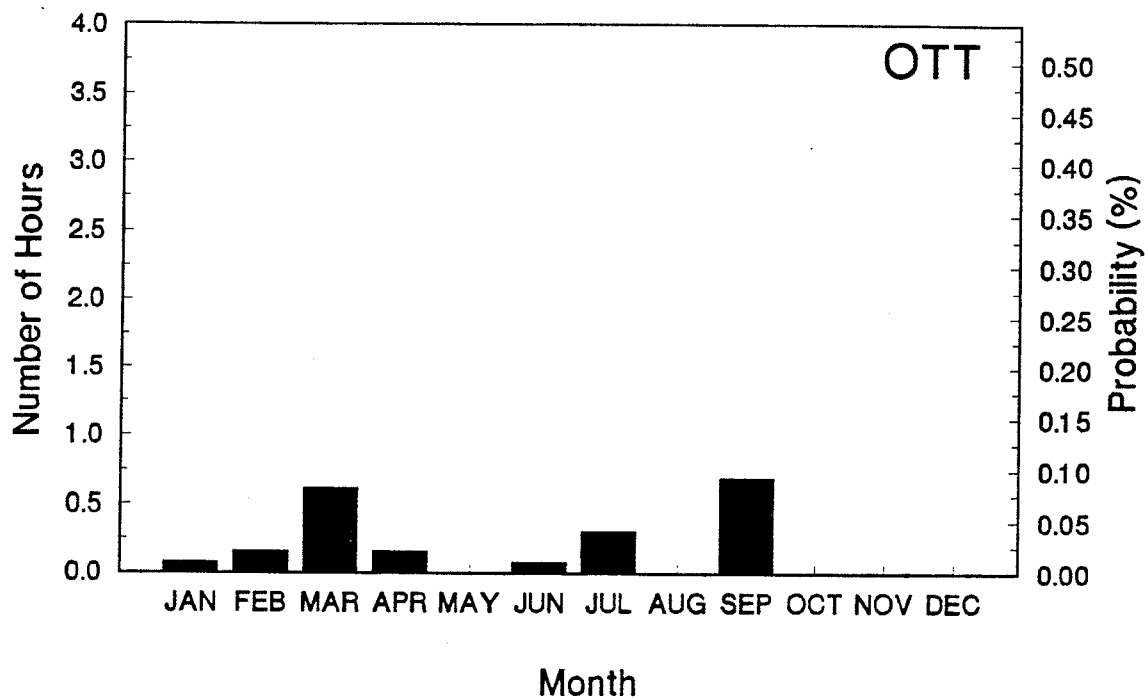


Figure 9a,b The average number of hours (left scale) and percentage probability (right scale) during which at least one event in any component equalled or exceeded 300 nT/min, as a function of month. Only those observatories for which the numbers are appreciable are shown.

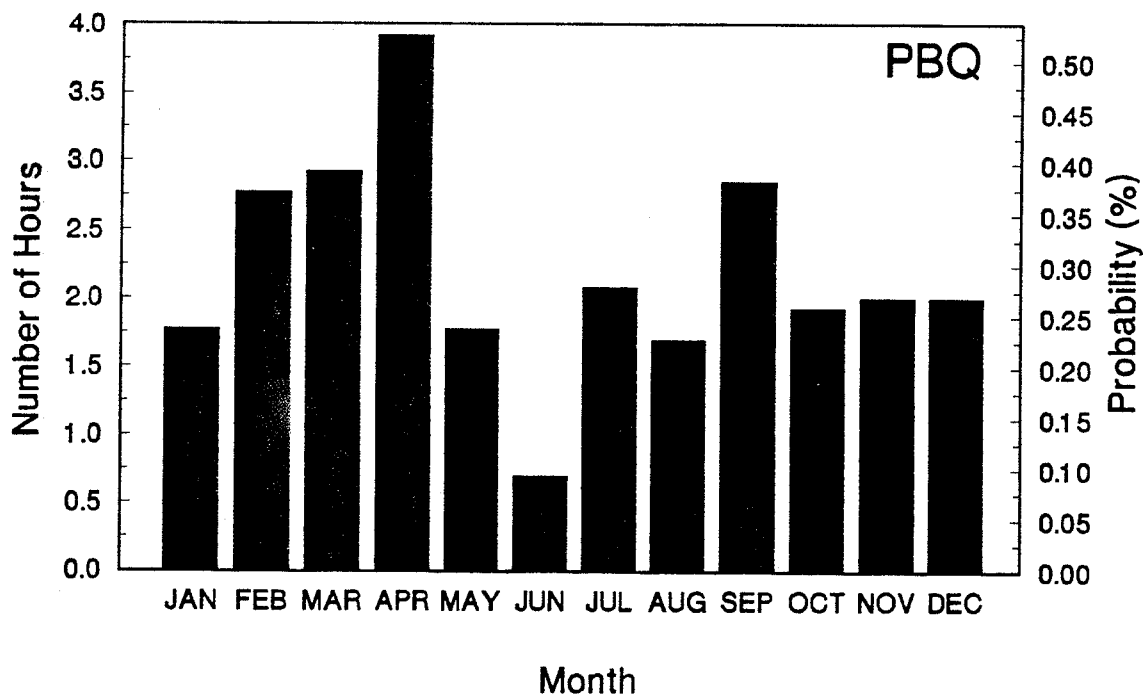
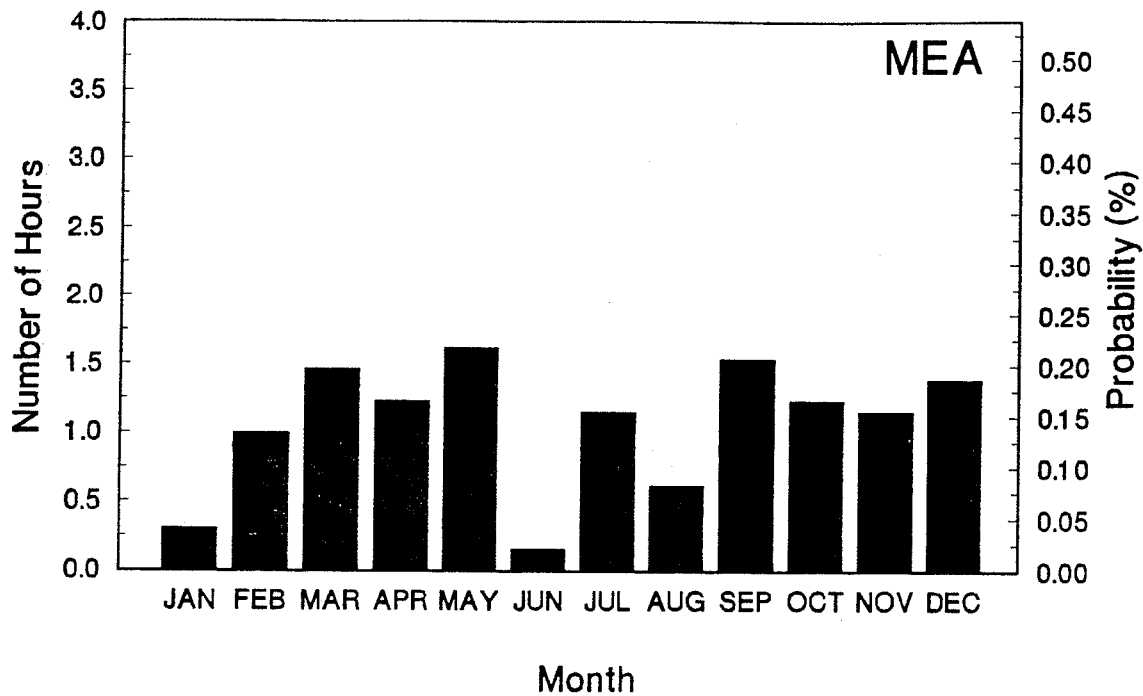


Figure 9c,d The average number of hours (left scale) and percentage probability (right scale) during which at least one event in any component equalled or exceeded 300 nT/min, as a function of month. Only those observatories for which the numbers are appreciable are shown.

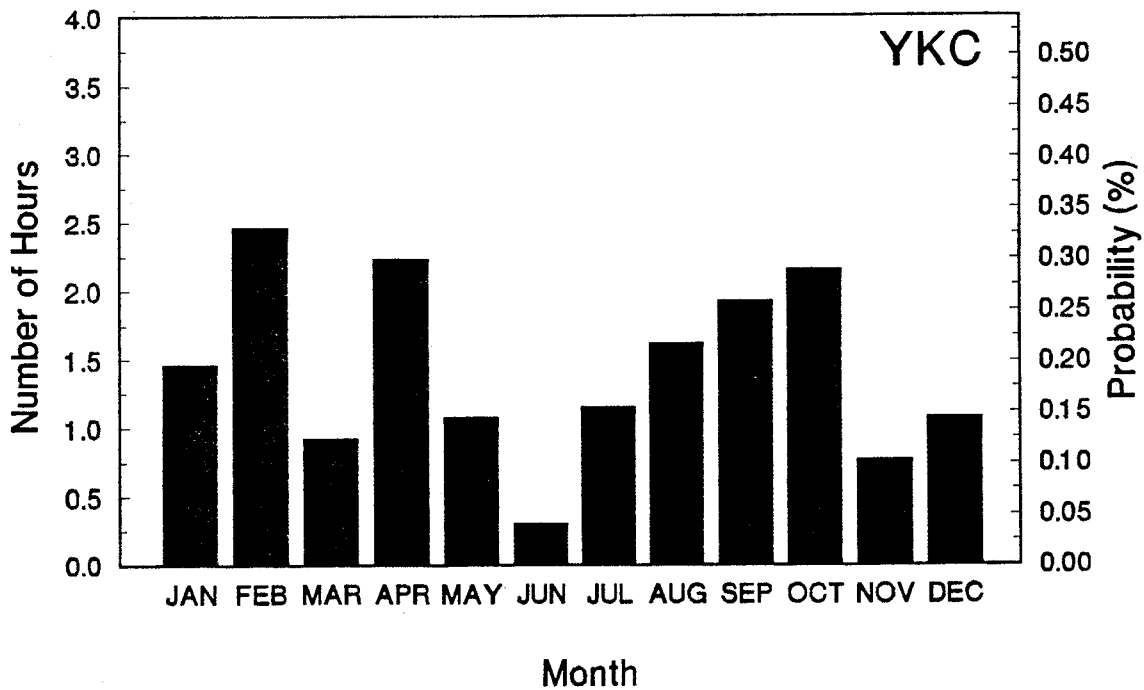
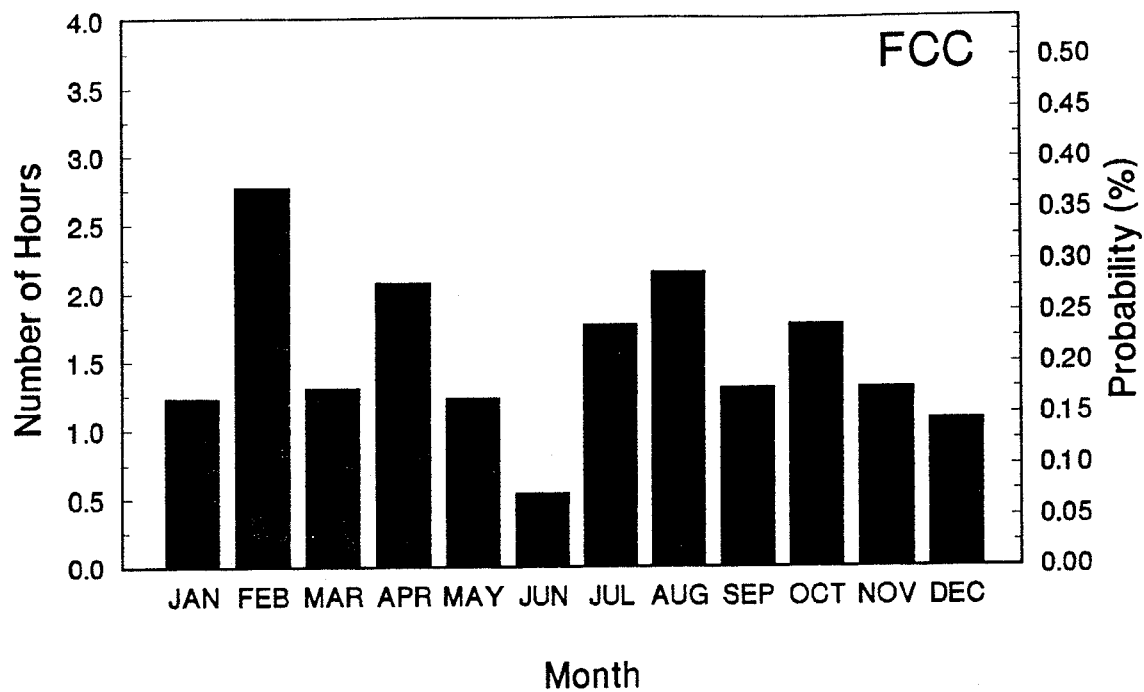


Figure 9e,f The average number of hours (left scale) and percentage probability (right scale) during which at least one event in any component equalled or exceeded 300 nT/min, as a function of month. Only those observatories for which the numbers are appreciable are shown.



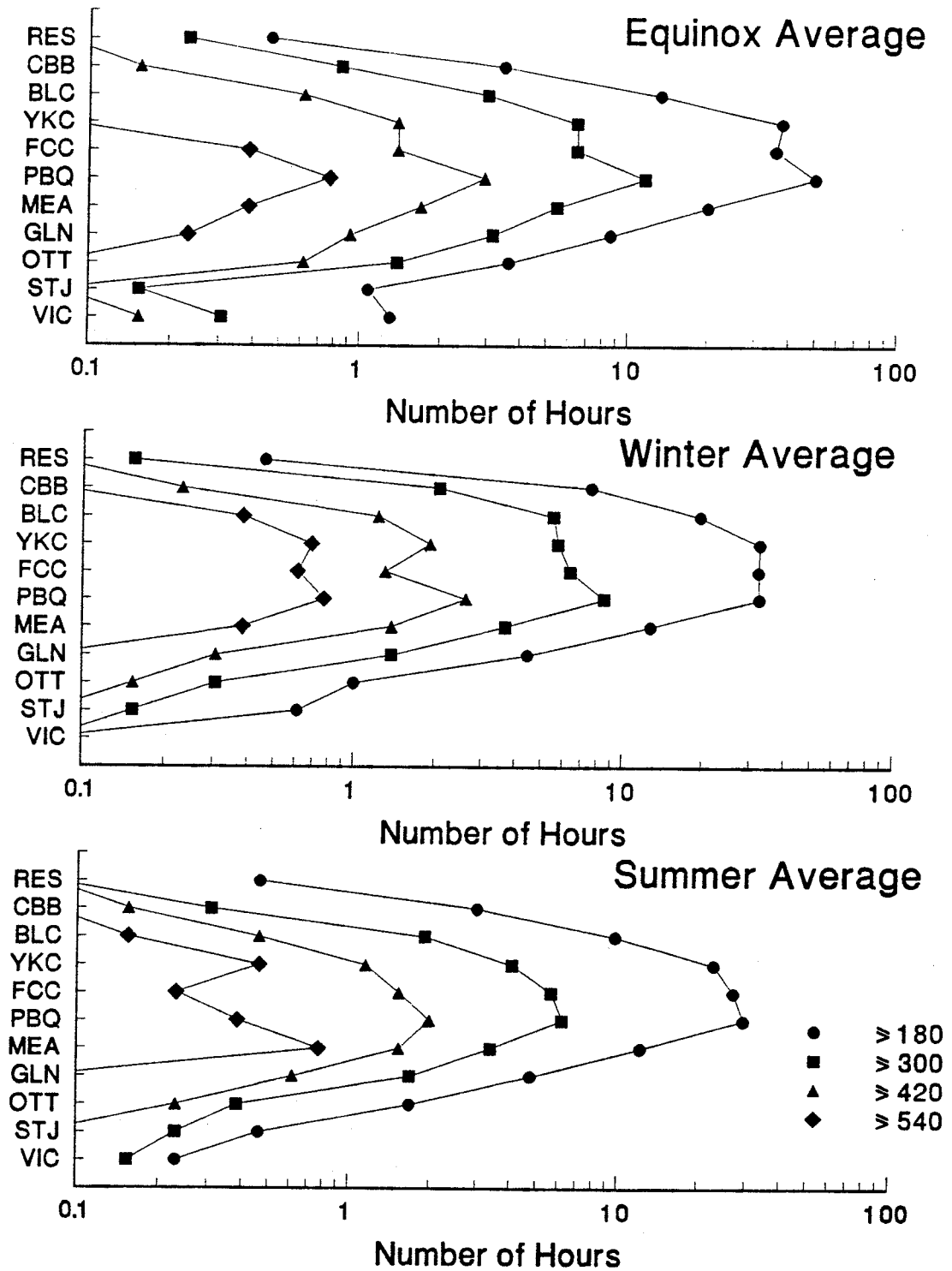


Figure 10 The average numbers of hours per season for which at least one event in any component equalled or exceeded 180 (solid discs), 300 (squares), 420 (triangles), 540 (diamonds) nT/min. Note the logarithmic horizontal scale. On the vertical scale, the observatories are sequenced according to invariant geomagnetic latitude.

The variation in occurrence with latitude can be illustrated by considering two examples. From Figure 10 it can be seen that, during the 4-month Equinox season, PBQ experiences, on average, 10 hours in which dB/dt exceeded 300 nT/min. In contrast, during the same season, OTT experiences, on average, approximately 1 hour in which dB/dt exceeded 300 nT/min.

### 3.5 VARIATION OF OCCURRENCE WITH LOCAL TIME

To determine the variation of activity with time of day (local time) at each observatory, the number of events in the X component of dB/dt > 300 nT/min in each hour was averaged over all years of data. The results, examples of which are presented in Figure 11, show that for most observatories, there is a clustering of events in the evening sector (approximately 1600 to 0100). In addition, from GLN northward into the auroral region, there is a second clustering in the morning sector (approximately 03.00 to 11.00).

This morning activity in the X component is particularly pronounced at MEA, FCC and YKC but is noticeably less at PBQ. Moving northward from the auroral region, at BLC and CBB, the morning peak is much diminished. At RES, in the polar cap, the activity shows a weak concentration in daytime hours.

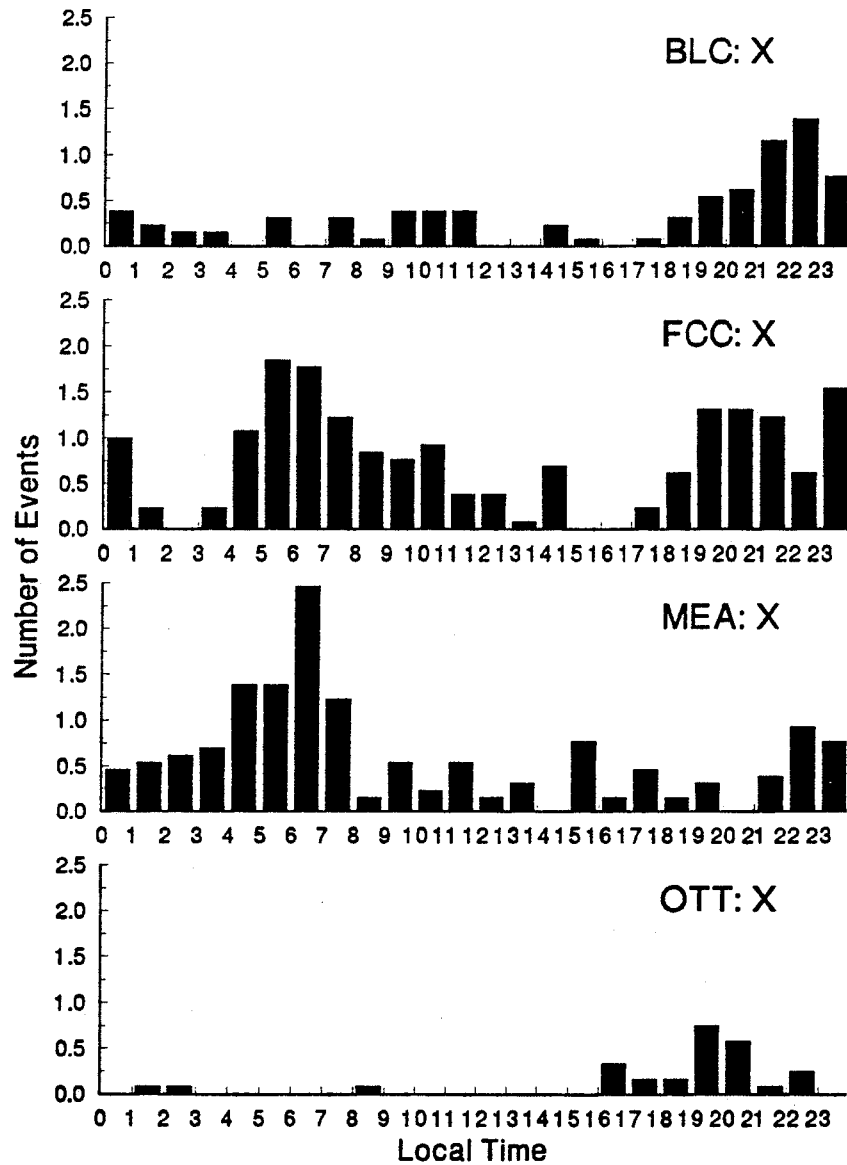


Figure 11 The average numbers of events equalling or exceeding 300 nT/min, for each hour in local time, for the X magnetic field component, for observatories OTT, MEA, FCC, and BLC as examples.

## 4 COMPARISONS OF dB/dt WITH GLOBAL INDICES

### 4.1 THE MAGNETIC INDICES $K_p$ , $a_p$ , and $A_p$

The complex nature of magnetic disturbances and the volume of data to be handled have led to efforts to characterize these disturbances by using indices of activity. The most well-known of these is the  $K_p$  index which is a code indicating the range of the disturbed magnetic field variation in a 3-hour interval. The  $K_p$  index is derived from a combination of  $K$  indices calculated from measurements made at 11 mid-latitude observatories around the world, mostly in the Northern Hemisphere (14). The quasi-logarithmic nature of the code, however, means it cannot properly be used to calculate means or other parameters. In this study, a linear equivalent of the  $K_p$  index is used: namely the  $a_p$  index and its daily mean  $A_p$ .

The occurrence of days with particular  $A_p$  values is shown in Figure 12. The values in the histogram at the left exceed the limits of the scale in order to emphasize the distribution of the occurrences of higher  $A_p$  values. The occurrence of  $A_p$  is shown to have an exponential fall-off with increasing  $A_p$ . Figure 13, using the 3-hour  $K_p$  index, shows that these severe storms (with  $K_p$  of 7, 8, and 9) occur more frequently 3 to 8 years after sunspot minimum (corresponding to sunspot maximum and the five years following). Figure 14 shows that these severe storms occur more frequently in equinoctial months than in summer or winter.

### 4.2 COMPARISONS BETWEEN THE $a_p$ INDEX AND RATE-OF-CHANGE

In this section we examine the relation between rate-of-change values and values of the global  $a_p$  index. The relation between dB/dt measurements at a particular observatory and  $a_p$  is likely to change with the time of day (local time) at the observatory.

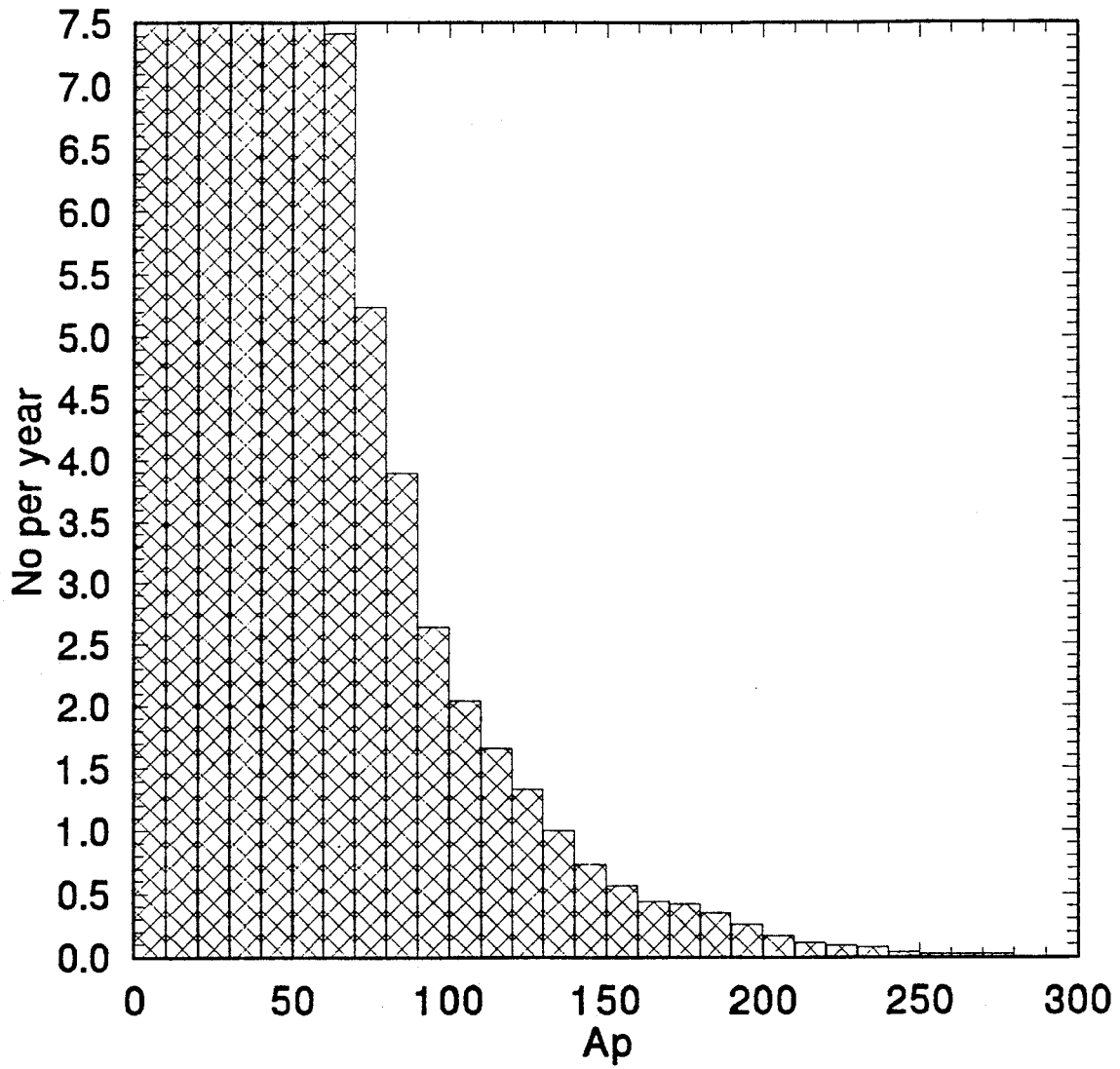


Figure 12 Histogram of the distribution of Ap values, in terms of number per year.

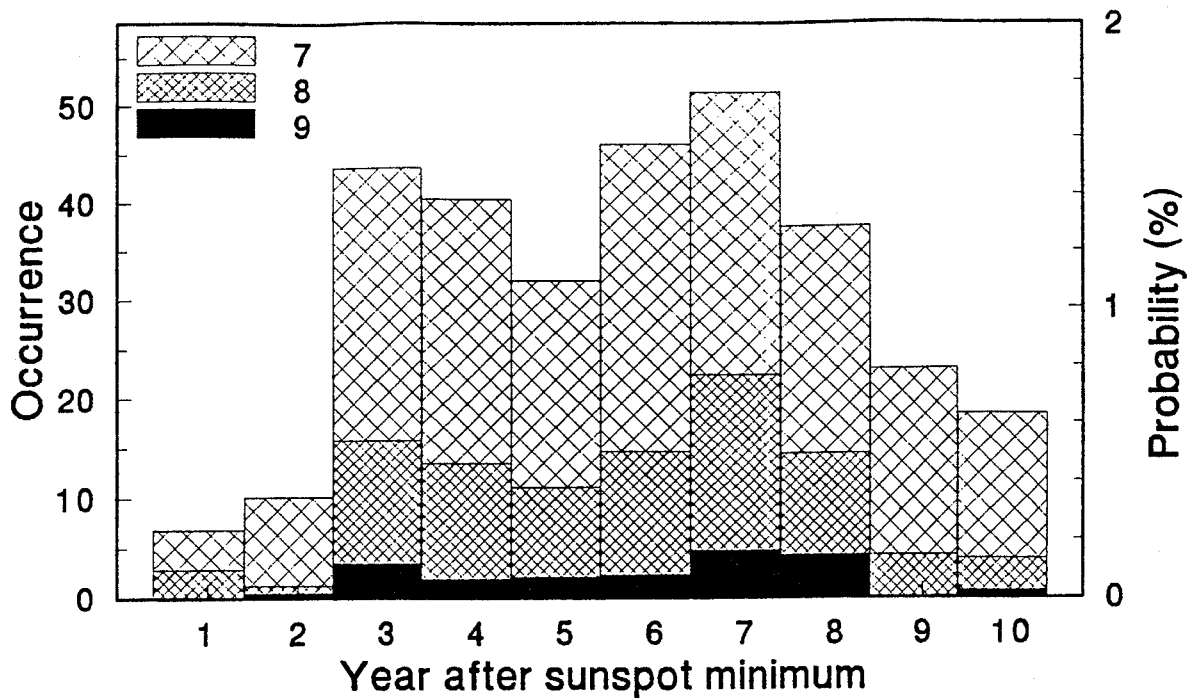


Figure 13 Average occurrence per year (left scale) and percentage probability per year (right scale) for 3-hour intervals with Kp=7, Kp=8, and Kp=9, in terms of number of years after the minimum in the solar sunspot cycle.

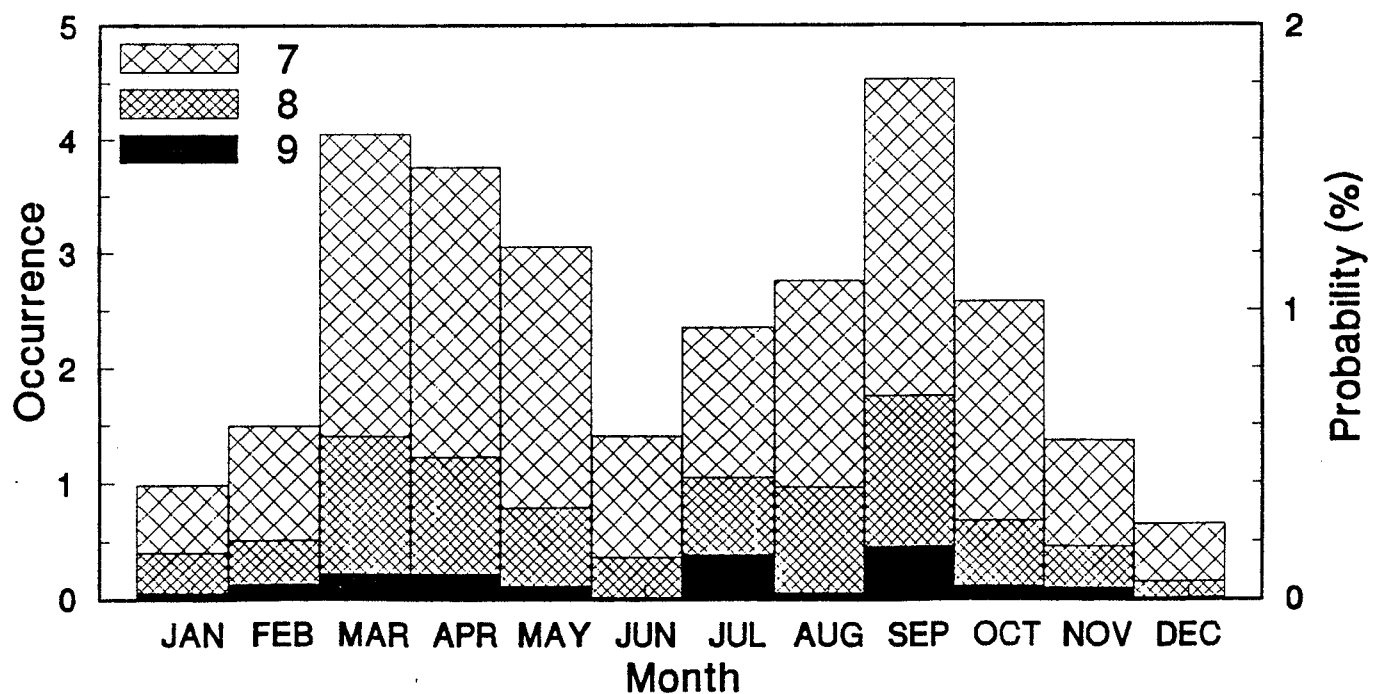


Figure 14 Average occurrence per month (left scale) and percentage probability per month (right scale) for 3-hour intervals with Kp=7, Kp=8, and Kp=9, according to month of the year.

To examine this change, the maximum dB/dt value in each 3-hour interval was compared with the  $a_p$  value for that interval. Examples of these relationships are shown in Figures 15 (the remaining plots can be found in the appendix). These figures are derived from the complete data set for the years 1977 to 1989 inclusive so include many disturbances. On each plot is drawn a regression line showing the best-fit linear relation of dB/dt to  $a_p$ . It will be seen that although there is a consistent trend, as expected, for increasing dB/dt to occur with higher  $a_p$  values, there is considerable scatter about this trend. This scatter is less at the sub-auroral observatories Meanook, Glenlea, and Ottawa, than at the auroral zone observatories Yellowknife, Churchill, and Poste-de-la-Baleine. The better correlation at sub-auroral observatories is not surprising because the  $a_p$  index is derived from mid-latitude observatories (data from both Meanook and Ottawa observatories are used routinely in the production of the global  $K_p$  and  $a_p$  indices); but this relationship deteriorates as one moves to auroral latitudes, as shown by the plot for FCC in Figure 15.

While remembering the scatter, the slopes of the regression lines can be used to give an indication of the mean ratio between the 3-hourly max dB/dt values and  $a_p$  values. Figure 16 shows how these dB/dt- $a_p$  ratios vary with local time. All of the original results in 3-hour UT intervals have been shifted so that local midnight and local noon coincide at all the stations. Also the results have been duplicated over part of a second day so that the complete variation during the night can be seen more easily. This figure shows that when there is a global magnetic disturbance, as measured by  $a_p$ , then the rates-of-change seen at individual observatories vary considerably with the time of day. For a particular  $a_p$  value, the dB/dt values are greater during the evening, night and morning hours than during the daytime. In spite of the large scatter in the regression plots for FCC and PBQ, the diurnal trends seen at these stations show the same pattern as those for the lower latitude stations.

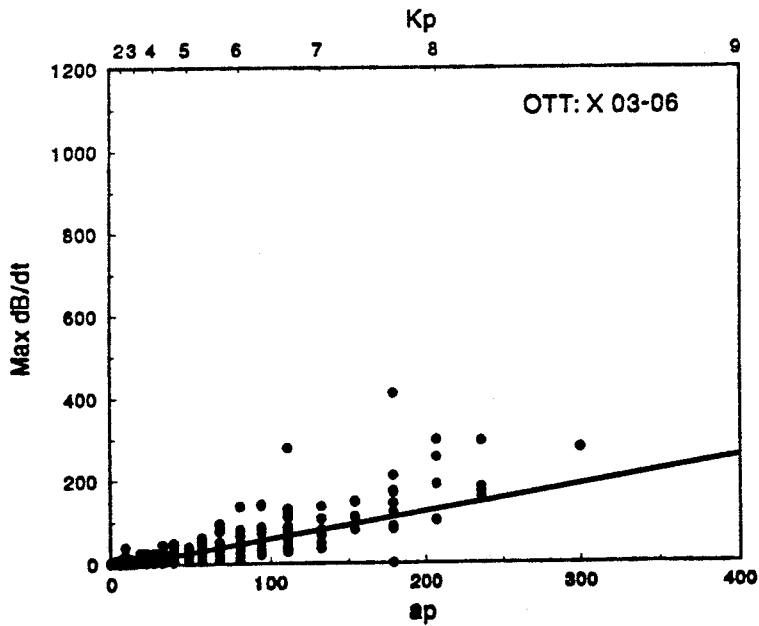
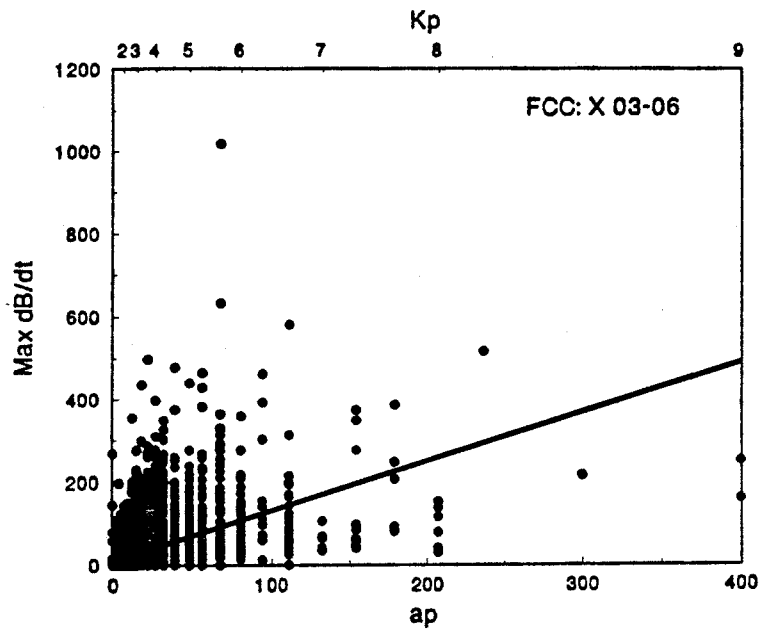


Figure 15 Examples of correlogram of the maximum dB/dt in a three-hour interval versus the ap value for that interval. The equivalent Kp values are noted on the top axis.



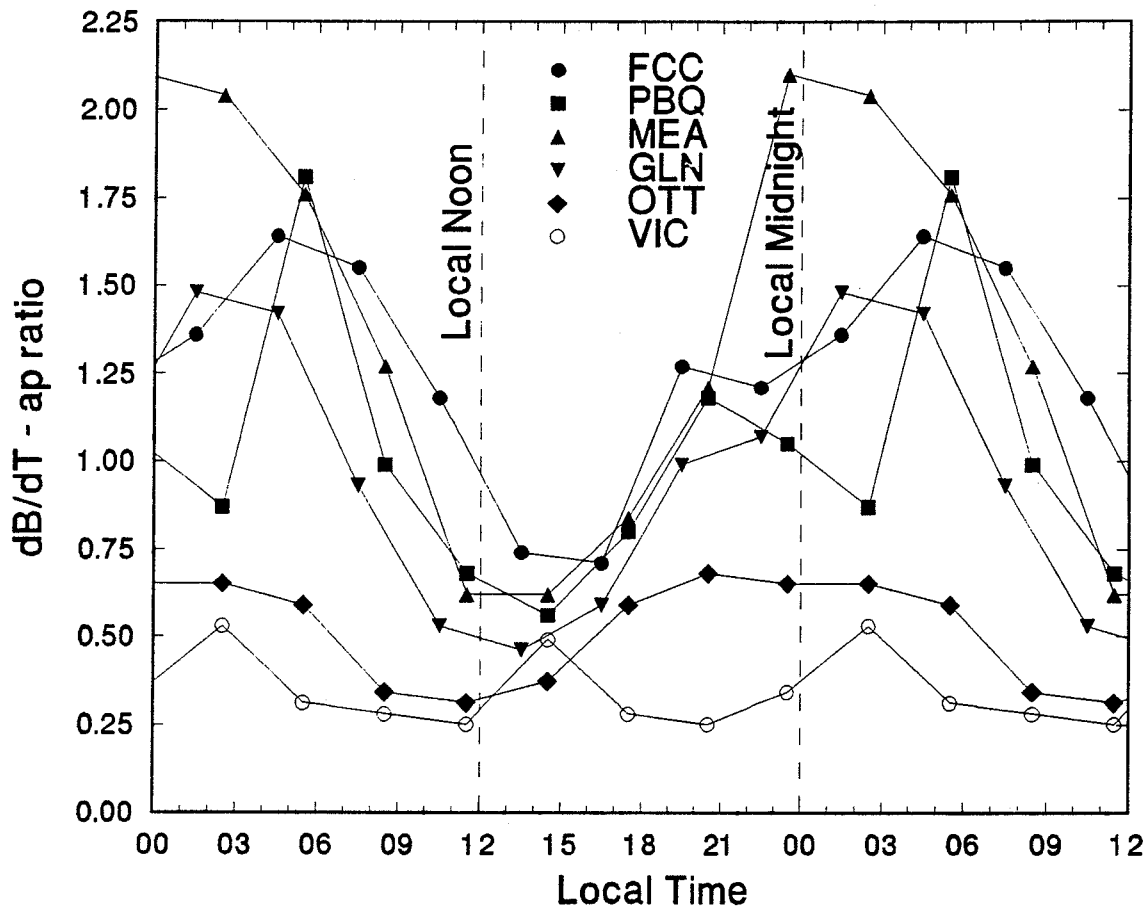


Figure 16 Plots of the slopes of the regression lines derived from the set of correlograms, as shown in Figure 14, for southern observatories, according to local time.

## 5 DISCUSSION AND CONCLUSIONS

### 5.1 INTRODUCTION

There are two types of variations in the occurrence of magnetic field fluctuations:

1. Temporal variations in the occurrence of magnetic disturbances, such as the solar cycle and seasonal effects.
2. Spatial variations in the occurrence of magnetic field fluctuations observed during a magnetic disturbance. The most marked of these is a variation in latitude, but there is also a longitudinal variation that, because of the rotation of the Earth, appears as a variation with local time.

Using the information on these variations, obtained in this study, allows the probability of different levels of geomagnetic hazard to be established for power systems at different locations across Canada.

### 5.2 TEMPORAL VARIATIONS

Solar cycle and seasonal variations are well-known features of the occurrence of large magnetic disturbances (as indicated by magnetic indices such as Kp and ap). However, these variations do not appear clearly in the results from many or all of the observatories in this study. There are several factors that can be said to contribute to this, and several more factors that require further research.

An underlying factor affecting all the results is that the occurrence of magnetic disturbances is essentially a random process. The solar cycle and seasonal variations are only modulations of the underlying random distribution of occurrence. It is expected that over a sufficiently long interval of time a random process will give an even distribution of occurrence. Therefore averaging over enough data will identify the solar cycle and seasonal variations. However, the variation of occurrence during an individual solar cycle or an individual year will show considerable differences from the mean variations. The data from

the Canadian observatories used in this study only cover just over one 11-year solar cycle, and although the seasonal variation results are obtained by averaging over 13 years this is still a short enough interval for the results to be distorted by the values from a few large disturbances.

The occurrence patterns for Kp (Figures 13 and 14), derived from 55 years of data covering 5 solar cycles, more clearly show the solar cycle and seasonal variation of disturbances. However, it is apparent from these plots that both the solar cycle and seasonal variations are predominantly a feature of larger disturbances.

Figure 14 shows the seasonal variation of Kp, with equinoctial peaks in occurrence. A similar pattern is seen at Ottawa (Figure 9) but this seasonal variation disappears as one moves to higher latitudes.

### 5.3 SPATIAL VARIATIONS

There is a distinct change in the occurrence frequency, for all rates-of-change, with invariant latitude. This is due to the position of the observatories relative to the auroral electrojets that are the principal source of the magnetic field fluctuations. Figure 10 can be used to determine the frequency of occurrence of a particular rate-of-change value, as a function of latitude.

Examination of the magnetic fluctuations recorded at the observatories in the Canadian network during several major and severe storms, along with the well-known observation that the region of occurrence of auroras expands southwards during such storms, has led to the idea that the peak occurrence of high dB/dt events may also move significantly southward. This suggestion has been pursued in this study for a few outstanding storms. However, the number of such storms is very small, and there are not enough within the interval of study (1977-1989) to permit a sound statistical statement. Nonetheless, the results are presented here. The storms examined all contained at least one 3-hour interval with a K9 level of activity. This amounts to five storms in the 13 year period from 1977 to 1989.

The storms selected are:

July 13-14 1982  
Sept 5,6,7 1982  
Feb 7,8,9 1986  
Sept 11,12 1986  
Mar 13,14 1989

Only the observatories from FCC southwards have been examined in detail for this purpose.

TABLE 2  
OCCURRENCES OF LARGE dB/dt DURING K9 STORMS

Observatory	No. of hours with dB/dt exceeding	
	180 nT/min	300 nT/min
FCC	45	15
PBQ	47	21
MEA	49	22
GLN	40	13
OTT	29	13
STJ	13	7
VIC	13	3

Note: The numbers above cannot be expressed in terms of frequency or probability, since there is no standard length of storm against which to compare.

Table 2 shows the occurrences of high dB/dt during these five storms. It is evident that at observatories such as MEA, GLN, and OTT, the numbers of occurrences have increased relative to those at PBQ and FCC, when compared to the average latitudinal profile graphs shown in Figure 10 in Section 3.3. Clearly there is a relatively increased occurrence of hours during which there are high dB/dt for the more southerly observatories, particularly MEA, GLN, and OTT. This suggests that during the rare severe storms the geomagnetic hazard is relatively greater for the lower latitude regions of the country than that indicated in the averaged graphs.

The occurrence of magnetic field fluctuations also shows a distinct variation with local time (see Figure 11), with most activity occurring in the morning or evening. This effect is really a longitudinal variation in occurrence due to the changing proximity of the observatories to the eastward and westward electrojets that occurs both in the evening and morning sectors. Electrojet activity may persist for some time in these sectors but only produce magnetic variations at an observatory when the rotation of the Earth carries the observatory into that sector. Because the electrojets are approximately fixed in space relative to the Sun-Earth direction, the magnetic variations they produce are seen when observatories are in the corresponding local time positions.

#### 5.4 GEOMAGNETIC HAZARD

Maximum rate of change in an hour has been chosen as the most appropriate index of the magnetic activity that may induce significant GIC in power systems. The occurrence of hours with high dB/dt values increases considerably as one goes north to the auroral regions and then shows a decrease as one moves from the auroral region to the polar cap. These results, obtained from observatories spread across all of Canada, show a well-ordered variation with invariant latitude. Thus the expected occurrences at any site across Canada can be found by reference to the results for the invariant latitude of the site. For example, for sites with an invariant latitude equivalent to that of Meenook magnetic observatory the probability of occurrence of an hour with maximum dB/dt equal to or greater than 300 nT/min is 0.14% (see Table 1 and Figure 4). Reference to Table 1 and to the figures in section 3 will provide indications of the variability about this average probability.

Maps have been created to provide a visual indication of geomagnetic hazard across Canada. Figure 17 shows averaged probability of the occurrence of an hour during which dB/dt will equal or exceed 300 nT/min. Figure 18 provides an indication of geomagnetic hazard during more active years.

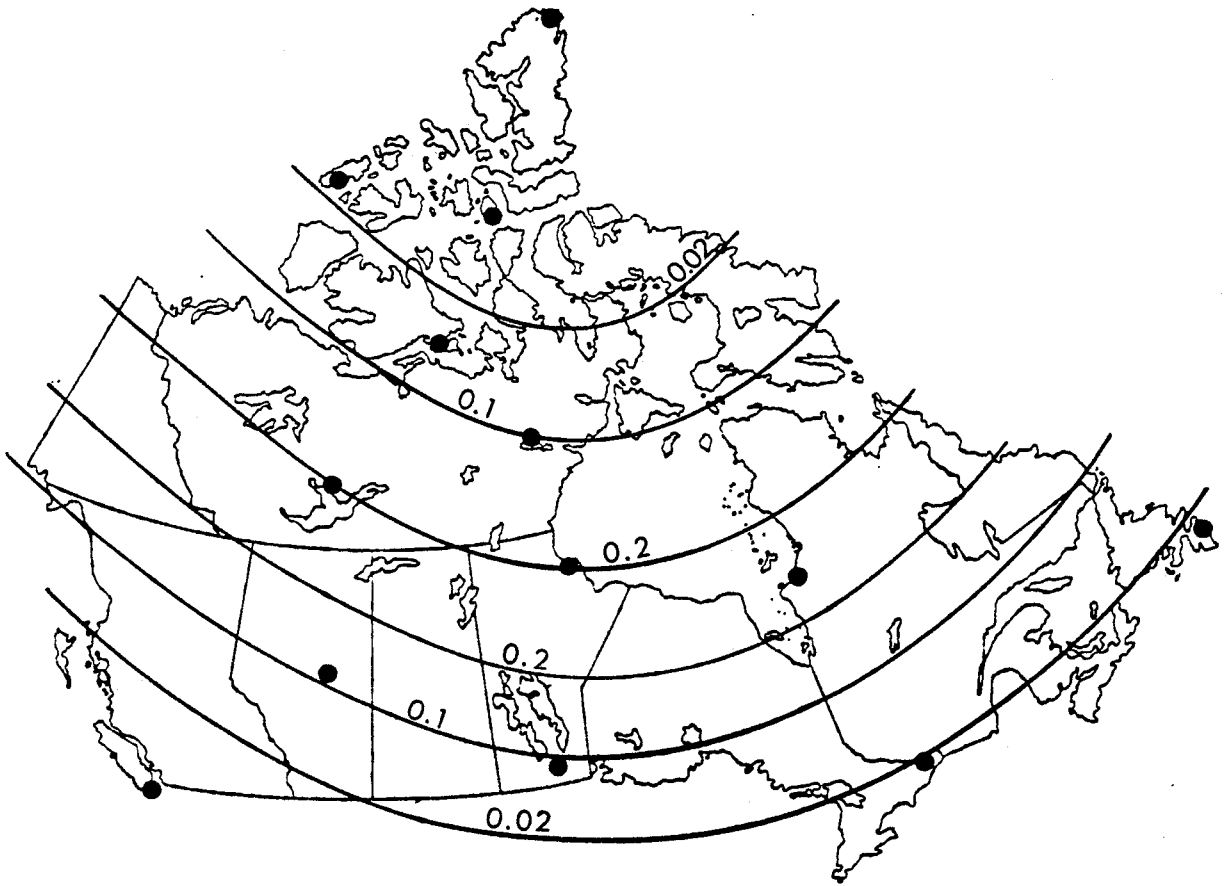


Figure 17 Map of average geomagnetic hazard, expressed as the percentage probability of occurrence of an hour during which dB/dt will equal or exceed 300 nT/min.

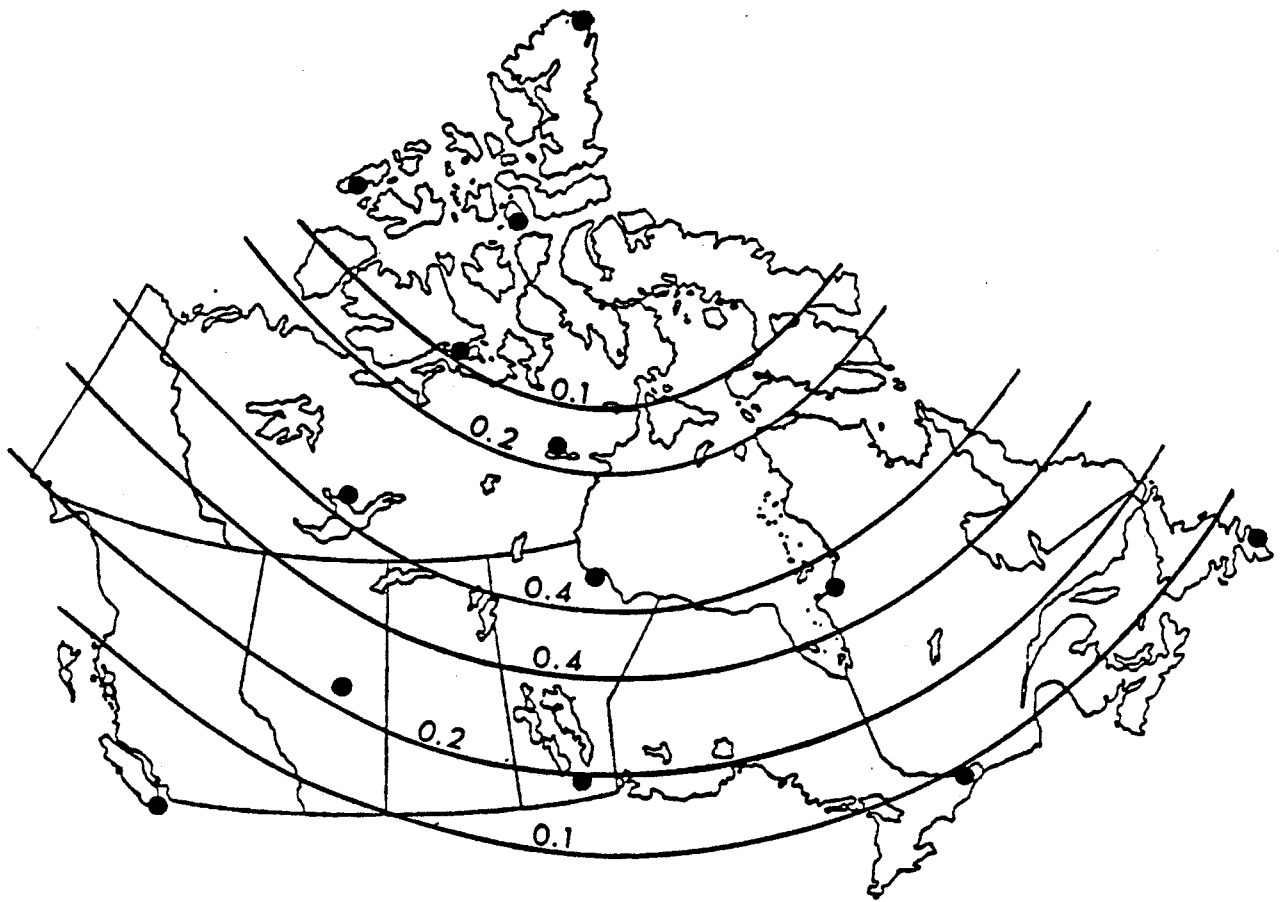
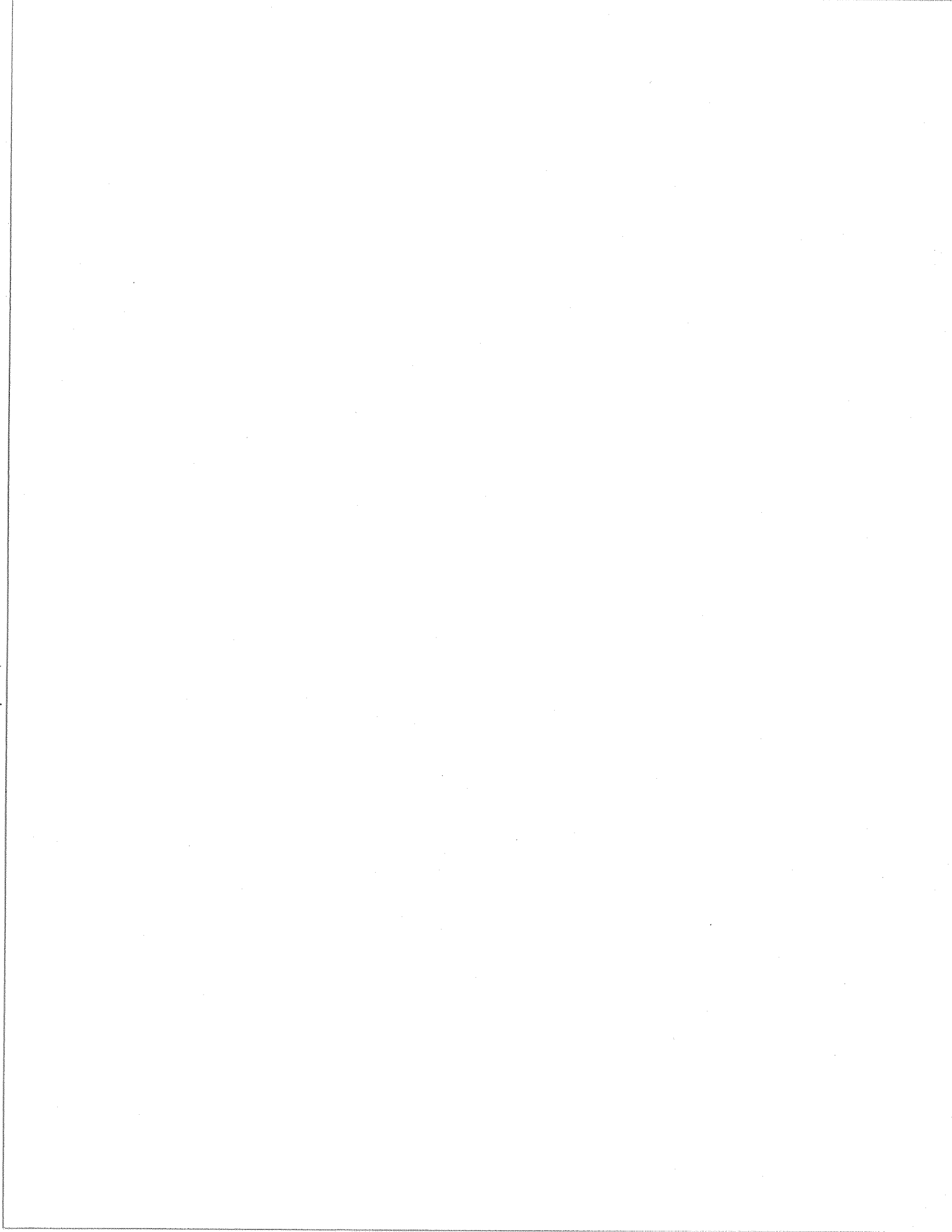


Figure 18 Map of geomagnetic hazard for more active years, expressed as percentage probability of occurrence of an hour during which  $dB/dt$  will equal or exceed 300 nT/min.

## 5.5 RECOMMENDATIONS FOR FUTURE WORK

Hourly maximum dB/dt values, used in this study, provide a convenient index of the level of higher frequency magnetic activity that may lead to power system problems. However the actual GIC produced during a geomagnetic disturbance depend, in a complicated way, on the frequency content of the magnetic field variations, the conductivity structure of the Earth, and the configuration of the power system. We recommend a study be made of the frequency content of the magnetic field variations and of the conductivity structure of the Earth. This will enable calculation of the electric fields produced during geomagnetic disturbances. Such electric field values can be used as input to a power system model to determine the distribution of geomagnetically induced currents (GIC). Combined with the geomagnetic hazard statistics determined in this study, these calculations will show the probability of GIC exceeding particular levels. Validation of the assumptions made in the modelling of the electric fields and GIC should be made by comparison of the calculated GIC values with actual measured GIC values from a number of power systems.





## 6 REFERENCES

1. Maguire, T., Woodford, D. "Geomagnetic Induced Current Effect on SVDC Operation," Canadian Electrical Association, Report 316 T 745, 1990.
2. Loomer, E.I., Whitham, K. "On Certain Characteristics of Irregular Magnetic Activity Observed at Canadian magnetic Observatories during 1960," Publications of the Earth Physics Branch, Ottawa, Vol. 27, no. 2, 1963.
3. Whitham, K., Loomer, E.I., Niblett, E.R. "The Latitudinal Distribution of Magnetic Activity in Canada," Jour. Geophys. Res., Vol. 5, p.3961-3974, 1960.
4. Loomer, E.I., Jansen van Beek, G. "The Effect of the Solar Cycle on Magnetic Activity at High Latitudes," Publications of the Earth Physics Branch, Ottawa, Vol. 32, no. 6, 1969.
5. Coles, R.L., Thompson, K., Jansen van Beek, G. "Comparisons between Changes in the Geomagnetic Field and the Geomagnetically Induced Currents in a Power Transmission System," presented at the IEEE T&D Conference and Exposition Panel #25 Session on Geomagnetically-Induced-Current (GIC) Effects on Electric Power Systems, Dallas, Texas, 1991.
6. Coles, R.L., Thompson, K., Jansen van Beek, G. "A Comparison between the Rate of Change of the Geomagnetic Field and Geomagnetically Induced Currents in a Power Transmission System," Proceedings: Geomagnetically Induced Currents Conference, TR-100450, Electric Power Research Institute, Palo Alto, California, p. 15.1-15.8, 1992.
7. Coles, R.L., Jansen van Beek, G., Newitt, L.R. "Annual Report for Magnetic Observatories and Repeat stations - 1985," GSC Paper 86-25, Geomagnetic Series no. 31, 1987.
8. Hruska, J., Coles, R.L. "A New Type of Magnetic Activity Forecast for High Geomagnetic Latitudes," J. Geomagn. Geoelectr., Vol. 39, p. 521-534, 1987.
9. Andersen, F. "An Automatic Magnetic Observatory System," Publication of the Earth Physics Branch, Ottawa, Vol. 44, no. 11, 1974.
10. Trigg, D.F., Nandi, A. "The Automatic Magnetic Observatory System AMOS III," Earth Physics Branch, Geomagnetic Series, no. 27, 1984.
11. McIlwain, C.E. "Coordinates for Mapping the Distribution of Magnetically Trapped particles," Jour. Geophys. Res., Vol. 66, p. 3681-3691, 1961.

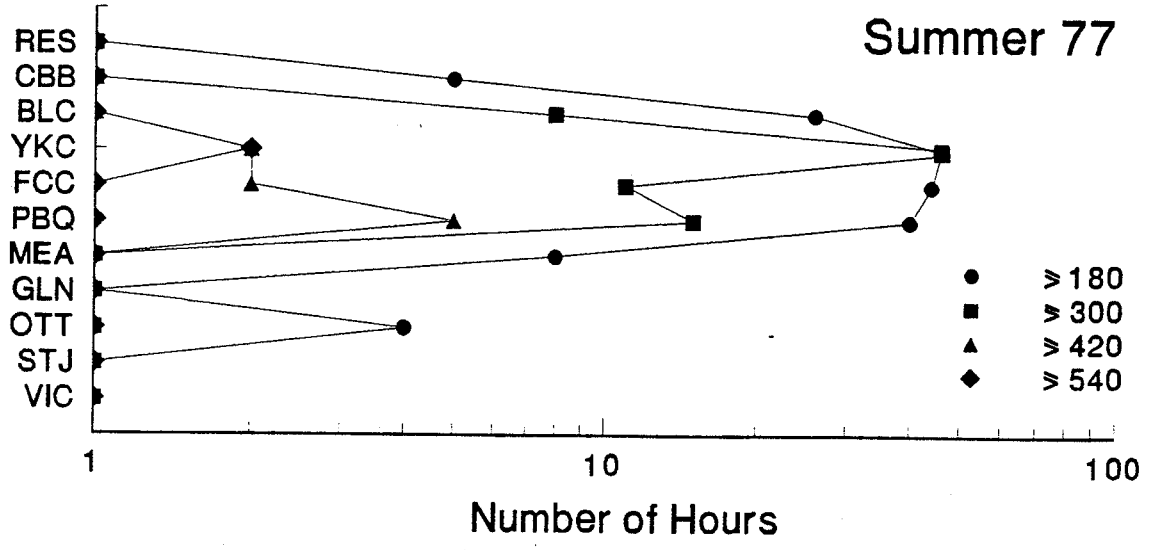
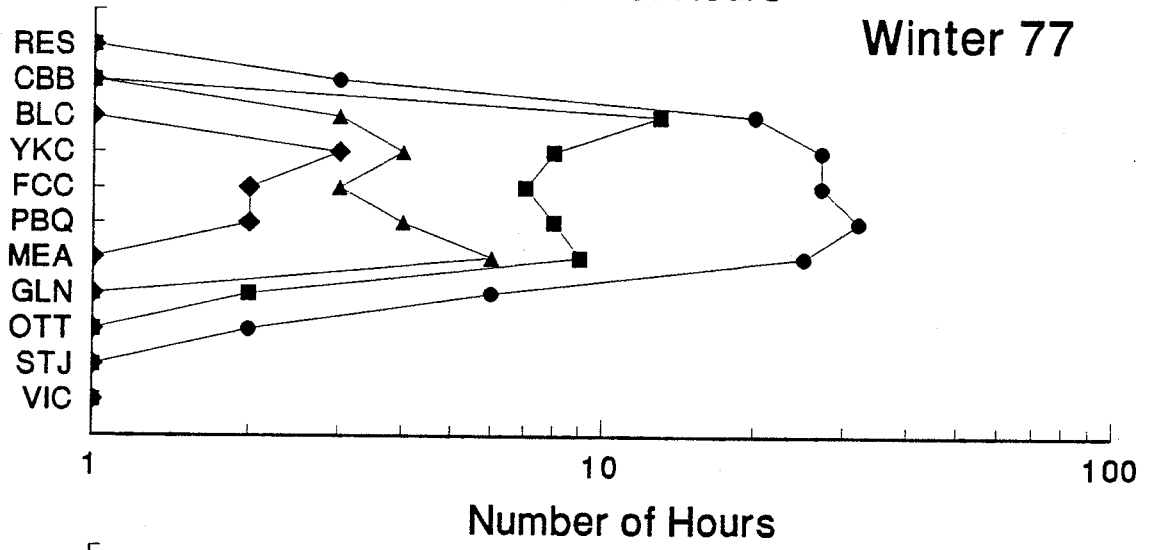
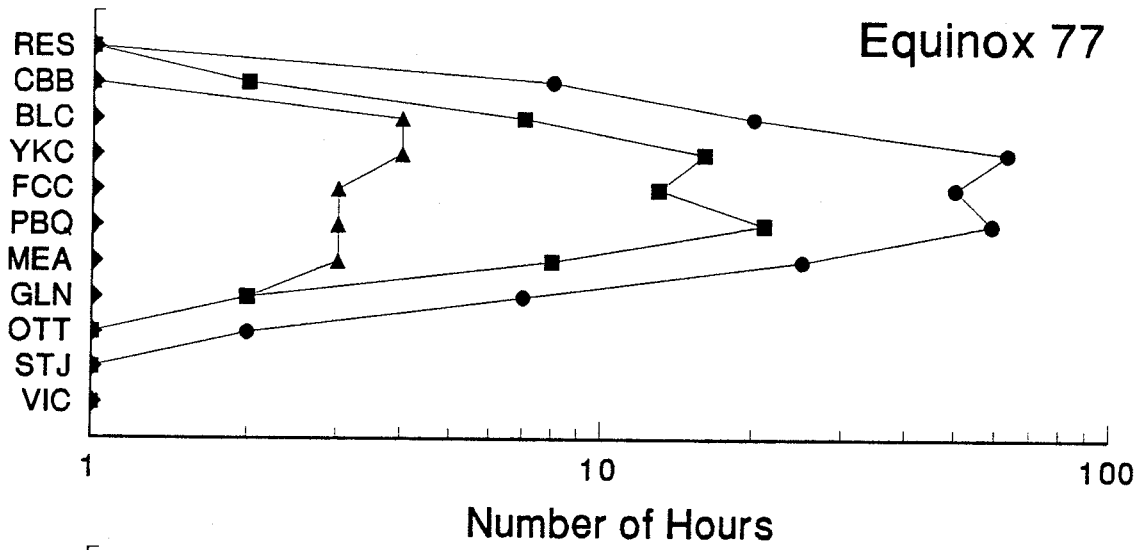
12. Evans, J.E., Newkirk, L.L., McCormac, B.M. "North Polar, South Polar, World Maps and Tables of Invariant magnetic Coordinates for Six Altitudes: 0, 100, 300, 600, 1000 and 3000 km," Lockheed Palo Alto Research Laboratory, Report DASA 2347, Palo Alto, California, 1969.
13. Parkinson, W.D. "Introduction to Geomagnetism," Elsevier, New York, 1982.
14. Mayaud, P.N. "Derivation, Meaning, and Use of Geomagnetic Indices," Geophysical Monograph, no. 22, American Geophysical Union, Washington D.C., 1980.

## APPENDIX

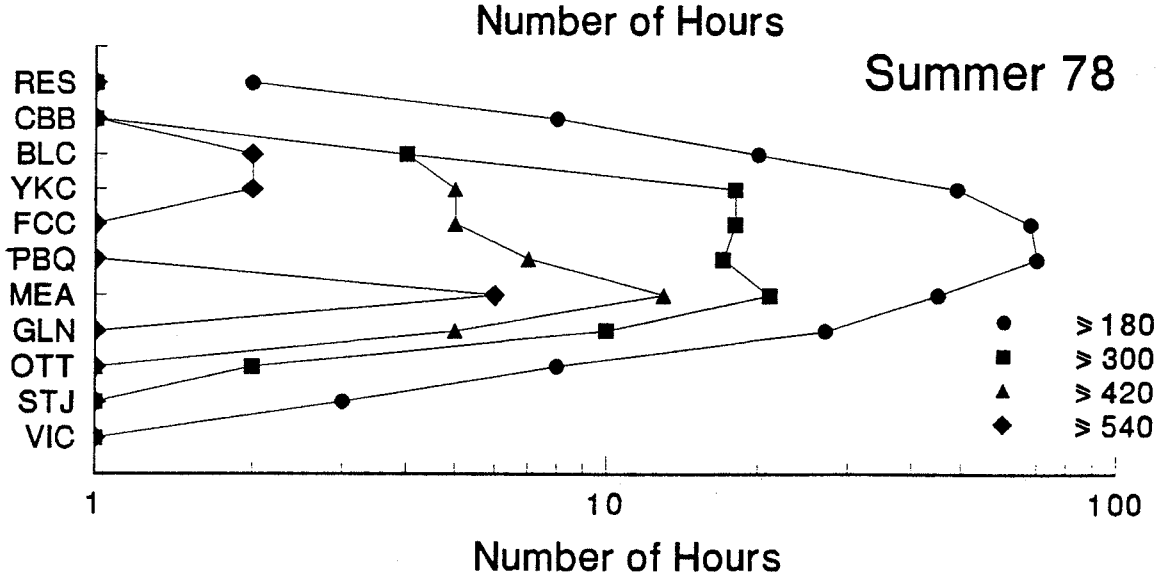
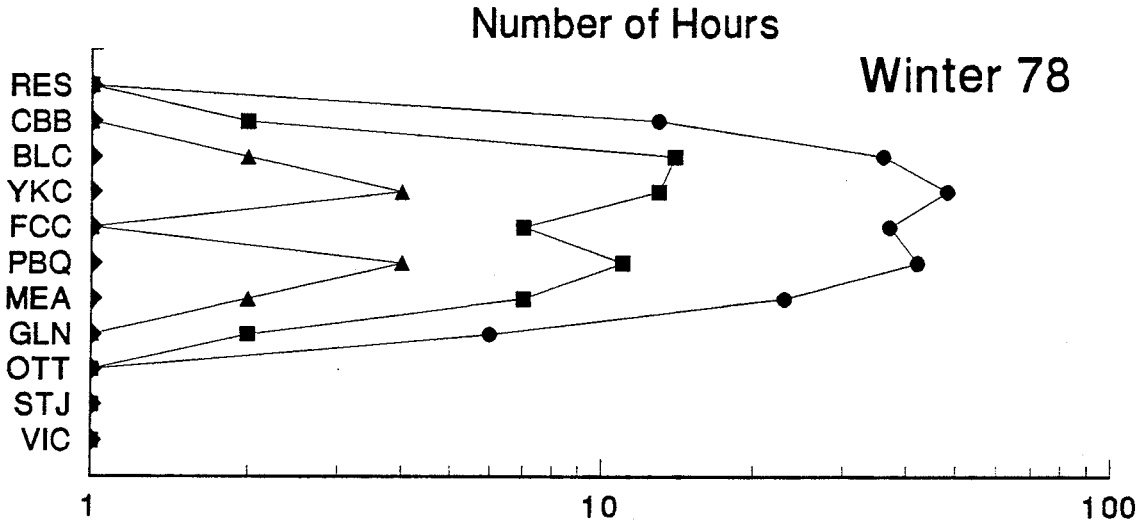
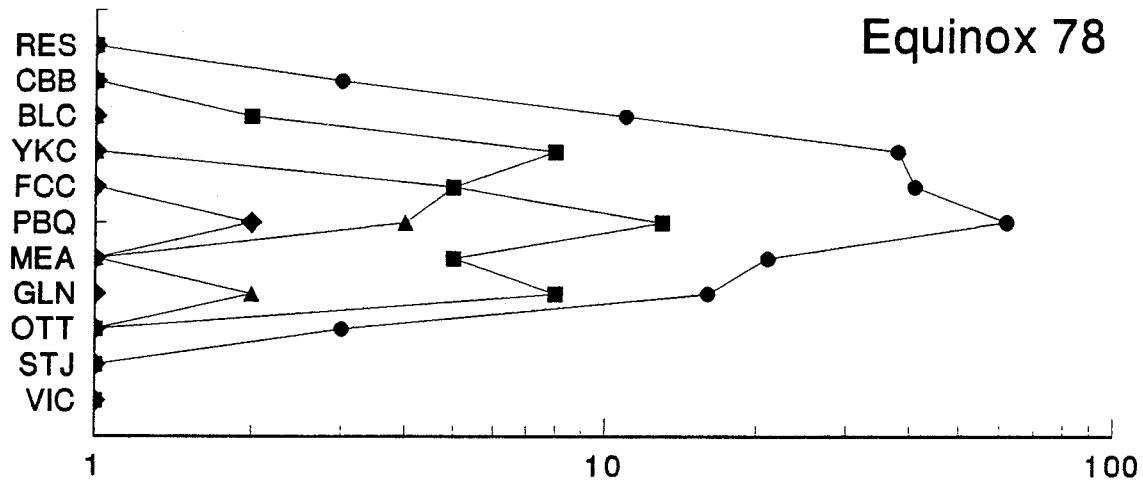
### A. LATITUDINAL AND SEASONAL VARIATIONS

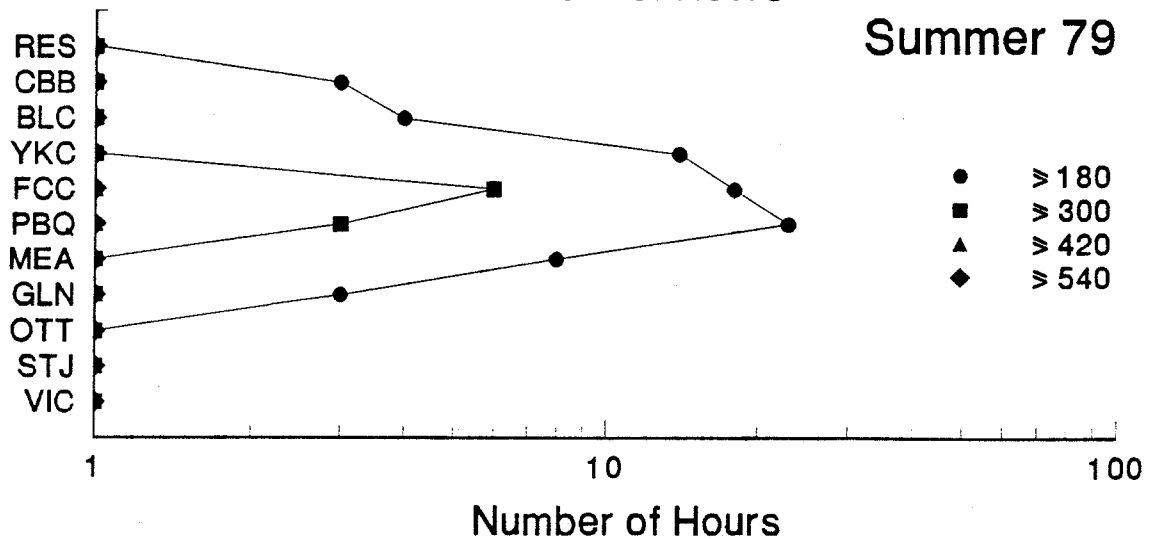
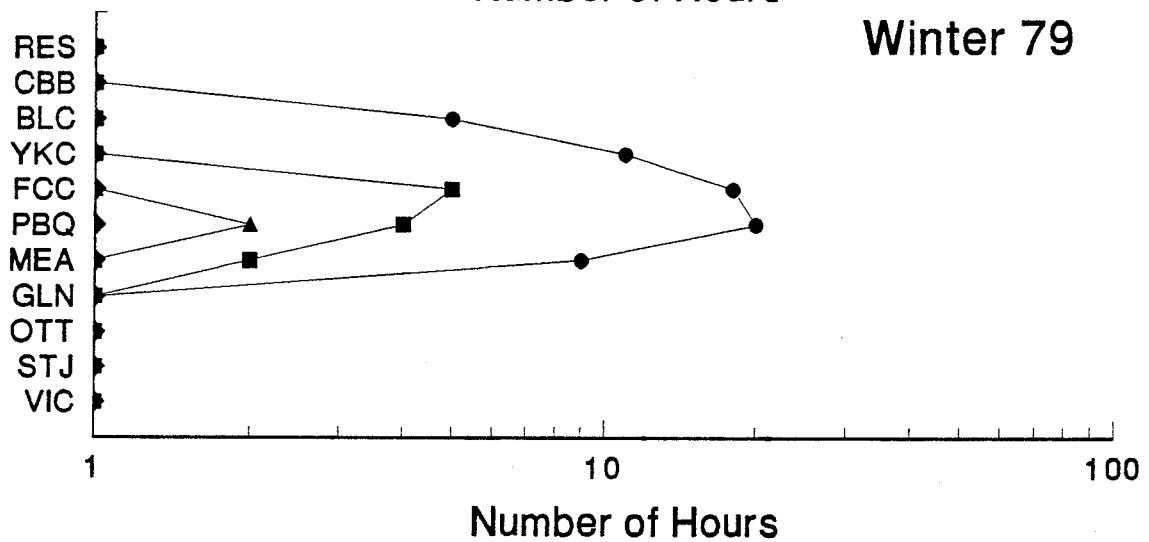
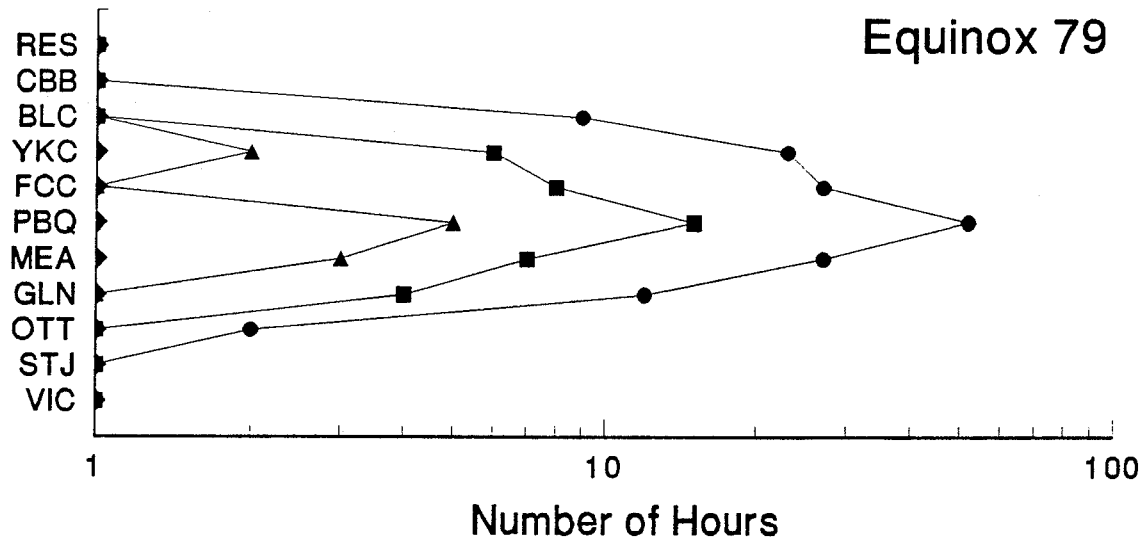
The following figures present results for each year, following the format of Figure 10 in section 3.

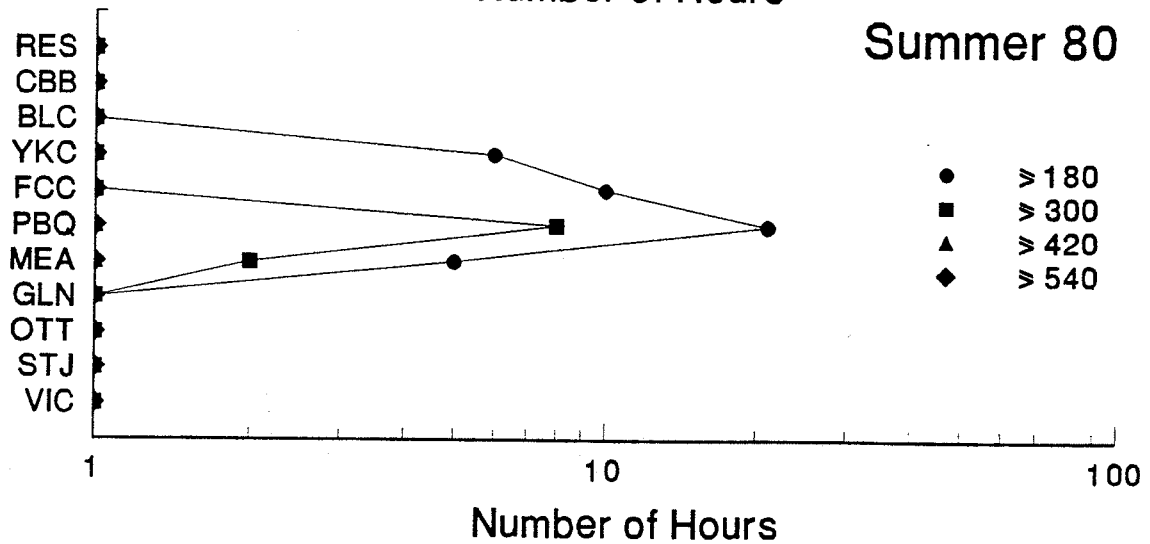
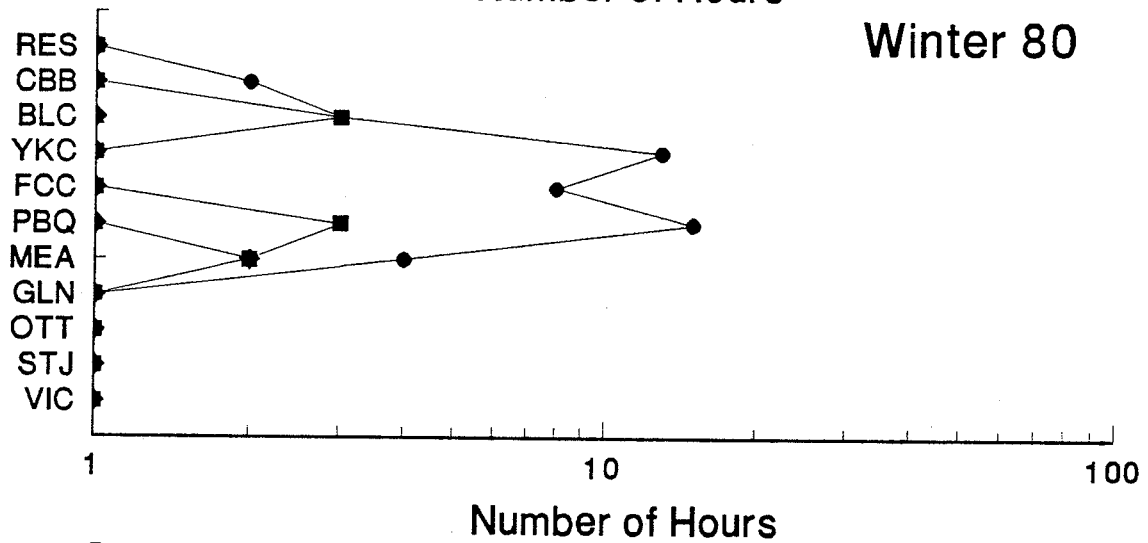
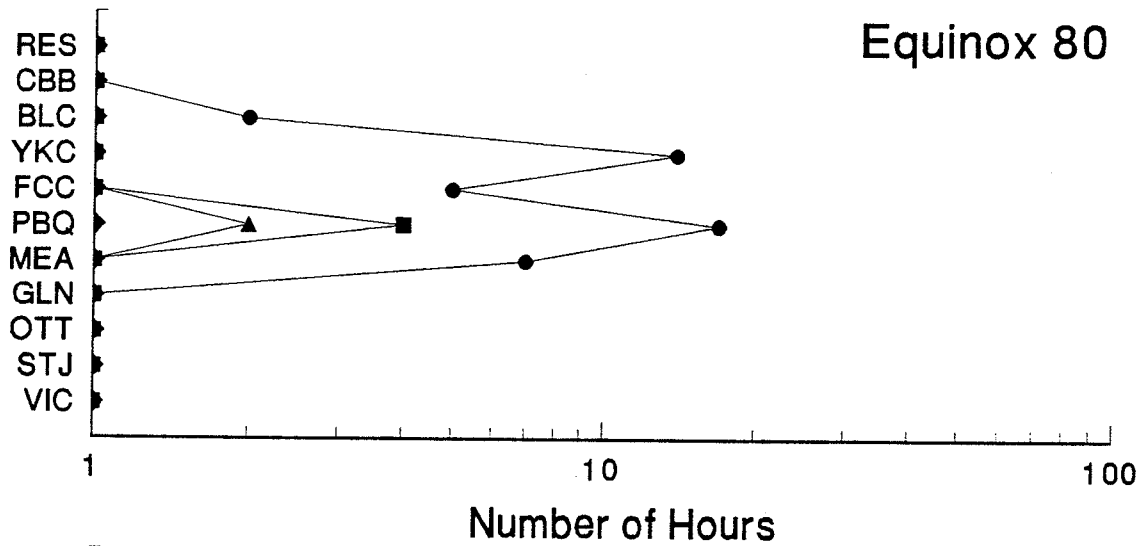
The average numbers of hours per season for which at least one event in any component equalled or exceeded 180 (solid discs), 300 (squares), 420 (triangles), 540 (diamonds) nT/min. Note the logarithmic horizontal scale. On the vertical scale, the observatories are sequenced according to invariant geomagnetic latitude.



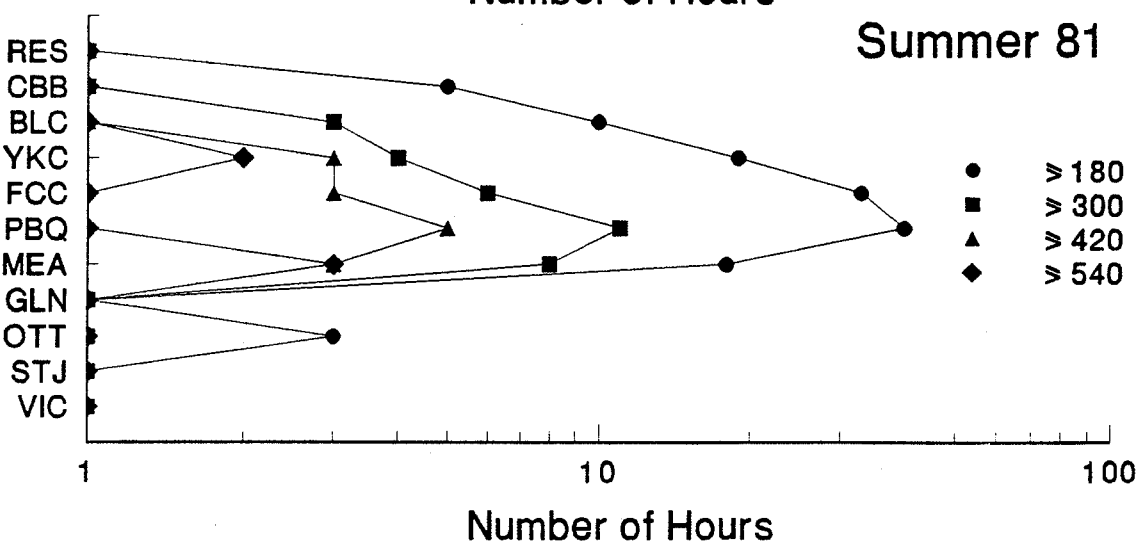
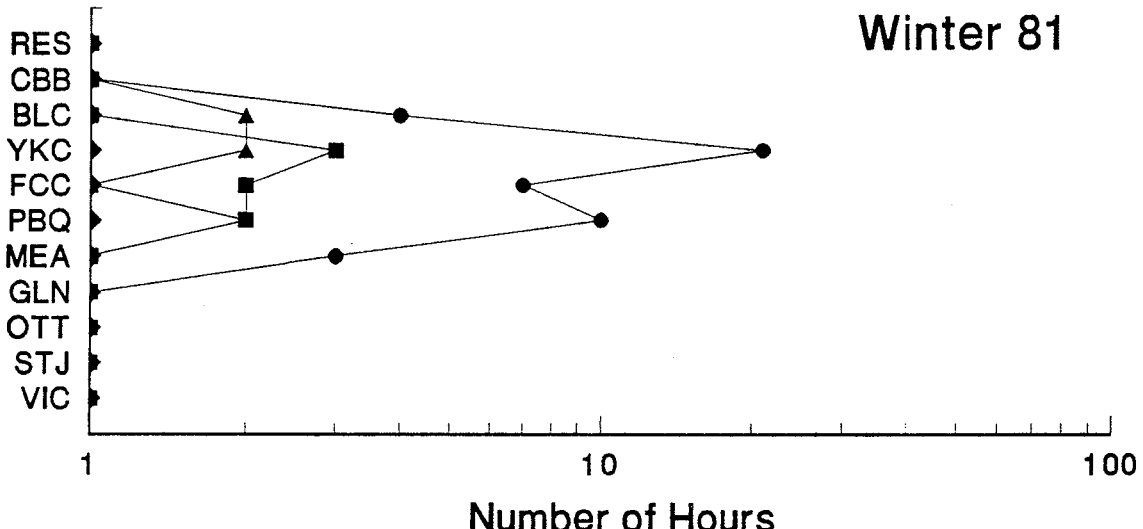
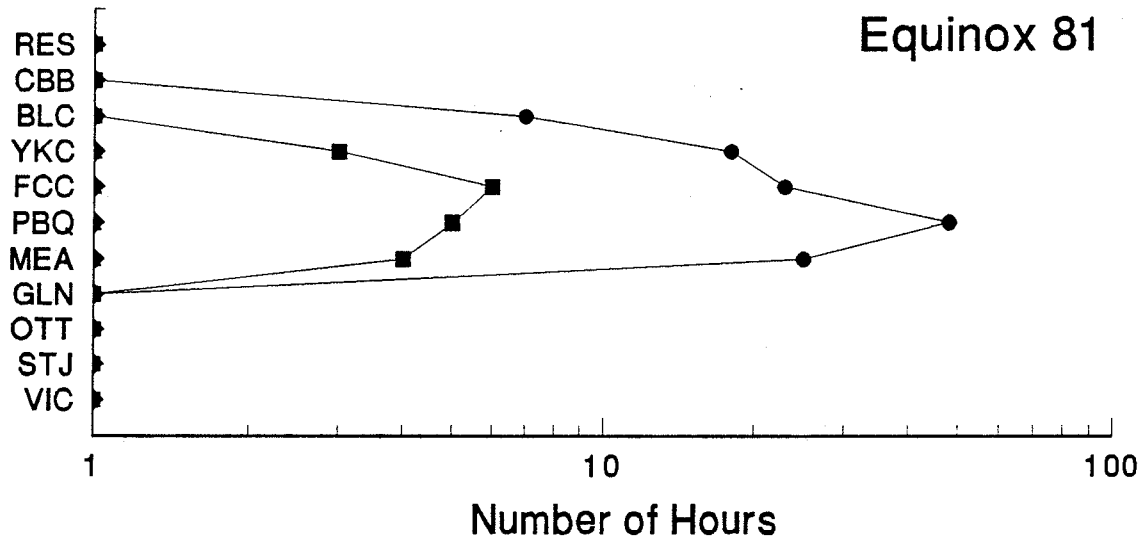
- $\geq 180$
- $\geq 300$
- ▲  $\geq 420$
- ◆  $\geq 540$

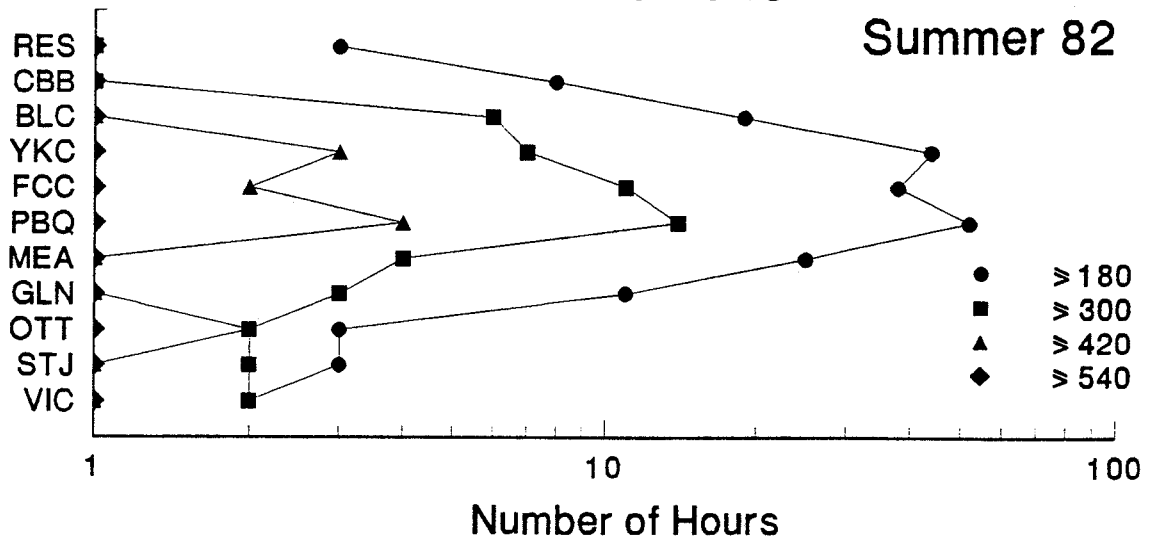
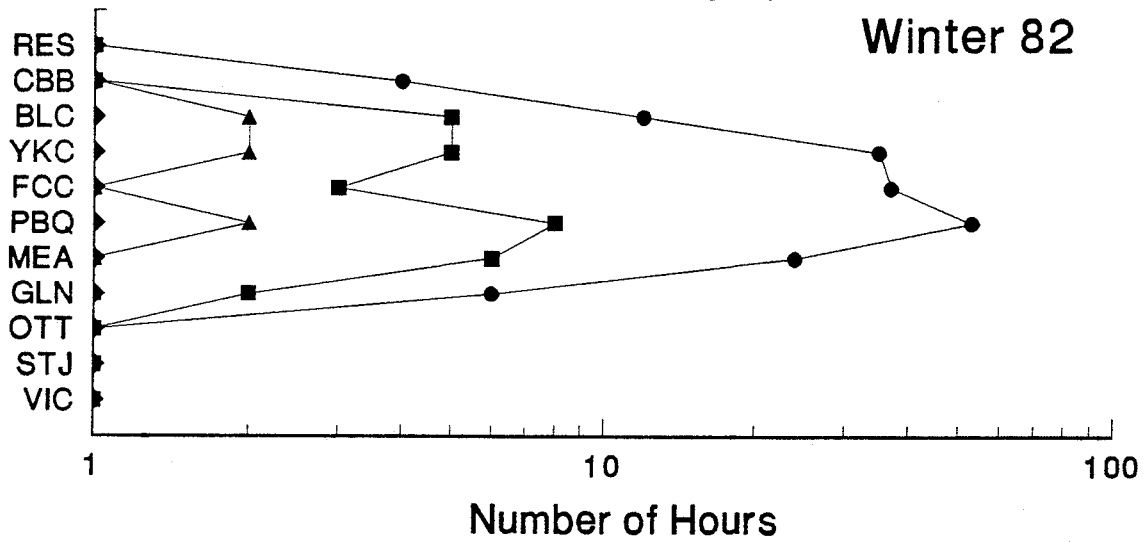
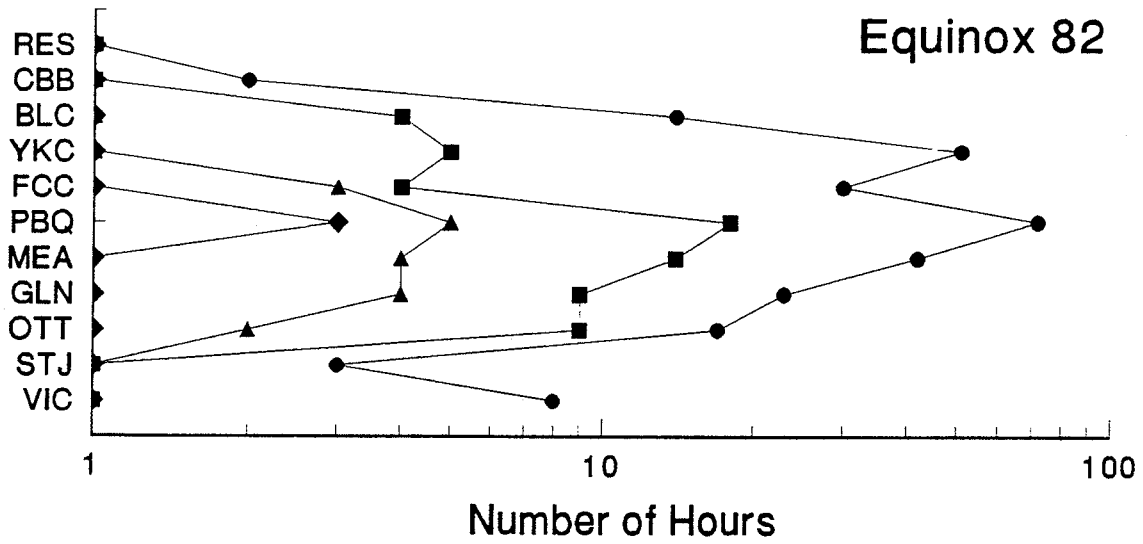


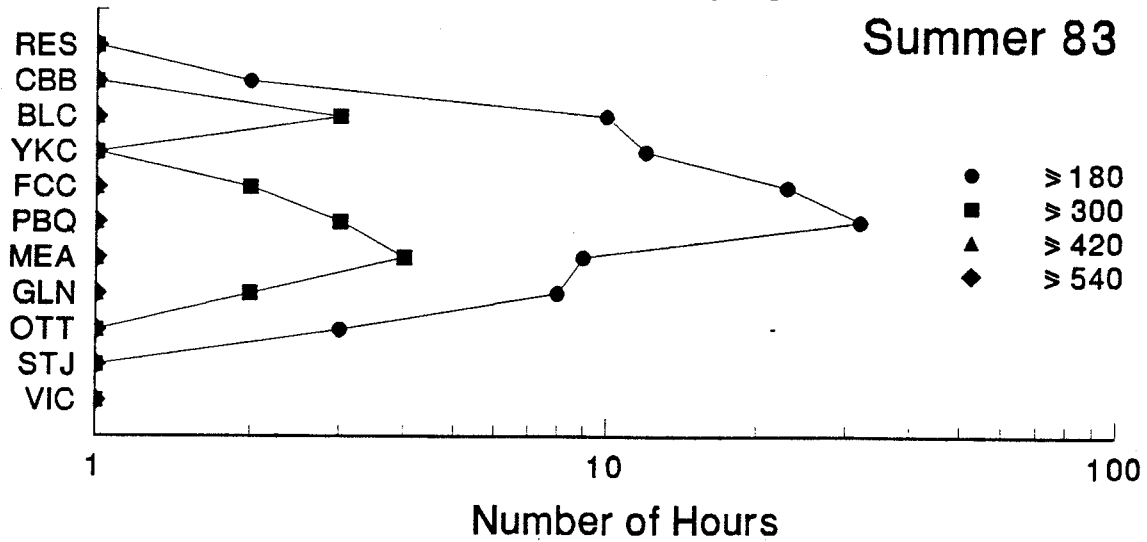
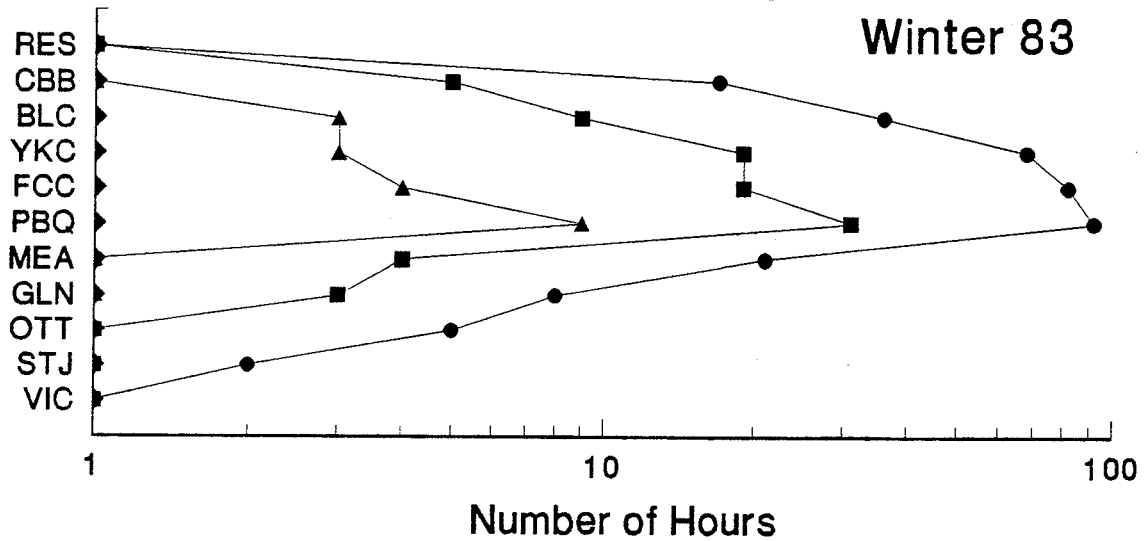
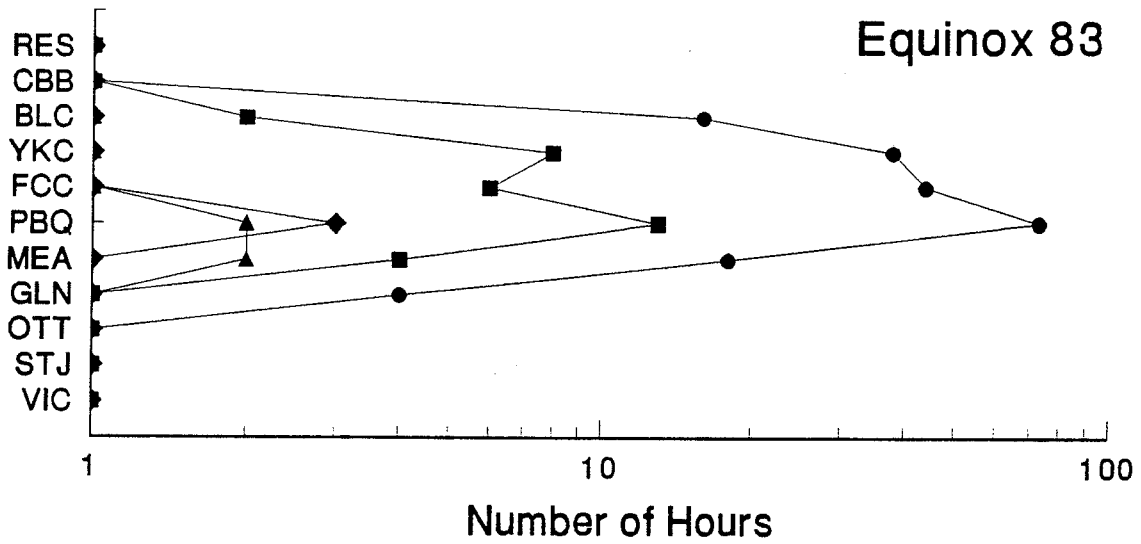


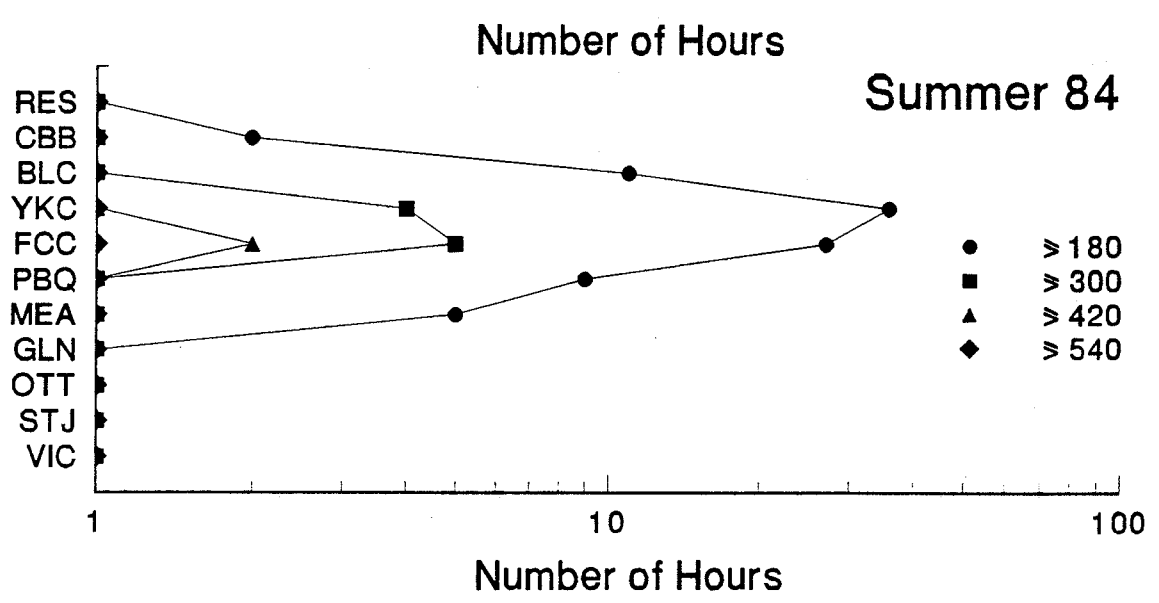
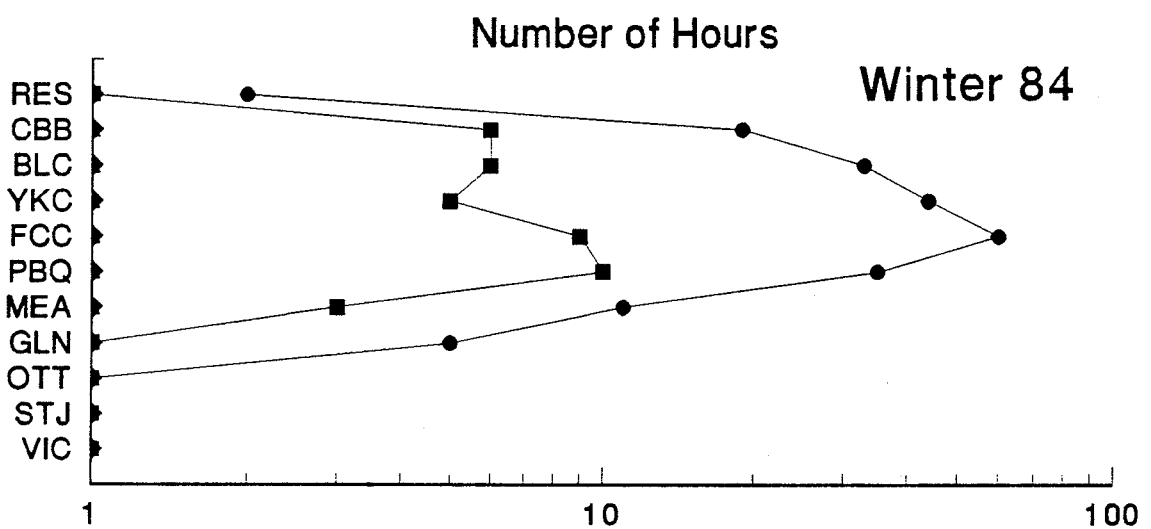
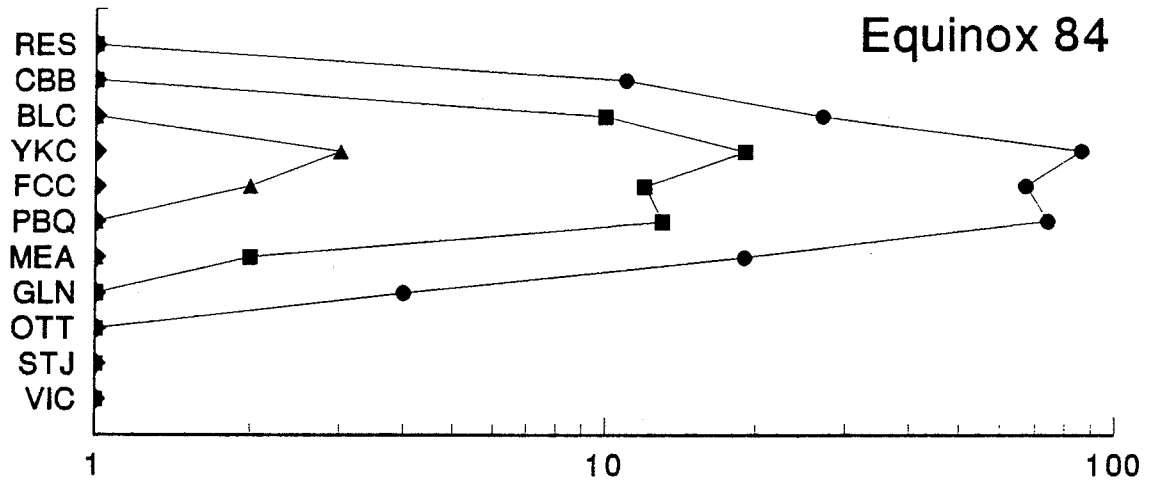


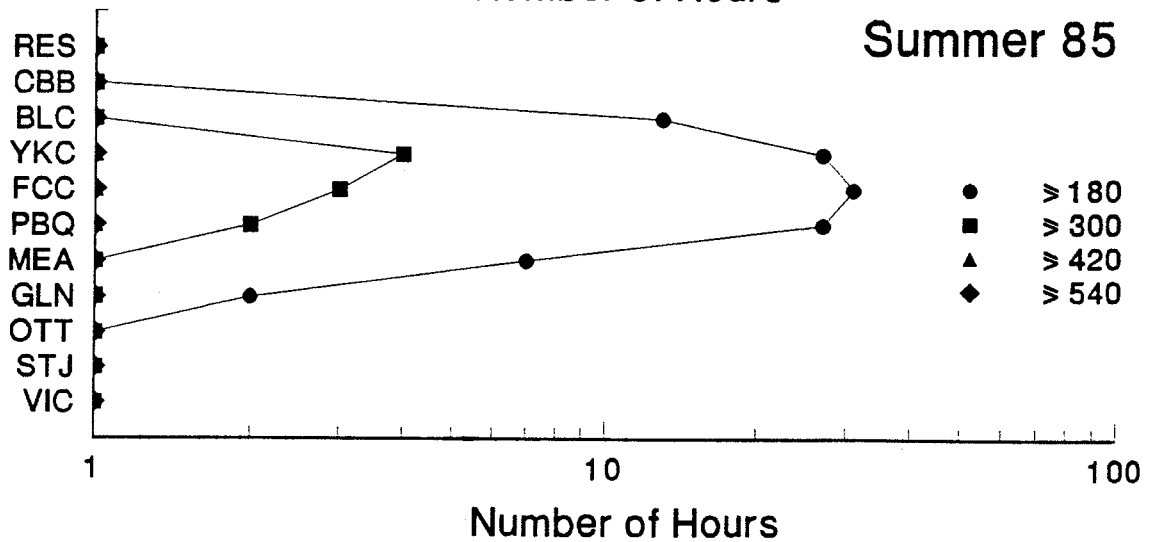
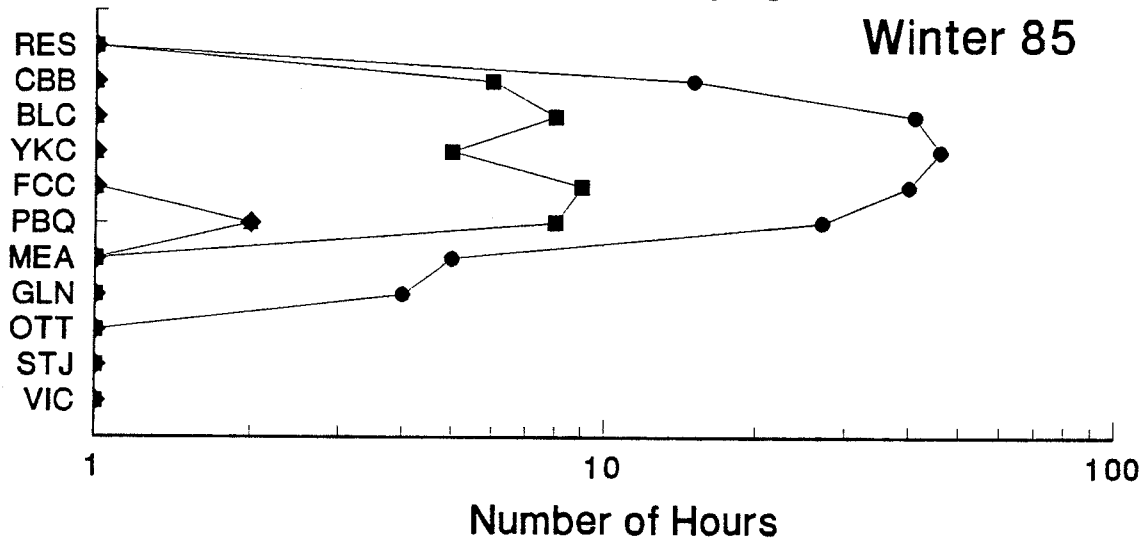
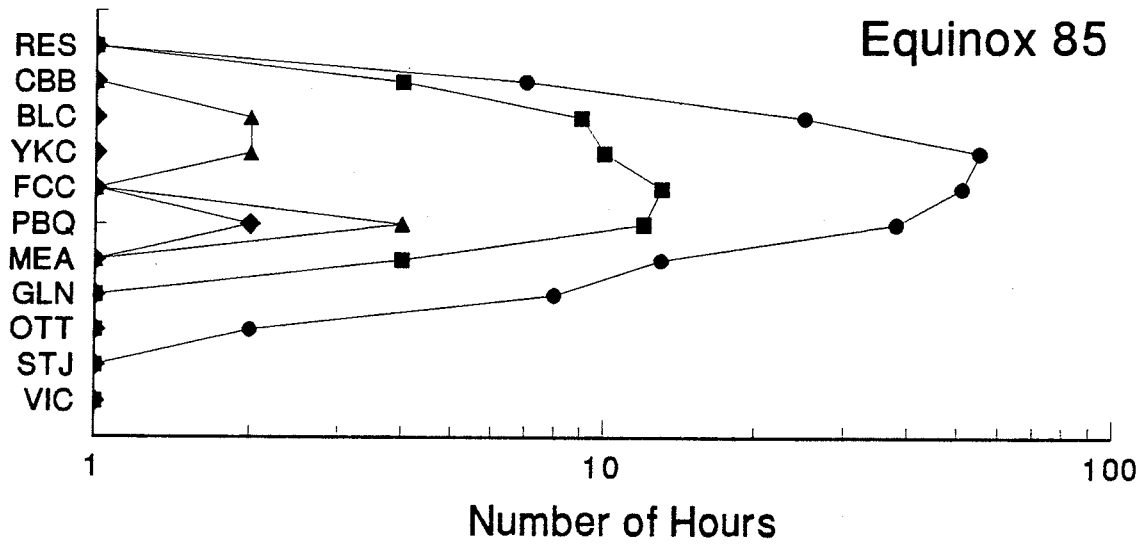


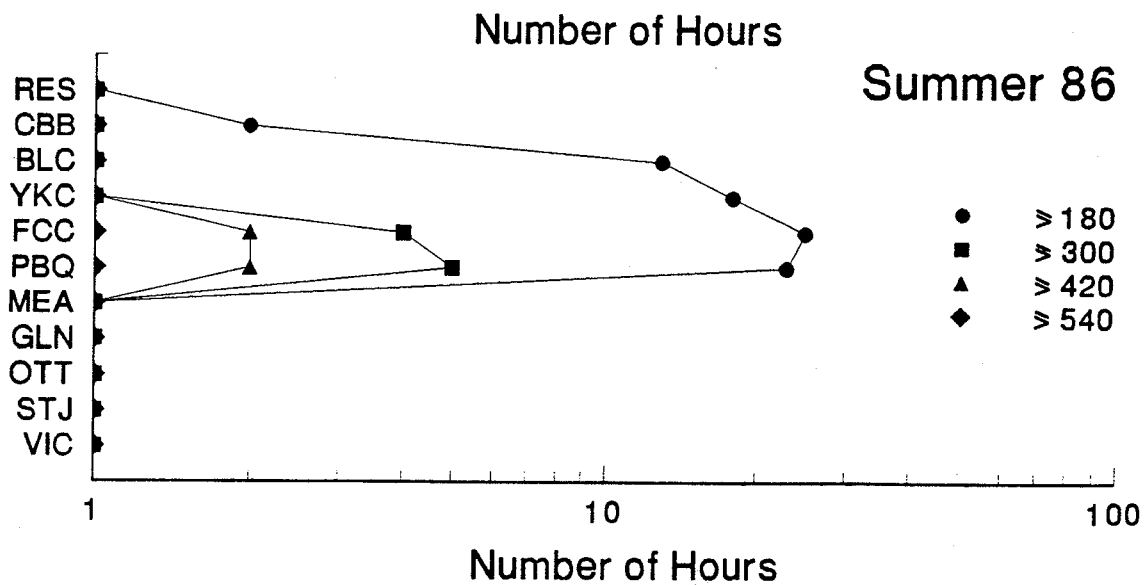
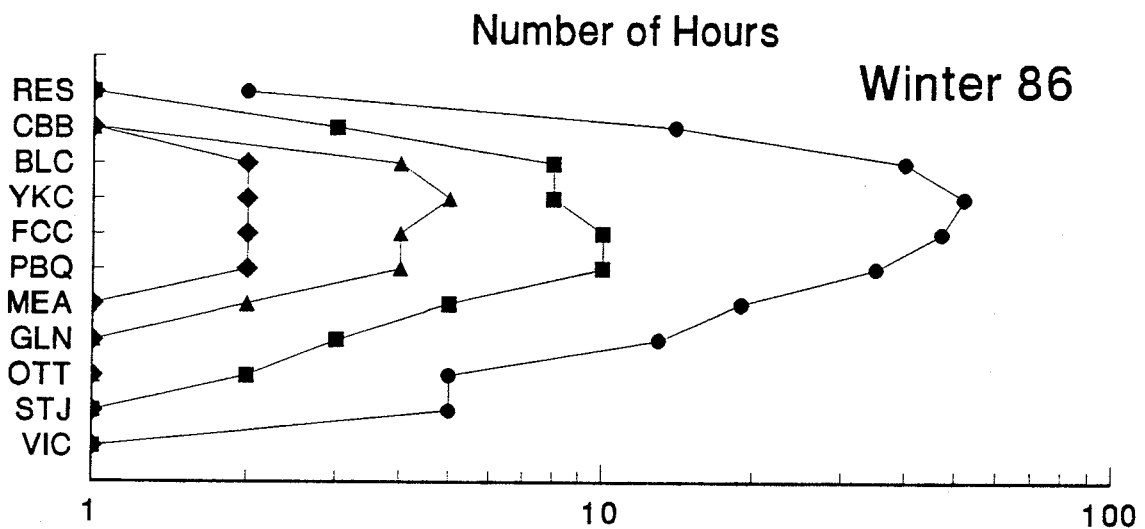
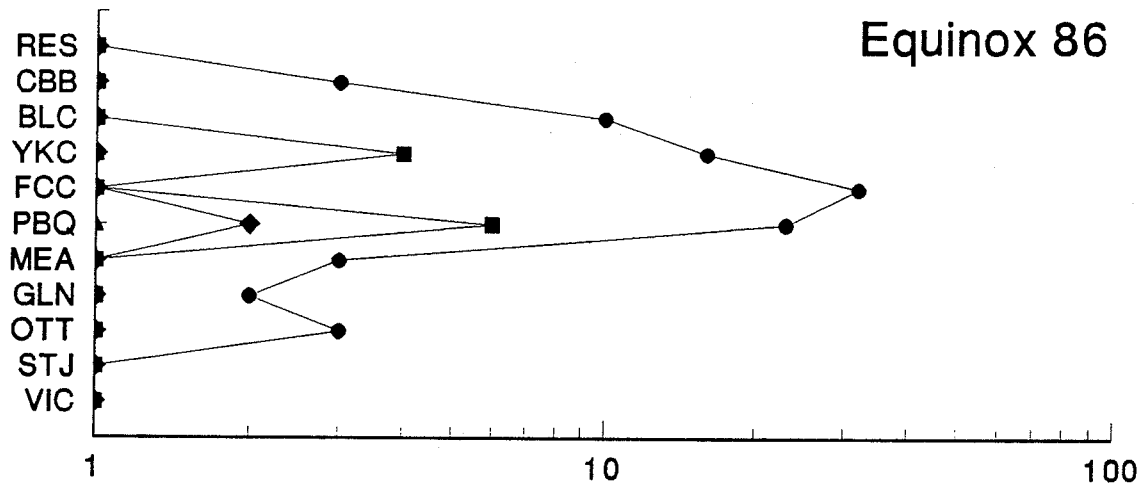


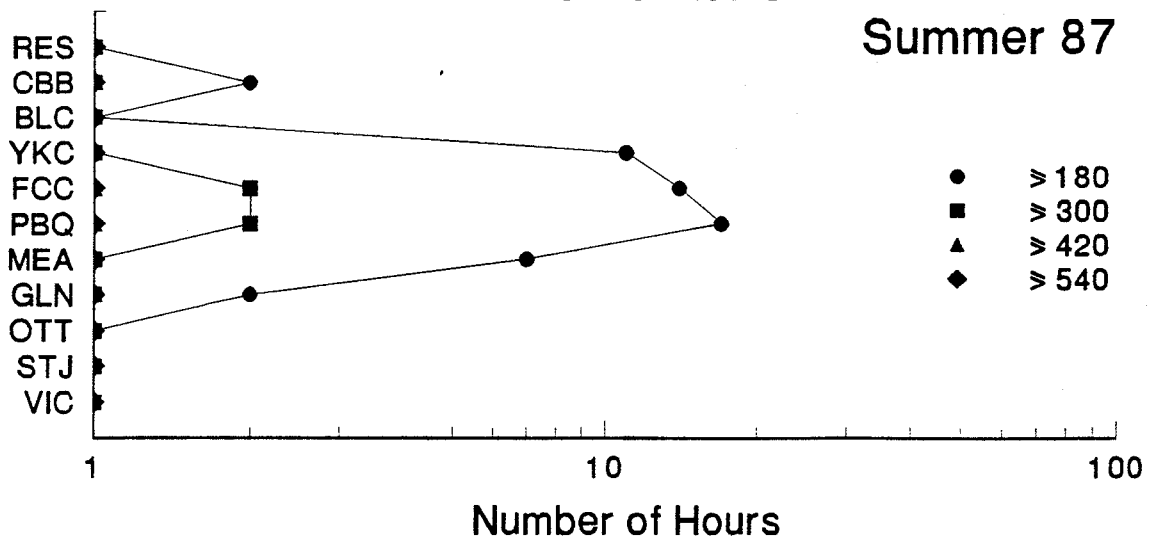
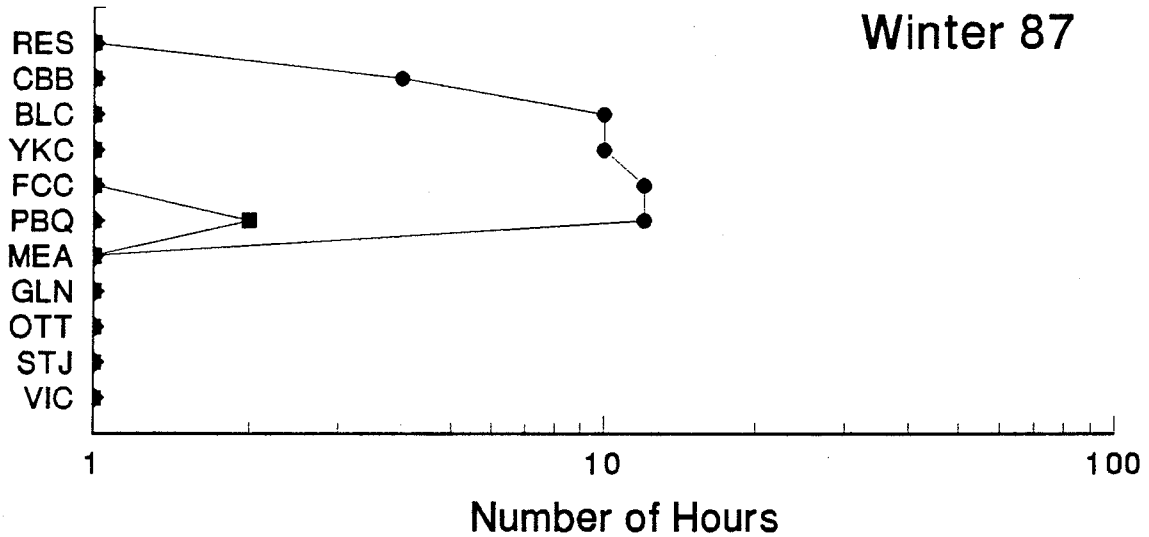
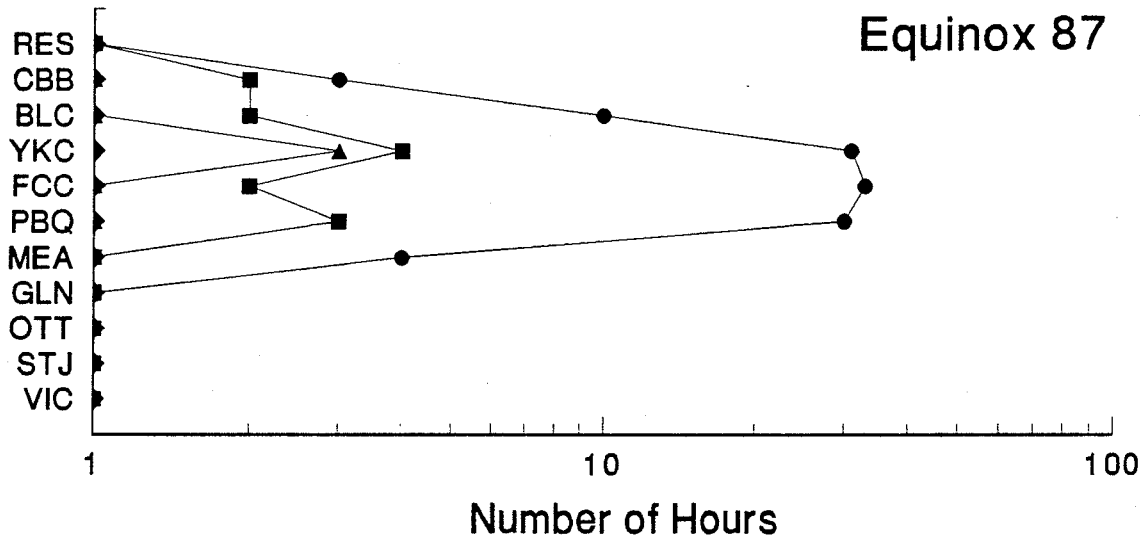


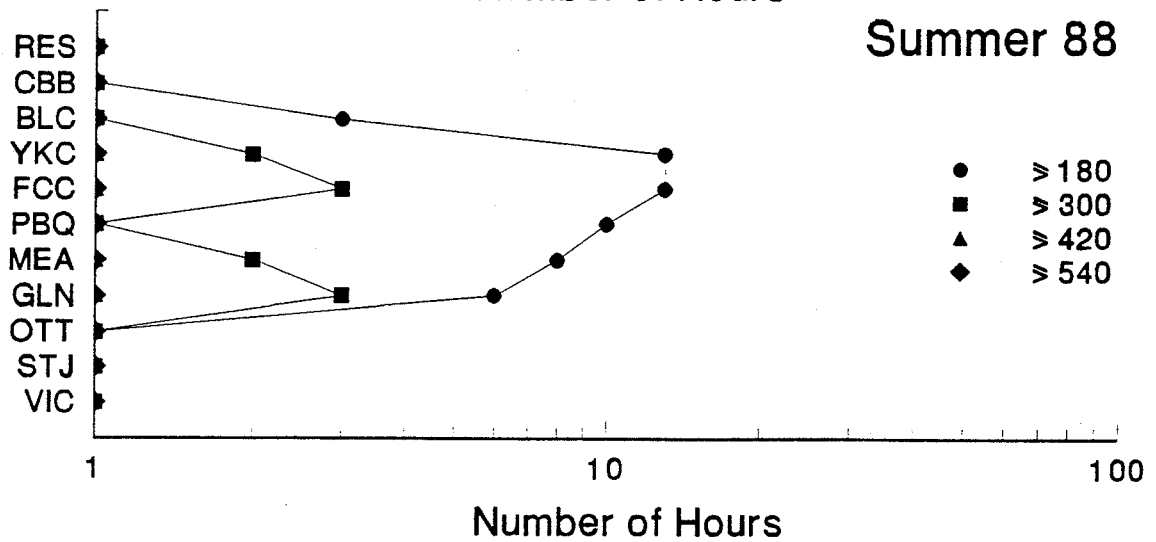
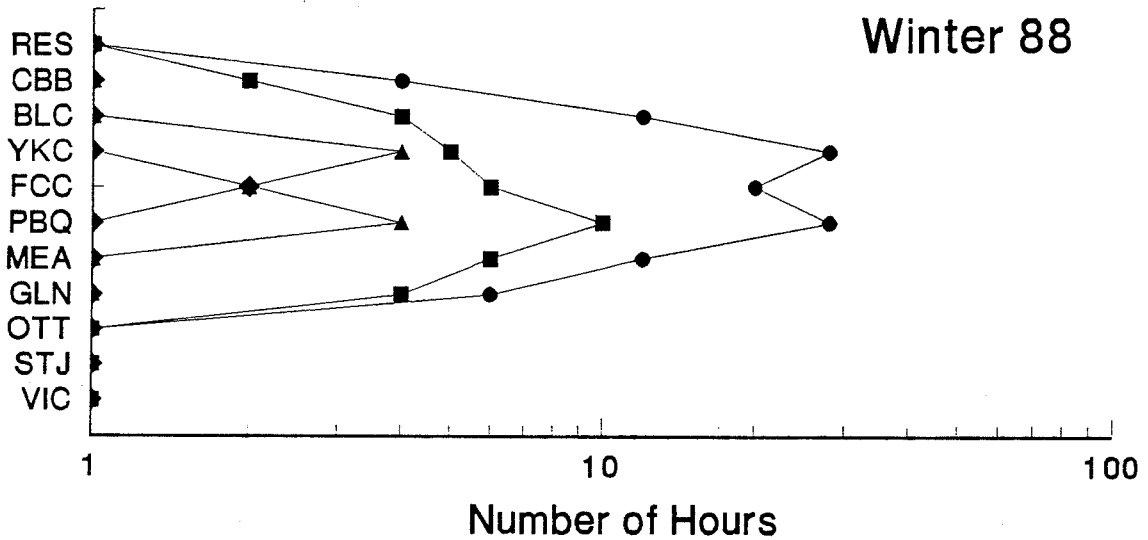
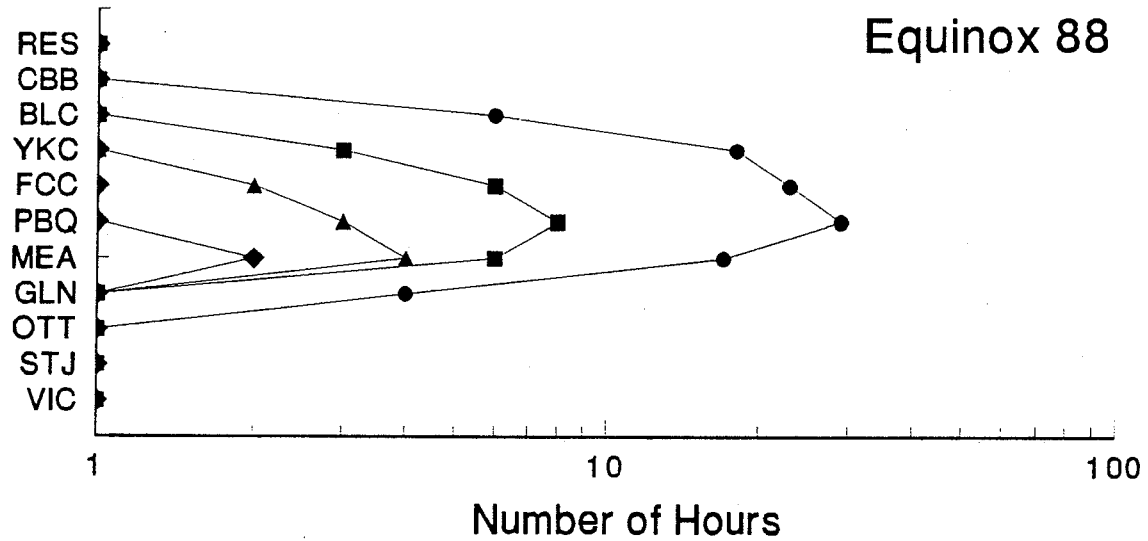




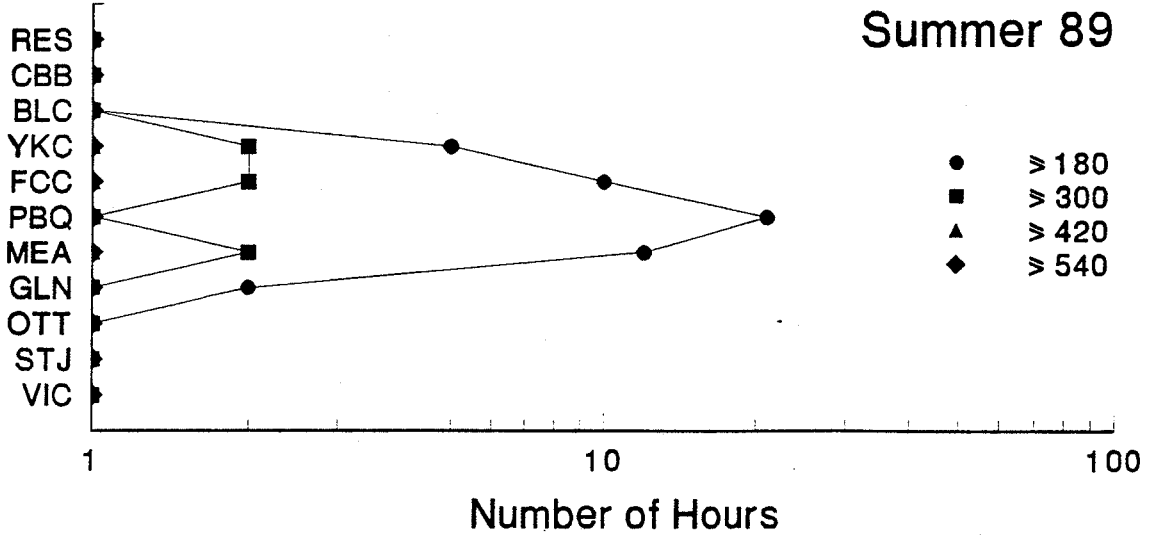
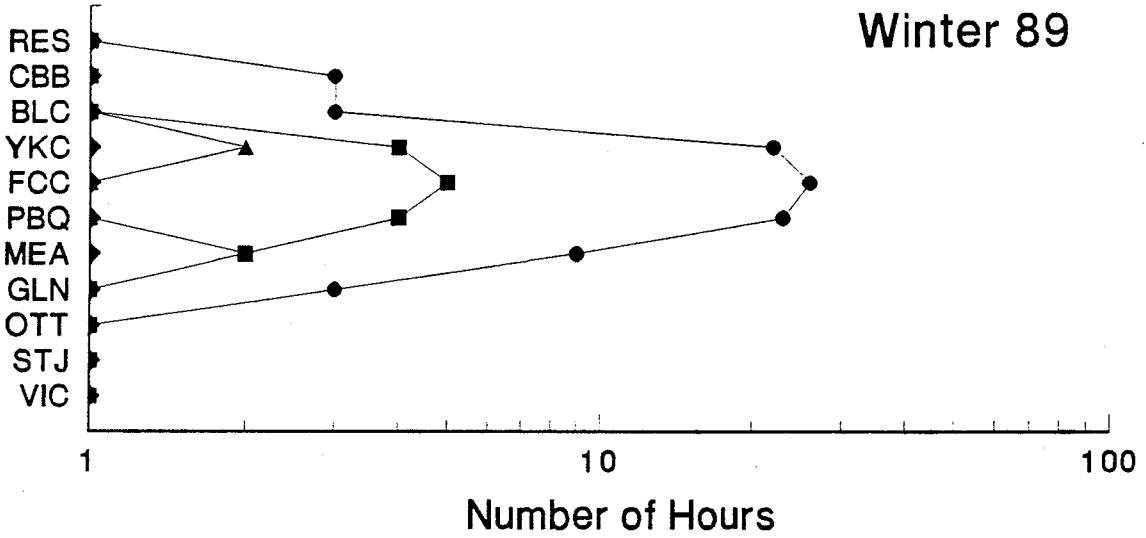
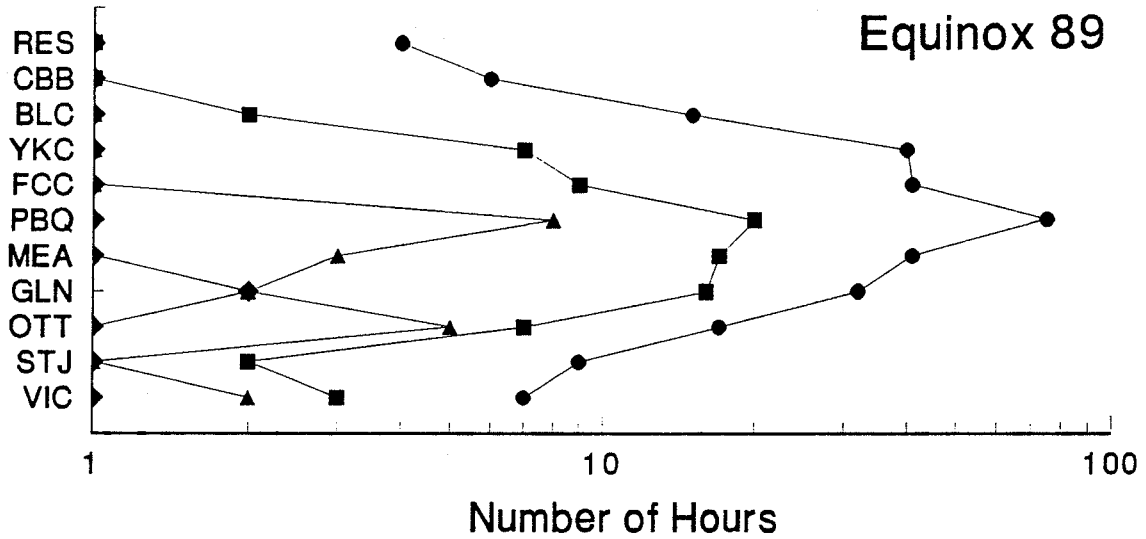








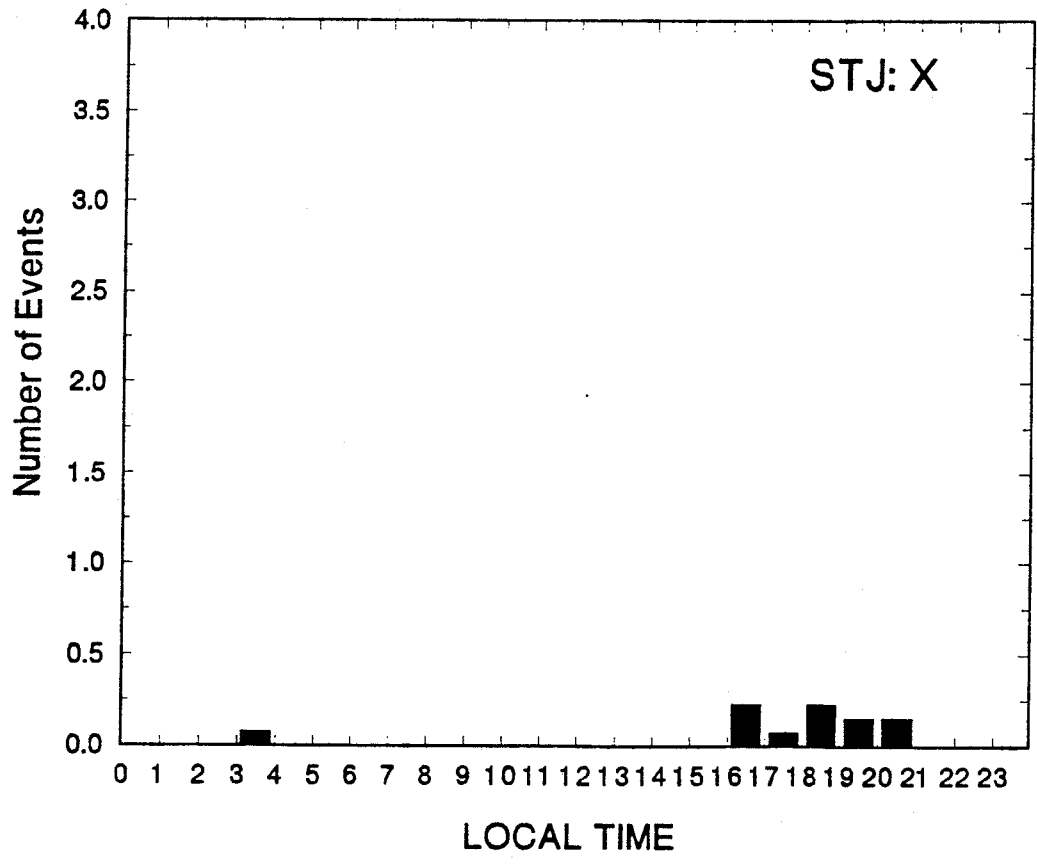
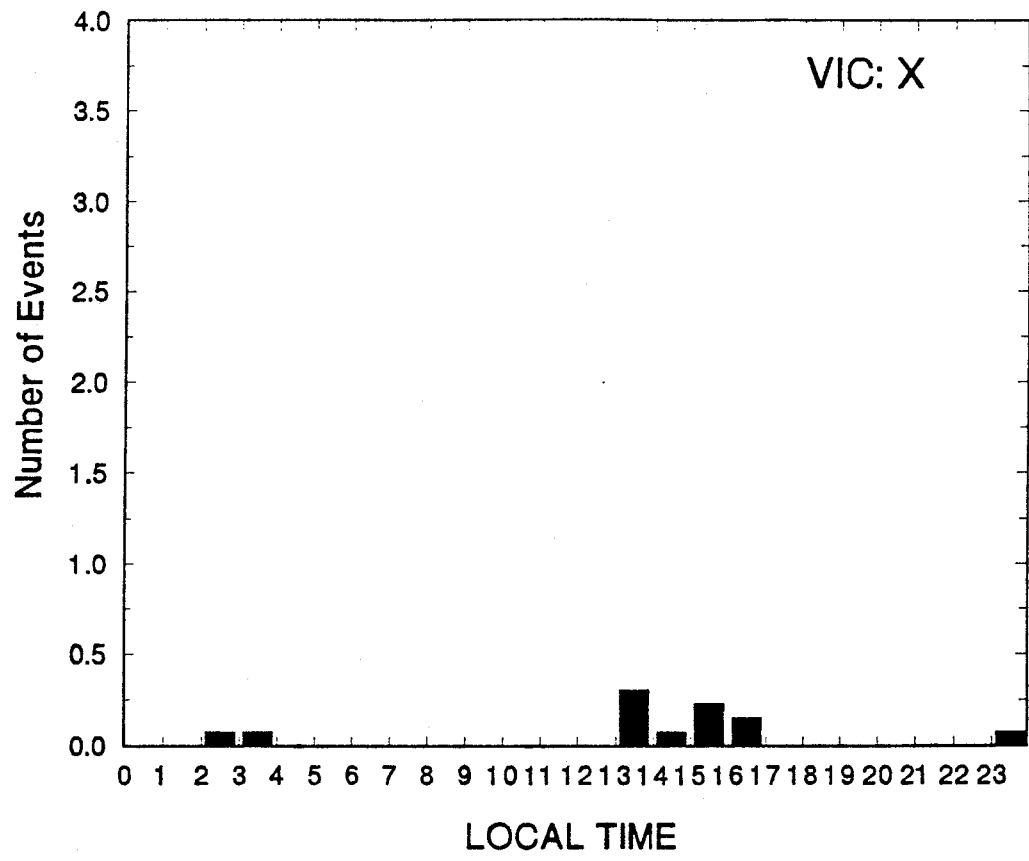


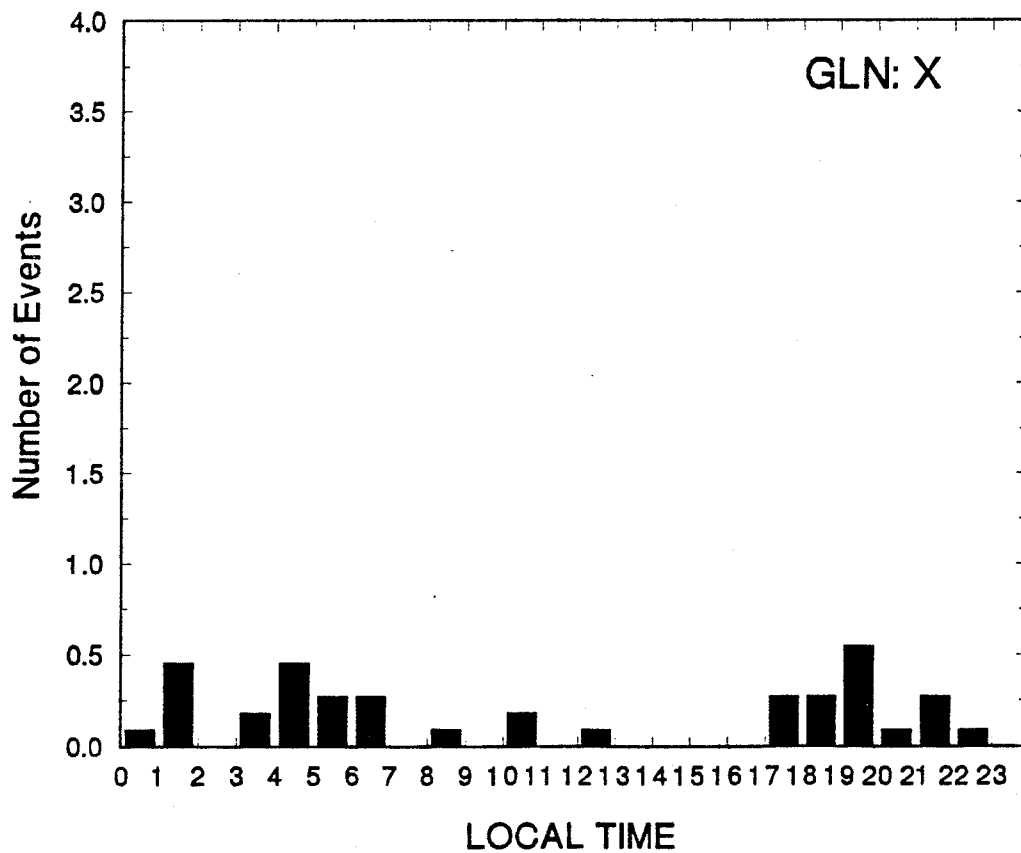
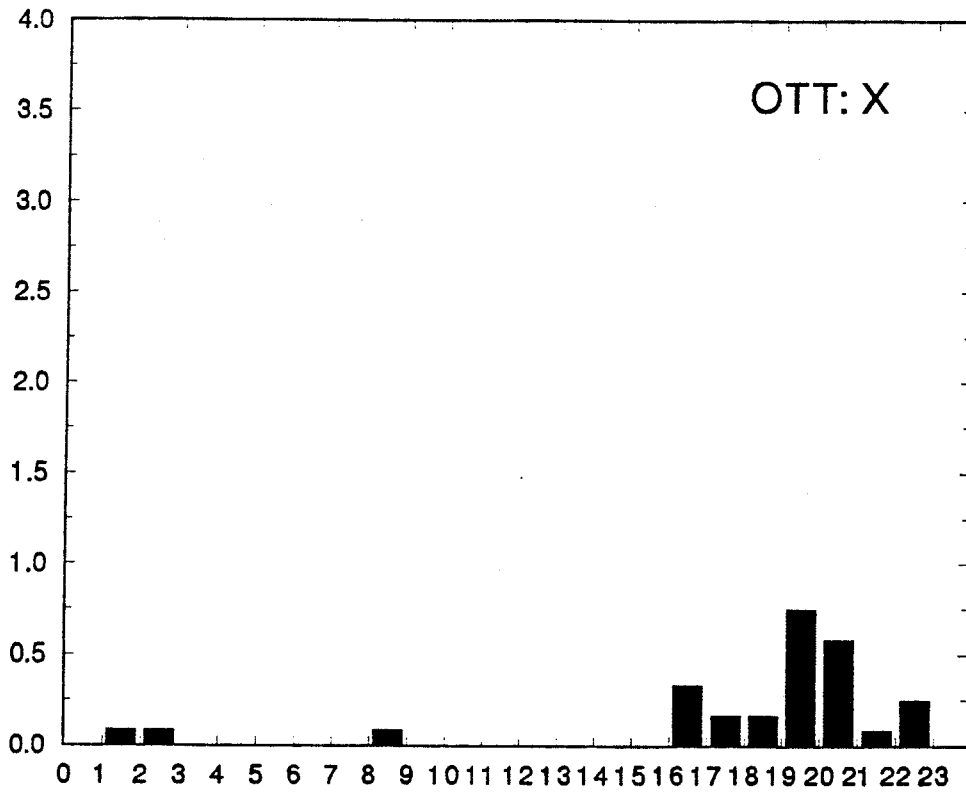


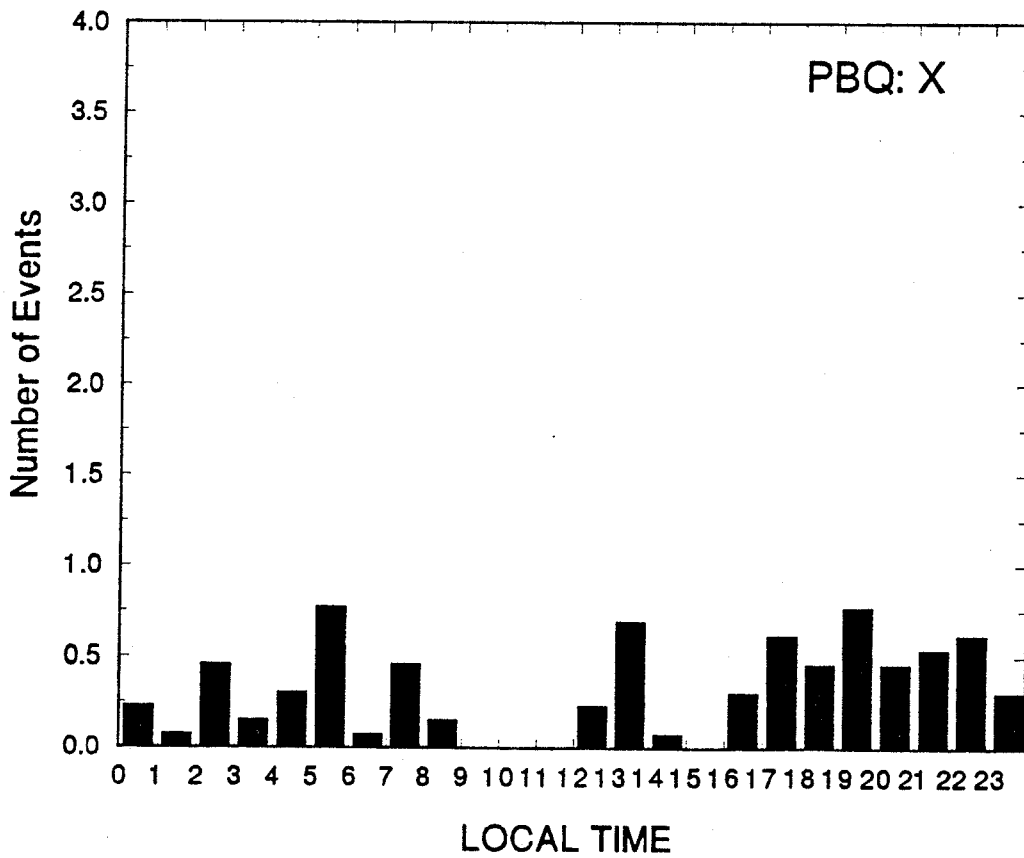
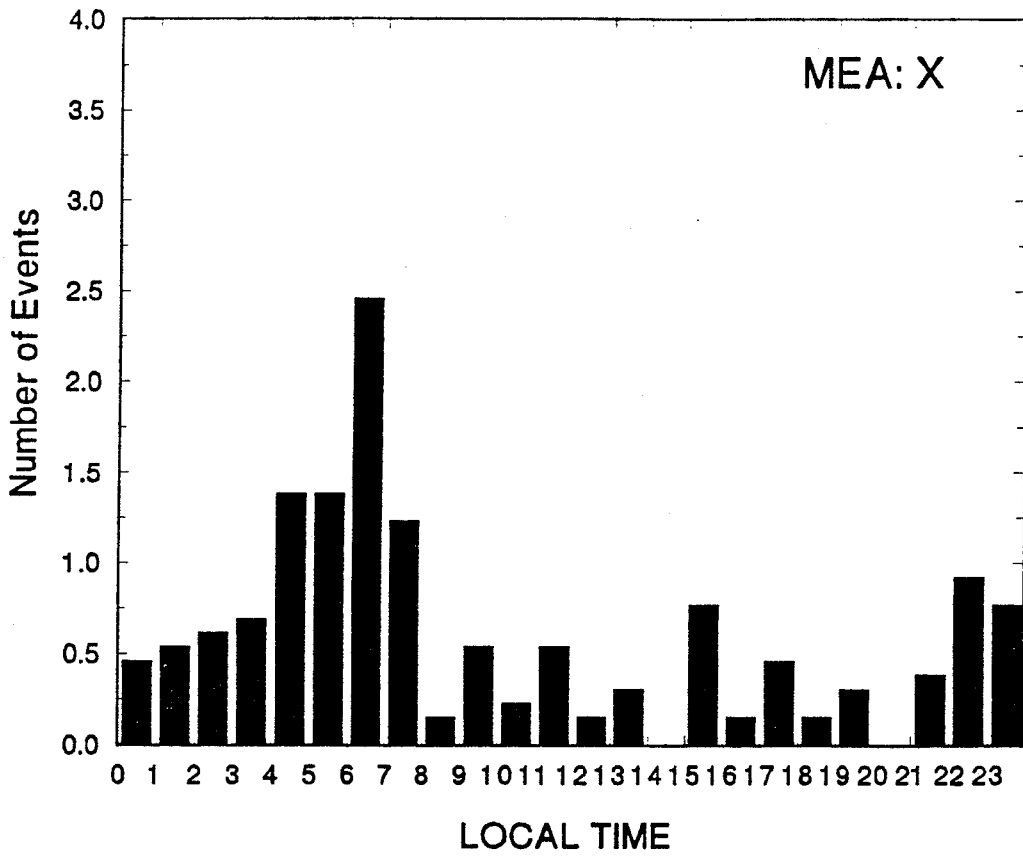
## APPENDIX

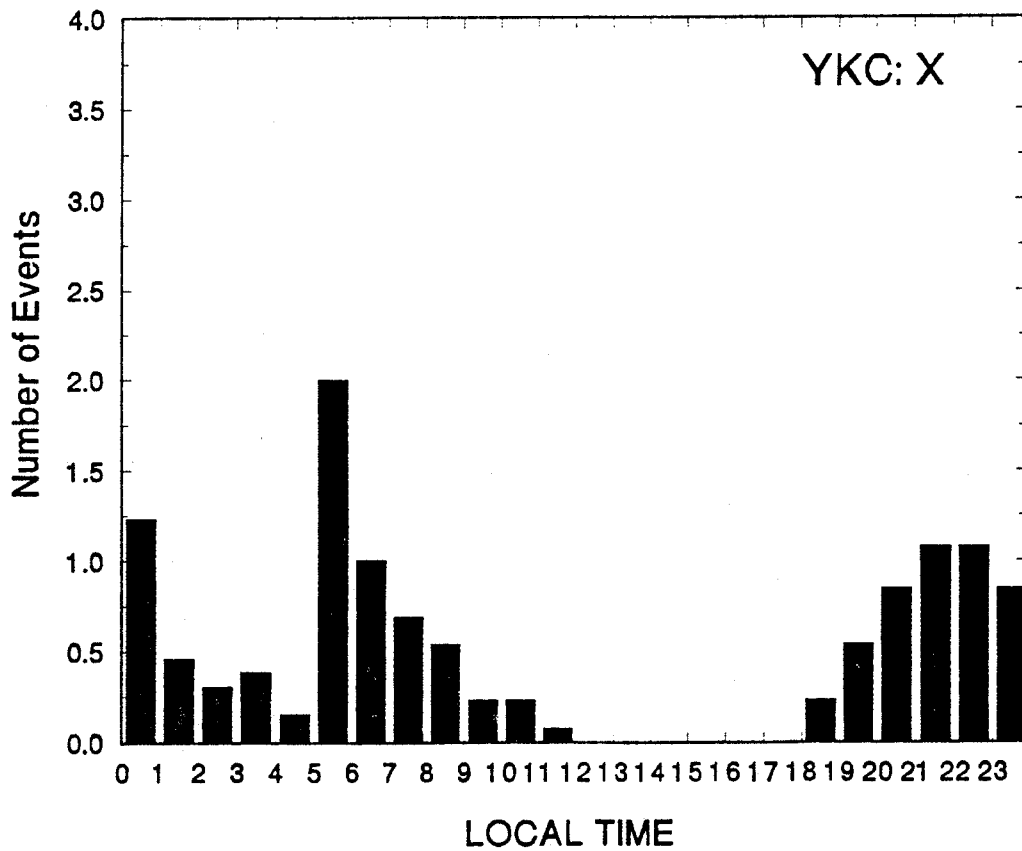
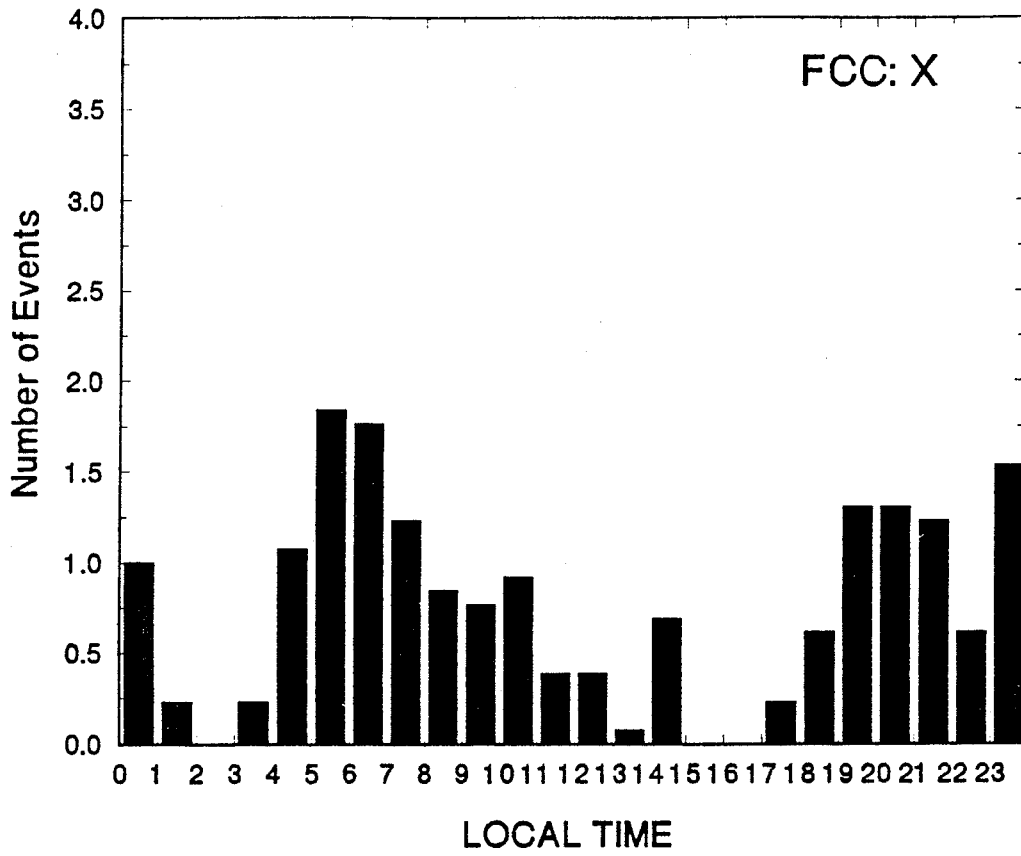
### B. VARIATION OF OCCURRENCE WITH LOCAL TIME

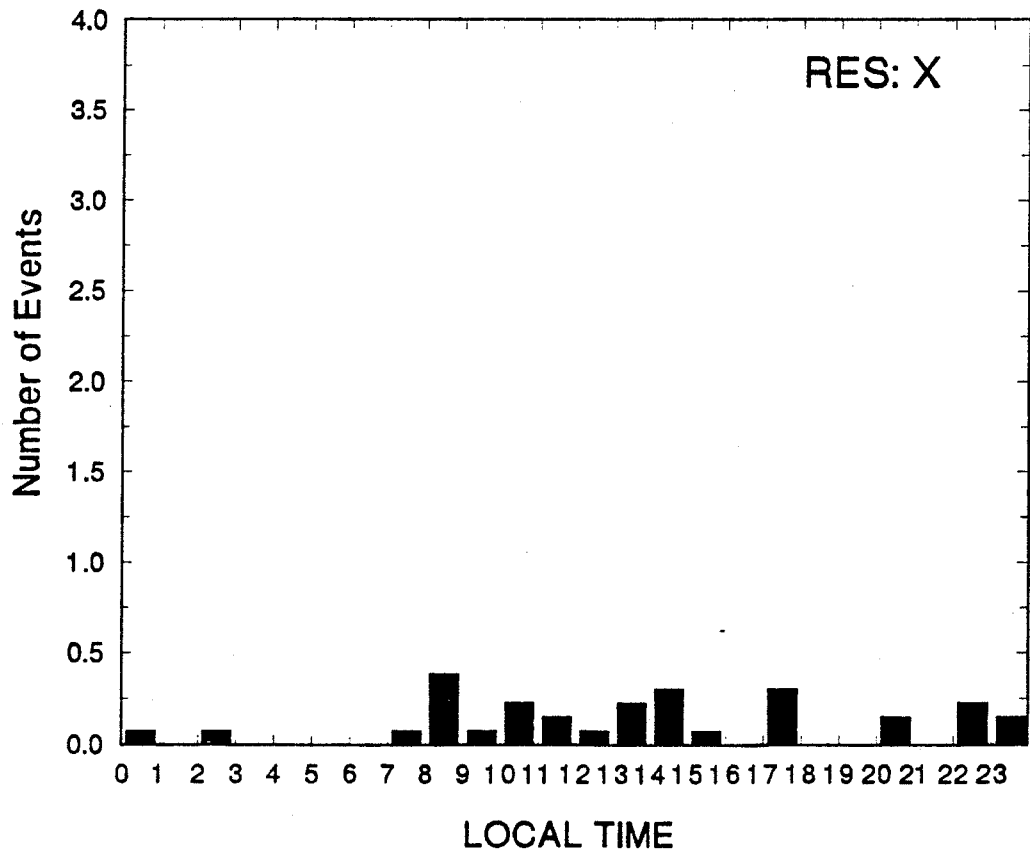
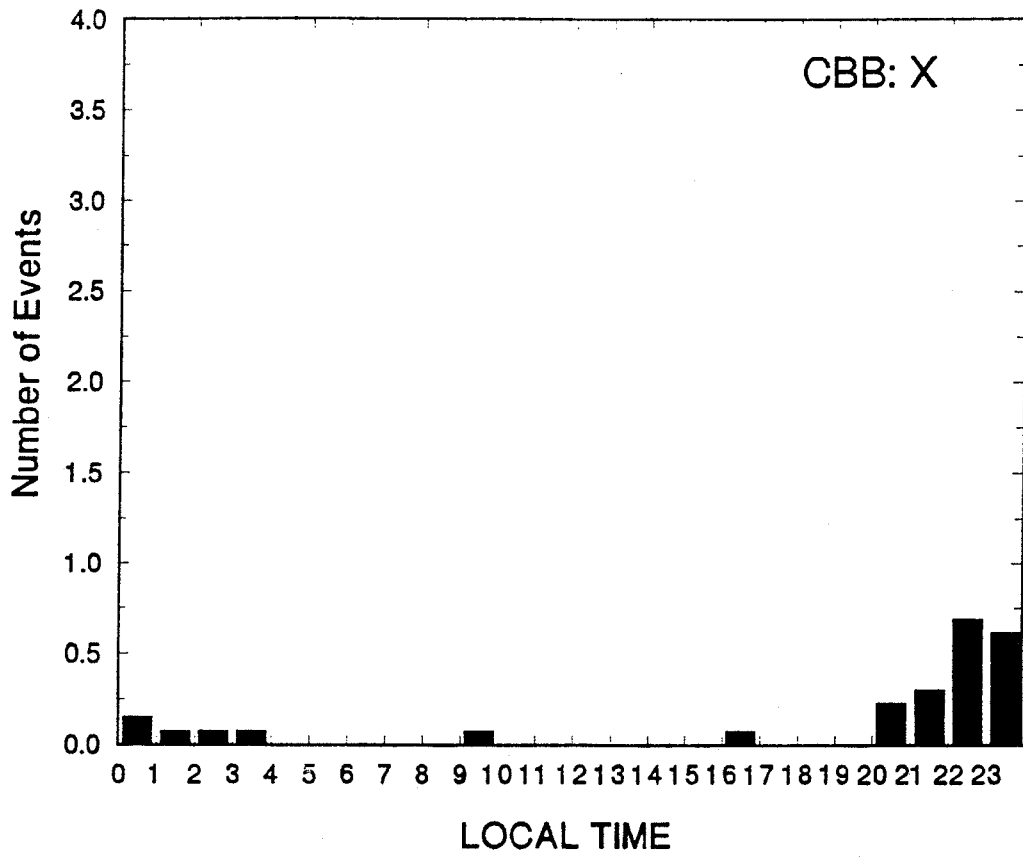
The following figures, as in Figure 11 of section 3, show the numbers of events equalling or exceeding 300 nT/min, for each hour in local time, for the X magnetic field component.











## APPENDIX

### C. RELATIONS BETWEEN $\text{dB}/\text{dt}$ AND $a_p$ ( $K_p$ )

The following figures, as in Figure 15 of section 4, show correlograms of the maximum  $\text{dB}/\text{dt}$  in a three-hour interval versus the  $a_p$  value for that interval. The equivalent  $K_p$  values are noted on the top axis.



